钱学森

力学手稿

9

钱学森

西安交通大学出版社
XI'AN JIAOTONG UNIVERSITY PRESS

ISBN 978-7-5605-4547-9
9 787560 545479 >
定价：70.00元

钱学森

力学手稿

⑨

钱学森

西安交通大学出版社
XI'AN JIAOTONG UNIVERSITY PRESS

图书在版编目(CIP)数据
钱学森力学手稿.9:英文/钱学森著. 西安:西安交通大学出版社,2013.2
ISBN 978-7-5605-4517-9

Ⅰ.①钱… Ⅱ.①钱… Ⅲ.①钱学森(1911~2009)-力学-手稿-英文 Ⅳ.①O3-53

中国版本图书馆CIP数据核字(2012)第200959号

书 名 钱学森力学手稿9
著 者 钱学森
责任编辑 杨 璠

出版发行 西安交通大学出版社
(西安市兴庆南路10号 邮政编码710049)
网 址 http://www.xjtupress.com
电 话 (029)82668357 82667874(发行中心)
(029)82668315 82669096(总编办)
传 真 (029)82668280
印 刷 中煤地西安地图制印有限公司

开 本 787mm×1092mm 1/16 印张 12.5 字数 300千字
版次印次 2013年2月第1版 2013年2月第1次印刷
书 号 ISBN 978-7-5605-4517-9/O·400
定 价 70.00元

读者购书、书店添货,如发现印装质量问题,请与本社发行中心联系、调换。
订购热线:(029)82665248 (029)82665249
投稿热线:(029)82664954
读者信箱:jdlgy@yahoo.cn

出 版 前 言

2011 年 12 月 11 日是西安交通大学杰出校友钱学森先生的百年诞辰。为缅怀钱学森学长，学习他的科学思想和卓越风范，展示其丰功伟绩和人格魅力，西安交通大学举办了“纪念钱学森诞辰 100 周年”系列活动：作为制片方之一，参与西部电影集团摄制传记故事片《钱学森》；与中央电视台合作，出品纪录片《实验班的故事——沿着钱学森走过的路》；扩建钱学森生平业绩展馆，向校内外开放；举办钱学森科学与教育思想研讨会；出版发行《钱学森力学手稿》、《钱学森年谱（初编）》、《钱学森第六次产业革命思想探微丛书》等。

钱学森先生在美国深造和工作期间留下大量珍贵手稿，这些手稿真实展示了钱学森先生博大精深的学识、开拓求实的精神和严谨奋进的作风，是钱老勇攀科学高峰和严谨治学的集中体现。这里，我们将部分原稿整理汇集成册，出版《钱学森力学手稿》，作为钱老百年诞辰的献礼。

《钱学森力学手稿》共 10 卷，包含两部分内容。第一部分是草稿，包括扁壳、球壳和圆柱壳屈曲分析的公式推导和数值演算。在研究圆柱壳轴压屈曲问题时，为了求得圆柱壳体的临界压力，在有关的五百多页草稿中，对多达二十多种可能的屈曲模

态逐一进行公式推演和数值计算，最终才找到满意的并在论文中采用的屈曲模态。仔细观察草稿中的数据列表，每个数字有效位数都长达八位，在手摇机械式计算机作为主要计算工具的年代，这串串数字凝聚着多少现今难以想象的艰辛劳动。

第二部分是手稿，以航空航天工程为核心，涵盖空气动力学、固体力学、火箭技术、工程控制论和物理力学等领域的部分学术论文手稿、打印稿和讲义。

《钱学森力学手稿》是在西安交通大学校领导的大力支持下，由西安交通大学航天航空学院沈亚鹏教授整理完成。图书出版过程中得到了西安交通大学党委宣传部、校友关系发展部、图书馆、航天航空学院等的积极协助，在此深表感谢。

Contents

Section 1

Wind-Tunnel Testing Problem in Superaerodynamics

orig. Scarborough
double space

1

Wind-Tunnel Testing Problems in Supersonic Aerodynamics

Hsue-shen Tsien
Guggenheim Aeronautical Laboratory
Massachusetts Institute of Technology

Wind-tunnels are, perhaps, the most powerful tool in aerodynamic investigations and certainly have contributed much in the modern development of fluid mechanics. It is natural, when one turns to the new field of aerodynamics, the aerodynamics of rarefied gases or supersonic aerodynamics, that one should think of using the wind tunnel again. Only here ~~the old faithful~~ it tool has to be adopted to entirely new circumstances and many new problems, both in its design and in its operation, appears. It is the purpose of this paper to discuss some of these problems, to so gain an orientation in the new field of experimentation.

1. Tunnel Design

To test models in the wind tunnel at its test section, it is of primary importance to obtain a uniform stream at the desired temperature, pressure and velocity. For subsonic wind tunnels with ordinary pressures, this can be achieved without much difficulty. For supersonic wind tunnels at ordinary pressures, the expansion part of the tunnel, or the nozzle, before the test section, is first designed to obtain a uniform stream at its exit without considering the thickness of the boundary layer. Then the boundary layer along the wall of the nozzle is calculated with the pressure gradient thus determined. Finally the thickness of the boundary layer, or rather the displacement of the boundary layer flow at lower velocity is provided by making the nozzle larger than the dimensions first determined by the calculated amount. (Ref 3) This design procedure is found to give satisfactory nozzles for supersonic wind tunnels.

[illegible] one tries to use the same design of [illegible] to the entrance cone [illegible] with the difficulty [illegible] the [illegible] the boundary layer will be so thick as to cut off [illegible] section of the nozzle downstream. To [illegible] this effect let us consider that the length of the test section [illegible] of the approach section [illegible] the [illegible] section as [illegible]

[illegible] the [illegible] test section. [illegible] a rough cut at it, we take the thickness of the [illegible] layer to be zero at the beginning of the test section and equal to [illegible] at the end of the test section, then

$$\delta = 3.65 L \frac{1}{\sqrt{Re}} \qquad (1)$$

[illegible] of [illegible] boundary layer actually occupies [illegible] of [illegible] such that

$$\frac{b}{2} = 2.5 L \frac{1}{\sqrt{Re}}$$

On the other hand the ratio of the area of the [illegible] boundary layer thickness of [illegible] to be equal to

$$\frac{A}{A} = \frac{1.07 \sqrt{Z} - \frac{11}{Re}}{3.65 \sqrt{Re}}$$

where [illegible] the ratio of effective [illegible] in the test section [illegible] contraction [illegible]

$$\frac{A}{A} = \frac{1}{\text{[illegible]}} \qquad (4)$$

This relation is shown [illegible] for a [illegible] section [illegible] to the [illegible] and [illegible] the boundary layer will [illegible] fill up

[illegible]

[illegible] calculating the section [illegible] section and the check [illegible] section [illegible]. Consider the [illegible] section, the pressure loss due to friction, Δp_1 is

$$\Delta p_1 = \frac{\text{[illegible]}}{b'}$$

$$= \frac{\rho}{2} \cdot u \cdot L \cdot \frac{f}{\text{[illegible]}}$$

Table [illegible]

$$\Delta p_1 = 2 \rho u^2 \frac{L}{h} \cdot \frac{f}{\text{[illegible]}}$$

In the plain duct it is situated as [illegible] duct with no recovery after the duct. Then if k is the pressure [illegible]

$$\Delta p_2 = \left[\frac{}{1 + \frac{k-1}{2} M^2} \right]^{\frac{\gamma}{\gamma-1}} = \left[\frac{2\gamma}{(\gamma+1)} M^2 - \frac{\gamma-1}{\gamma+1} \right] p_1$$

[illegible]

$$\frac{\Delta p_2}{p_1} = \frac{2\gamma M^2 \left(\frac{L}{b}\right) \frac{1.32}{\sqrt{R_L}}}{1 + \frac{\gamma-1}{2} M^2} \qquad (9)$$

Introducing the free path ratio given by (3), we have

[illegible]

[illegible] plotted in fig. 2. Therefore if Mach number M is 2 [illegible]

the ratio of frictional loss to shock loss is 0.628 therefore the frictional loss and the shock loss are of the same order of magnitude.

[illegible] design of the nozzle and test section for a supersonic wind tunnel, it is no longer possible to separate the [illegible]

Rayleigh, a number encountered. Therefore to actually design such a nozzle to obtain the correct effect on the ideal uniform flow, it will be necessary to use the exact Navier-Stokes [illegible]

Of course, it may be argued that for uniform supersonic, the Navier-Stokes equations are no more correct and added viscous corrections must be added (Ref. 4). However, recent investigations by R. Schamberg (Ref 3) have shown that these additional corrections [illegible] essentially alter the "flow" pattern. Hence for a first approximation, just like the one-dimensional isentropic flow as a first approximation for subsonic supersonic nozzles, we can use the Navier-Stokes equations. The simplest case to be considered is certainly the axially symmetric nozzles. If x is the axial axis of the [illegible] r the coordinate in the radial direction and [illegible] the corresponding velocity components (Ref 3) the [illegible]

$$\frac{1}{r}\frac{\partial}{\partial r}(rv) + \frac{\partial u}{\partial x} = 0 \qquad (9)$$

$$\rho \frac{Du}{Dt} = -\frac{\partial p}{\partial x} - \mathrm{grad}(\tau)_x \qquad (11)$$

$$\rho \frac{Dv}{Dt} = -\frac{\partial p}{\partial r} - \mathrm{grad}(\tau)_r \qquad (12)$$

$$\rho \left(\frac{D}{Dt} \left(u^2 + v^2 + \hat{p}T \right) \right) = \Phi - \mu \, \mathrm{grad}(\tau)_x + v \int d\tau$$

$$+ \frac{\partial}{\partial x} \lambda \frac{\partial T}{\partial x} + \frac{1}{r} \frac{\partial}{\partial r} \left(\lambda r \frac{\partial T}{\partial r} \right)$$

$$\frac{p}{Dt} = u \frac{\partial}{\partial x} + v \frac{\partial}{\partial r}$$

Φ = dissipation function

τ = stress tensor

(9), (10), (11) together with the equation of state

$$\frac{p}{\rho} = RT \qquad (13)$$

[illegible]

[illegible]

The quantities [illegible] and [illegible] may be
three variables f, P, T and are [illegible]
f, P, T are related by the equations of state and [illegible]
is necessary for the determination [illegible]
work, the quantities [illegible] f [illegible]

[illegible] pressure, we assume a fluid surrounded [illegible]
[illegible] pressure. However for the extremely [illegible]
[illegible] the most usual type is the Perrin gauge. The
[illegible]
[illegible] by the rise of [illegible]
of the gas surrounding it. The temperature [illegible]
the change in the resistance of the wire. The [illegible]
[illegible] The method [illegible]
[illegible] The practical [illegible]
[illegible] by S. A. Schaff. (Ref 5)

To [illegible] the amount of the constant needed [illegible]
the range in the different [illegible] liquid range as manometers of different sizes
[illegible]
[illegible]
[illegible] is a variety of these methods described [illegible]
[illegible]

---

* 1000 microns = 1 mm Hg.

proportional to the density of the gas. The measurement of the

The conventional method for the measurement of the [illegible] makes the use of dynamic pressure [illegible] great disadvantage as pointed out in the previous section. Thus the

[illegible]

$$a = \sqrt{\frac{R}{\pi U}}$$

and the stagnation point is located at

$$r_s = \sqrt{\frac{3R}{4\pi U}} - \frac{\sqrt{3}}{2} R a$$

The velocity introduced by the source is then

$$-U \frac{3}{4} \frac{R^2}{r^2}$$

In calculating the viscous stress from the approximate disturbance

[illegible]

$$U \frac{\partial u}{\partial r} + \frac{1}{\rho} \frac{\partial p}{\partial r} = +3\nu U R^2 \frac{3}{2 r^4} \qquad (16)$$

Hence if p_0 is the stagnation pressure and p' the ~~free stream~~ static pressure,

$$p_0 - p' = \frac{1}{2}\rho U^2 + \mu U R^2 \frac{3}{2} \int_r^\infty \frac{dr}{r^4}$$

$$= \frac{1}{2}\rho U^2 - \frac{1}{2}\mu U R^2$$

or $$p_0 - p' \simeq \frac{1}{2}\rho U^2 \left[1 - \frac{8}{3\sqrt{3}} \frac{\nu}{aU}\right] \qquad (17)$$

[illegible]

[illegible]

The displacement flow is bounded when the amount of any fluid element that is the same free path. Since the actual flow, the

[illegible] have this a simple physical situation. If ϑ is the inclination [illegible]

$$E_{i_{kr.}} = \rho \frac{c}{2\sqrt{\pi}} \int e^{-\frac{k^2}{c^2}\sin^2\vartheta} \cdots \left(c^2 + \tfrac{1}{2}u^2\right)$$

[illegible] (8)

[illegible] the gas stream. (But in consideration [illegible] $\vartheta = 0$, then

$$\cdots_{kr} = \rho \frac{c}{2\sqrt{\pi}} \left(c^2 + \tfrac{1}{2}u^2\right), \quad \vartheta = 0$$

The total incident energy per unit area is then

$$E_i = \rho \frac{c}{2\sqrt{\pi}} \left[\tfrac{1}{2}u^2 + \left(\tfrac{1}{2}R + c_v\right)T\right] \qquad 9)$$

where α is the accommodation coefficient of the gas at constant volume of the wall temperature, and α the accommodation coefficient for molecules striking the energy E_i incident upon the surface and the energy E_r carried by the molecules reflected from the surface is given by

$$E_r - E_i = \alpha (E_i - E_w) \tag{9}$$

where E_w is the energy that would be carried away by the reflected molecules if the gas were in thermal equilibrium at the temperature of the wall T_w.

[illegible] the number striking unit area of the surface per unit time is given by

$$\frac{n\sqrt{RT}}{\sqrt{2\pi}} \left[\left(\tfrac{1}{2}R + C_v\right)(T - T_w) + \tfrac{1}{2}u^2 \right] \tag{10}$$

[illegible] energy carried from the surface is $\varepsilon \sigma T_w^4$ where ε is the emissivity, and σ the Stefan-Boltzmann constant [illegible] the heat [illegible] the energy balance requires

$$\alpha \frac{n\sqrt{RT}}{\sqrt{2\pi}} \left[\left(\tfrac{1}{2}R + C_v\right)(T - T_w) + \tfrac{1}{2}u^2 \right] = \varepsilon \sigma T_w^4 \tag{11}$$

If ρ is the resistivity coefficient of the material of the wire [illegible] temperature T, then

$$r = r_0 \left[1 + \beta (T_w - T)\right] \tag{12}$$

where r_0 is the resistance of the wire at the temperature T. By elimination of T_w from (11) and (12), we have

$$\frac{i^2 r}{2\pi} = \frac{2\pi}{\gamma - 1}(\beta T)^2 \left(\frac{r}{r_0} - 1\right) + \left[\frac{\varepsilon \sigma T^4}{\alpha \rho \frac{n\sqrt{RT}}{\sqrt{2\pi}} \gamma RT}\right] \cdot \left(\frac{r}{r_0}\right)^4 \cdot \left(\frac{r}{r_0}\right)$$

where M is the Mach number of the gas stream, γ is not [illegible]

To be more specific, let us assume that the cone current be maintained at a constant value i such that when the air velocity is zero, $T_w = T$ at $r = r_0$. Then

$$\frac{T}{T_0} = \frac{1}{\left[1 + \frac{\gamma-1}{2} M^2\right]} + \frac{\left[\frac{i^2 R T^*}{\left[1 + \frac{\gamma-1}{2} M^2\right]^{\gamma}}\right]^{\frac{1}{2}}}{\left[1 + \frac{\gamma-1}{2} M^2\right]^{\frac{\gamma}{2}}} \left(\frac{r}{r_0}\right)^{\frac{1}{2}} \qquad (14)$$

[illegible]

Therefore the performance of such a cathode heat source is given by

$$\frac{1}{2} M^2 = 2.14 \left(\frac{r}{r_0} - 1\right) + \left(\frac{r}{r_0}\right)^4 - \left(\frac{r}{r_0}\right) \qquad (17)$$

This equation is plotted in Fig. 5. It is seen that the sensitivity of such an enhancement is quite satisfactory.

[illegible]

3. Parameters of Flow

[illegible] field are the Reynolds number Re, defined as

$$Re = \frac{UL}{\nu^0}$$

where ν^0 is the kinematic viscosity, L the typical linear dimension of the body, and the Mach number M^0 of the free stream. Thus

a boundary layer with flows and free molecule flows due to the fact that the mean free path is the typical dimension of the object. The Reynolds number and the Mach number [illegible] the flow is continuum, [illegible] the flow enters into the free molecule regime [illegible] the interaction of the molecules and the wall be considered and that the radiation of energy to and from the wall be taken into account. The interaction of the molecules with the wall [illegible] the molecules are diffusely re-emitted from the wall and the accommodation [illegible] we have reason to believe that [illegible] the temperature of the wall and the [illegible] the wall temperature, the gas temperature and the [illegible] considerations seem to indicate then that for the model test [illegible] the same pressure, the model must be made [illegible] same Mach number, and furthermore the following parameters must be the same:

1) Reynolds number Re^*
2) Mach number M^*
3) free stream temperature, T^*

[illegible] that [illegible] the wall temperature equal to $\frac{T_w}{T^*}$ for exact [illegible] however, if the model is surrounded by the [illegible] then also the heat transfer [illegible] and the [illegible] is to be [illegible] the wall temperature equal to $\varepsilon \sigma T_w^4 - q_c$ [illegible] the heat transfer, in the [illegible] to be determined as a [illegible] call this new parameter Λ_w, [illegible]

$$\Lambda_w = \left[\frac{\varepsilon \sigma T_w^4 - q_c}{\rho^* u (c_p T^*)} \right]_w \qquad (45)$$

on the f[illegible] the heat fr[illegible] the [illegible]ells of the test element .. assert that there can be other reactions and the radiation from the walls and surroundings at temperature T_s [illegible] can [illegible] by a [illegible] the parameter Λ, for the prototype.

$$\Lambda = \left[\frac{F \sigma T_w^4 - q}{\sigma \alpha (T_p - T^\circ)} \right]_m \qquad (6)$$

in order for this flow to be same also with the model, must have,

$$\Lambda = \Lambda_m \qquad (7)$$

From [illegible] we [illegible] conditions on the [illegible] and free stream temperature, [illegible] we must have

$$\frac{\xi \xi - \xi^\circ}{\xi \sigma T_w^4} = \frac{L}{\quad} \qquad (8)$$

[illegible] the typical linear dimension of the [illegible] and T_w the wall temperature of the test element. It is [illegible] that [illegible] satisfy [illegible]

[illegible] set of [illegible] at the [illegible] wall for model testing in a [illegible] flow is certainly different to satisfy [illegible] that [illegible] can be selected [illegible] the [illegible] of the [illegible]

References

1) A.E Puckett, "Supersonic Nozzle Design"
[illegible] (1946)

2) H. S. Tsien, "Supersonic Mechanics & Transonic Flows"
[illegible]

[illegible]

[illegible]

[illegible]

6) R.A. Evans, "Flow Visualization at Low Pressures"
[illegible]

[illegible]

Table 1

The functions F_1 and F_2 of [illegible]

U/c	F_1	F_2
	[illegible]	
	1.73751	0.07020
"	1.63260	0.27269
	1.49248	0.58566
"	1.32024	0.97843
"	1.14328	1.42053
	0.97825	1.88555
"	0.83480	2.35492
"	0.71628	2.81412
"	0.62153	3.27117
"	0.54683	3.71356
	0.48790	4.14672
"	0.44090	4.57300
"	0.40268	4.99395
"	0.37100	5.41117
"	0.34420	5.83748

Then since

$$F_2(z) = \sqrt{\pi}\, z^2\, e^{-\frac{z^2}{2}} \left[I_0\left(\frac{z^2}{2}\right) + I_1\left(\frac{z^2}{2}\right) \right]$$

where I_1 is the modified Bessel function of first kind ...

Hsue-shen Tsien

Guggenheim Aeronautical Laboratory

Massachusetts Institute of Technology

Wind-tunnels are, perhaps, the most useful tool in aerodynamic investigation. It can certainly have contributed [illegible] development of fluid mechanics. It is thus natural, when one turns to a new field of aerodynamics, [illegible] that one should think of using the wind tunnel again. Only here it has to be adopted to satisfy new circumstances and new problems, which in its design and in its operation, appear. It is the purpose of this paper to discuss some of these problems, so as to gain an orientation in the new field of experimentation.

1. Tunnel Design

To test models in the wind tunnel at its test section, it is of primary importance to obtain a uniform stream at the desired temperature, pressure and velocity. For a tunnel with primary pressures, this can be achieved without much difficulty. For a tunnel with primary pressure, the expansion part of the nozzle or the test section or the nozzle is first designed to obtain a uniform stream at its exit without considering the effects of the viscosity of air. Then the boundary layer along the wall of the nozzle is calculated with the pressure gradient thus determined. Then, the displacement [illegible] boundary layer, or the needed space [illegible] under layer [illegible] provid-

ed by making the nozzle larger than the theoretical [illegible] calculated amount. (Ref. 1) This design procedure is found to give satisfactory nozzles for supersonic wind tunnels.

However when we tried to use the same design principle for the supersonic aerodynamics wing tunnel, one is immediately faced with the difficulty of extremely large viscous effect. In other words, the boundary layer will be so thick as to occupy the entire passage. To demonstrate this effect, let the length of the constant area part of the nozzle and the width of the square test section be L. Then the ratio of the area at the condition in the test section is $\frac{L^2}{L^2 - 2\delta^2}$ where U is the velocity in the test section. If, as a rough estimate, we take the thickness of the boundary layer to be zero at the beginning of the test section and equal to a value calculated by the two-dimensional case at the end of the test section, then

$$\delta = 3.65\, L/\sqrt{Re} \tag{1}$$

Now if this boundary layer is to fill only half of the tunnel width, then

$$\delta = \frac{L}{2} = 3.65\, L/\sqrt{Re} \tag{2}$$

In other words, the ratio of the mean free path / [illegible] boundary layer thickness δ is known (Ref. 2) to be equal to

$$\frac{l}{\delta} = \frac{1.255\sqrt{\gamma}}{3.65}\,\frac{M}{\sqrt{Re}} \tag{3}$$

where γ is the ratio of specific heats and may be taken as 1.4, l is the Mach number in the test section. By combining (2) and (3), we have

$$\left(\frac{l}{\delta}\right)\left(\frac{L}{\delta}\right) = 0.0557\, M \tag{4}$$

This relation is shown in Fig. 1. The [illegible] number equal to 4, and L/b = 2, the boundary layer will completely fill up the test section, if the mean free path is equal to 5.6% of the boundary layer thickness or 2.8% of the tunnel width. It is seen from the above, although use of [illegible] totally inapplicable.

The extremely thick boundary layer where the velocity increases from a small value near the wall to some supersonic velocity at the center of the nozzle, also gives a [illegible] of the nozzle. Since pressure disturbances can be transmitted upstream in subsonic flows, the flow in the test section of a low pressure tunnel will be sensitive to changes in the diffuse even if the main stream velocity at the center of the nozzle is supersonic. This is of course a new phenomenon in [illegible].

The large viscous effects can be also demonstrated by calculating the ratio of frictional loss on the walls of the test section and the shock loss in the diffuser after the test section. For simplicity the diffuser is assumed to be a straight tube of approximately the same cross sectional area as the test section, then the pressure loss due to friction, is

$$\Delta p_1 = \frac{1}{2}\rho U^2 \left(\frac{L}{b}\right) C_f$$

Taking C_f to be Blasius value or $C_f = \frac{1.328}{\sqrt{Re}}$ we have

$$\Delta p_1 = 2\rho U^2 \left(\frac{L}{b}\right) \frac{1.328}{\sqrt{Re}} \qquad (5)$$

Now if is the ot[illegible] pressure in the [illegible] as p_2 [illegible] ress re by ideal isentropic compression in the diffuser is . If the actual press e rise in the diffuser is es imated as [illegible] ue to a normal shock without further recovery, then the actual pressure rise is

Therefore the pressure loss due to shock is

(5)

By combining (5) and (6), the ratio of these two pressure losses is

(6)

Introducing the mean free path ratio given by (3), we have

(8)

This relation is plotted in Fig. 2. Therefore if the Mach number is 2, and L/b = 2 as before, then when the ratio ( ) is 0.056, the ratio of frictional loss to shock loss is 0.428. Hence the friction loss and the shock loss is of the same order of magnitude.

These large viscous effects are fully confirmed by the recent tests on the 1" x 1" low pressure wind tunnel at the University [illegible]* The test nozzle Fig. 3, was designed for Mach number with consdering the viscous e[illegible] the medium. During test, the st[illegible] pressure on the

* Experimental work [illegible] under contact with the [illegible] Naval research. The author is deeply indebted to Professors R. G. Folsom and E. D. Kane for permission to use their unpublished results.

wall at the exit [illegible] is measured. This pressure is equal to 175 microns* for the two tests presented in Figs. 4 and 5. The apparent Mach number "M" is the Mach number calculated from the dynamic pressure measured by a Pitot tube having the straight form. Since there is the complication of large gradients in the Pitot tube reading as shown in the following section, this apparent Mach number is only quantitative and cannot be taken as the exact value. However it is apparent from Figs. 4 and 5 that the boundary layer in the test section is indeed very thick, and fills up the whole space. This large boundary layer thickness makes this space available for the expansion of the central potential flow if it exists, very small. Therefore the maximum Mach number reached at the center of the test section is very much smaller than the design Mach number of 4. At low pressure, the influence of slip at the wall is also evident. This has the tendency to make the flow more uniform. However the very low Mach number at the test section indicates that the strong viscous effect in decreasing much of the pressure energy into heat energy.

These experiments, calculations and preliminary test results make it clear that for the design of the nozzle and test section for a supersonic wind tunnel, it is no longer possible to separate the compressibility effects and the viscous effects. In fact, the concept of boundary layer is also of doubtful value due to the extremely small Reynolds number encountered. Therefore to actually design a nozzle to obtain the nearest approximation to the ideal uniform flow it will be necessary to use the exact Navier Stokes equations instead of the approximate boundary layer equations. Of course, it may be argued that for supersonic speeds, the Navier-Stokes equations for no slip exact and additional conditions must be used (Ref. 2). However, recent investigations by

---

* 1000 microns = 1 mm Hg_1 one atmosphere = 0.760×10^6 microns.

R. Schamberg Ref. 9 have shown that these additional corrections are small in case of slip-flows concerned here and will not essentially alter the flow pattern. Hence for a first approximation just like the non-viscous isentropic flow as a first approximation for ordinary supersonic nozzles, we can use the Navier Stokes equations. The simplest case to be considered is certainly the axially symmetric nozzles. If x is the coordinate in the axial direction, the coordinate in the radial direction and u and v are the corresponding velocity components, the equations are:

(9)

(10)

(11)

(12)

where

= dessipation function

= stresses tensor

(9), (10), (11) and (12) together with the equation of states

= R T (13)

then determines the unknowns u, v, , and T. Of course, the actual process of making this calculation will be extremely tedious and some approximation method of solution may have to be developed. One possibility would be to adopt

the Karman-Pohlhausen method of boundary layer theory is used. We integrate the differential equation with respect to r and thus only try to satisfy the equation "on the average" over the cross section of the nozzle. The "distribution" of u, v over the cross-section will then be set in the form of a polynomial. Initial guess in this procedure is already made by S. A. Schaaf (Ref. 4) at the suggestion of the author.

For ordinary supersonic diffuser, the efficiency of pressure recovery can be generally quite good. However, for a supersonic wind tunnel, due to the extreme large loss in separation, long diffusers are used. As a fact, the pressure loss may be reduced by using a shortest possible diffuser.

2. Flow Measurement

The quantities which determine the flow field are two out of the three variables , , T and the velocity components. The quantities , , T are related by the equation of states and therefore only two is necessary for the determination of the flow. For a supersonic wind tunnel work, the quantities to be measured are , , and , the magnitude of the velocity.

For the measurement of pressure, a manometer is used. For ordinary pressure, the manometer used may be water, alcohol or mercury. However for supersonic flow, some more sensitive manometer is necessary. One of the most successful type is the Pirani gage. It utilizes the change of the pressure of a wire heated with a constant current to measure the pressure of the gas surrounding it. The temperature of the wire is decided by the resistance of the wire. The wire is usually in a small chamber which is connected to the

point o measurement [illegible], from which the gas stream t static pressure is to be measured. The question of best design of the connecting tube for quick response is studies by S. A. Schaaf. (Ref. 5).

To measure the density , the conventional method utilises the difference in the velocity of a light rays in medium of different density. With different optical arrangements we have the shadowgraph method, the schlieren method and the interferometer method. However, if the density of the medium is very low as in the case of rarefied dynamic flow, the sensitivity of these methods is the exception rather than the rule. The schlieren method, the per centage illumination by passing through a region of thickness b is given by

(14)

where is the air density at 32°F and 1 atmosphere pressure, and is the density gradient normal to the light ray. and are the local length and width of the light source image perpendicular to the knife edge. K is a constant, determined by the particular optical path used. The sensitivity of the schlieren method decreases with the increase in . Some improvement can be made by altering the quantitive f and , but practical limitations and diffraction difficulties do not allow the increase of sensitivity to satisfactory values.

A new method of the pressure density measurement is the method of absorption. It has been found that oxygen at low pressures shows a strong absorption spectrum in the region around 1,700 A or ultra violet light. The percentage absorption is proportional to the number of molecules that meet the light ray and, therefore, proportional to the density of the gas. The measurement is thus similar to that of the interferometer method where the density is determined. A similar method is the utilisation of the after-flow in nitrogen. These

methods are now being studied by J. A. Evans (Ref. 1).

The conventional method for the measurement of velocity is through the use of dynamic pressure rise in a Pitot-tube. A straight forward application of this method is, however, difficult for rarefied gases. The formula used is, however, based upon the neglection of viscosity effects. But for rarefied gases the viscosity effect is of great importance as pointed out in the previous section. Then the dynamic pressure would be quite different than that given by the usual formula. To estimate this effect, let us consider the case of low Mach number so that compressibility effects can be neglected. Then as a first approximation, take the flow field around the Pitot tube as that of a source of strength in a non-viscous flow of uniform velocity J. The "radius" of the tube a is

$$a =$$

and the stagnation point is located at

(15)

The velocity introduced by the source is then

Neglecting the viscous stress from this approximate disturbance velocity, we have for flow along the axis

(16)

Hence if is the stagnation pressure and the static pressure,

$$\frac{\partial}{\partial r}$$

)

For rarefied gases, the value of $\frac{1}{\gamma}$ or the reciprocal of the Reynold's number of the Pitot-tube could be of the order of unity. Then the dynamic pressure rise - is not the usual value $\frac{1}{2}$ but a value much less than that. In fact previous investigation by Baker (Ref.) and F. Homann (Ref. 8) indicate that the Reynolds number where a' is the radius of the mouth of tube, must exceed 30 in order to reach the usual dynamic pressure rise $\frac{1}{2}$.

When the velocity of flow is high, we have the additional complication due to the shock. The conventional Rayleigh formula for Pitot tubes in supersonic flow is based upon the assumption that the shock wave at the mouth of the Pitot tube. Now the thickness of the shock is proportional to the mean free path. Hence in rarefied flows, the thickness of the shock will be so increased as to cause interference with flow in the neighborhood of the Pitot-tube. This together with the viscous effect mentioned in previous paragraph definitely show the inapplicability of the Rayleigh formula for supersonic velocity of rarefied gases.

3. Hot-Wire Anemometer

With the great complications in applying the conventional velocity measuring device to supersonic flows, one is naturally led to the thought of other avenues of approach. One possibility is the use of hot-wire. If the wire diameter is of the order of several inches, and if the pressure of the gas stream is approximately 140 microns, the ratio of the mean free path to the wire diameter will be approximately 140. Therefore the flow around the wire is definitely the free molecule flow (ref.). We have thus a simple physical situation, which is an improvement over the rather uncertain circumstances involved dynamic and viscous effects for the measurement of velocity by Pitot tube. It thus seems worthwhile to explore this possibility by a trial calculation of the performance of such a hot-wire anemometer.

If is the inclination of the solid surface to a gas stream which has a macroscopic velocity U and a Maxwellian molecular velocity distribution, the translational energy of molecules incident upon the unit area is,

(18)

where $c^2 = \frac{1}{2}RT$, T temperature of the gas stream and erf is the error function. Now let r be the radius of the hot-wire. Then the total energy E_i incident upon a unit length of the wire is the sum of translational energy and internal energy. If C_v is the specific heat at constant volume, w is total energy per unit length of wire is

(19)

The integrals in equation (19) can be expressed in terms of tabulated functions, (see Appendix) Thus

(20)

where

(21)

(22)

The I_o and I_1 are the modified Bessel functions of the first kind of orders zero and one respectively. The functions F_1 and F_2 are tabulated in Table 1.

If T_w is the wall temperature, and x the accomodation coefficient, the

Diffuse reflection of the molecules incident upon the surface and the energy E_r carried by the molecules re-emitted from the surface is given by

$$E_i - E_r = \quad (E_i - E_w)$$

where E_w is the energy that would be carried away by the molecules if the re-emission were at the temperature T_w of the wire. Therefore

$$E_i - E_r = \quad c\,r \quad \tfrac{1}{2} U^2 + (\tfrac{1}{2} R + C_v)(T - T_w) F_1 \left(\frac{U}{a}\right)$$

$$+ \quad \tfrac{1}{2} U^2 + (R + C_v)(T - T_w) \quad F_2 \left(\frac{U}{a}\right) \qquad (23)$$

This difference of energy is then the net energy input to the wire per unit length of the wire by the air stream.

If i is the electric current heating the wire and is the resistance o. the wire per unit length at the wire temperature, the heat input per unit length of wire by the heating current is i^2 . Heat is lost from the wire by radiation. If is Stefan-Boltzmann constant and is the emissivity of the wire surface, the radiation heat loss per unit length is .

Therefore if the wire has reached a steady condition, the heat balance requires

(24)

This equation can be put into somewhat simpler form by using the relation that

$$R = C_p - C_v = C_v (\quad - 1) \qquad (25)$$

The [illegible] T_0 [illegible] temperature at which the resistance is [illegible], and the corresponding temperature coefficient of the resistance is [illegible]. Then the resistance [illegible] can be expressed as

$$= {}_{o}\,1 + \quad (T_{\theta} - T_{o}) \tag{26}$$

Now let

$$- \tag{27}$$

Then from equation (2[illegible]),

$$\frac{r_m}{r_o} = \frac{-\lambda}{T_o} + 1 \tag{28}$$

Now introduce $_{o}$ as the reference density and i_o as the reference heating current, then equation (24) can be written as

(29)

The particular values of the reference temperature T_o, the reference density $_{o}$ and the reference current i_o are not yet fixed. We fix these quantities now by requiring that

$$T_o = 1 \tag{30}$$

(31)

and

Then equation (29) simplified to

(33)

This is then the performance equation of the hot wire in free molecular flow.

Now let us investigate in greater detail the case of a straight platinum wire. To satisfy equation (30),

$$T_o = 492^\circ \text{ R.}$$

The value for and can be taken to be 0.08 and 0.90 respectively. Then equation (31) gives the corresponding pressure p_o for $_o$ and T_o as

Let the radius r of the wire be 0.0001 inch. Then equation (32) gives the reference heating current i_o as

$$i_o = \frac{\qquad\qquad}{\qquad\qquad} = 0.274 \text{ milliampere.}$$

where the resistivity of the platinum is taken as 10.9×10^{-6} ohm-cm. Therefore the order of magnitude of the different quantities is entirely satisfactory.

If the wire is used with a constant heating current, then equation (33) can be used to calculate the relation between the resistance ratio and the velocity ratio ($\frac{U}{C}$) at constant air stream density and temperature. This is done for $_o = 1$, $T/T_o = 1$ and $i/i_o = 1$* and the result is given in Fig. 5. It is seen that the sensitivity of the instrument is good. Of course, the behavior of the hot-wire anemometer will be actually determined by calibration for any experiment.

---

* The author is indebted to Mr. L. Mack for the numerical computations.

above the wall is the same. [illegible] to indicate that that for the model test to be similar to the prototype, the model must be made of same surface material as the prototype, and the flight must be the same, and furthermore the following parameters must be the same:

(1) Reynolds number Re

(2) Mach number M°

(3) free stream temperature T°

The radiation heat loss from the surface is equal to per unit area. However, if the model is surrounded by the walls of the test chamber, there is also an heat input due to radiation from walls of the test section to the model. Let us call this quantity . Then the net heat loss per unit area of the surface of the model is . This quantity can be rendered non-dimensional by dividing it by . Call this new parameter , then

(34)

For the prototype, the heat from the walls of the test chamber is a part of there may be solar radiation and the radiation from the earth and surrounding atmosphere. (Ref.). Denoting this amount by , then the parameter for the prototype is

(35)

In order for the flow to be same also with respect to the radiation heat transfer,

(36)

Because of the previous conditions on the Reynolds number and free stream temperature, (36) is the same as

Since the performance of the wire is strongly influenced by the accommodation coefficient as shown by equation (29), it will be necessary to find materials which can hold this coefficient constant over a considerable period of time so that no frequent calibration is required. However the present analysis seems to indicate the feasibility of such an instrument for measurements in rarefied gases and further research is definitely desirable.

4. Parameters of Flow

The two parameters that are directly connected with the flow field are the Reynold's number Re, defined as

$$Re = \frac{Ul}{\nu}$$

where ν is the kinematic viscosity, L the typical linear dimension of the body, and the Mach number M^{∞} of the free stream. This is true even for slip flows and free molecule flows due to the fact that the ratio of mean free path to typical dimension can be also expressed in terms of the Reynold's number and the Mach number.

However, as the pressure or density is reduced, the solid boundary of the flow enters actively into the flow conditions by requiring not only that the microscopic stream velocity be tangential to the surface but that the interaction of the molecules and the wall be considered and that the radiation of energy to and from the wall be taken into account. The interaction of the molecules with the wall is so far expressed through the fraction of molecules that are diffusely re-emitted from the wall, and the accommodation coefficient . It is known that both and are functions of the temperature of the wall and we have reasons to believe that they are also functions of the molecular velocity distribution. Therefore the interaction of the molecules with the wall is the same only if the wall temperature, the gas temperature and the Mach number of the gas

The Functions F_1 and F_2 (cf. equation 21)

U/c	F_1	F_2
0	[illegible]	0
0.[illegible]	[illegible]	[illegible]
0.[illegible]	[illegible]	[illegible]
0.[illegible]	[illegible]	[illegible]
0.[illegible]	[illegible]	[illegible]
1.0	[illegible]	[illegible]
1.2	[illegible]	[illegible]
1.[illegible]	[illegible]	[illegible]
1.[illegible]	[illegible]	[illegible]
1.[illegible]	[illegible]	[illegible]
2.0	[illegible]	[illegible]
[illegible]	[illegible]	[illegible]
2.[illegible]	[illegible]	[illegible]
2.[illegible]	[illegible]	[illegible]
2.[illegible]	[illegible]	[illegible]
2.8	[illegible]	[illegible]
3.0	[illegible]	[illegible]

Appendix

Evaluation of the Functions F_1 and F_2

For the function F_1,

where I_o is the modified Bessel function of first kind and order zero. The

last step is made possible by the substitution =

For the function F_2,

By the definition of the error function, we have

This form can be simplified by partial integration. Thus

where L_m is the [illegible] linear dimension of the model and L_p is the [illegible] linear dimension of the prototype. This means that the wall temperature of the test chamber must be so controlled that [illegible] satisfies (37).

This set of rather strict similarly rules for model testing in super-aerodynamic flows is certainly difficult to satisfy. In what way the rules can be relaxed is the problem of future research.

Therefore

where I_1 is the modified Bessel function of first kind and order one.

June 12, 1948

Mr. Robert R. Dorter, Secretary
Institute of the Aeronautical Sciences
2 East 64th Street
New York 21, N.Y.

Dear Mr. Dorter:

Enclosed are two manuscripts which I am submitting for consideration of publication in the Journal of the Aeronautical Sciences.

The first paper, "Wind-Tunnel Testing Problem in Supersonic Aerodynamics", is the revised form of my paper presented in the Annual Meeting. I apologize for the long delay in getting the manuscript into this form.

The second paper, "Two Dimensional Airfoils in Hypersonic Flows", is written by Mr. Richard D. Linnell and is taken from his Thesis at the Massachusetts Institute of Technology.

Very sincerely yours

H. S. Tsien
Professor of Aerodynamics

INSTITUTE
OF THE
AERONAUTICAL SCIENCES
INC
2 EAST 64TH STREET
NEW YORK 21 N Y

July , 19 A

Dr. H. S. Tsien
Guggenheim Aeronautical Laboratory
Massachusetts Institute of Technology
Cambridge, Massachusetts

Dear Dr. Tsien:

We are now preparing your paper, "Wind-Tunnel [illegible] Pressures in Supersonic Flow," for publication, and there does not seem to be an abstract or summary included. Since we feel that some sort of an abstract should be published with the paper, I should appreciate your sending one as soon as possible.

Very truly yours,

Clarence N. Jarcke

Managing Editor

July 24, 1948

Miss Bernoice H. Jarok
Associate Editor
Journal of the Aeronautical Sciences
2 East 64th Street
New York 21, N.Y.

Dear Miss Jarok:

Enclosed is the Summary for my paper, "Wind-Tunnel Testing Problems in Superaerodynamics". This is to answer your request in your letter of July 20, 1948.

Very sincerely yours

H. S. Tsien
Professor of Aerodynamics

Wind-Tunnel Testing Problems in Supersonic Aerodynamics

Hsue-shen Tsien

Summary

The problems in the experimentation of rarefied gas are discussed. First the extremely large viscous effects in a wind-tunnel nozzle is shown. Then the difficulties of flow measurement are surveyed, pointing out particularly the unconventional behavior of the Pitot tube in rarefied gas. The performance of a hot-wire anemometer is then studied in some detail to show its feasibility. Finally the rules for achieving complete flow similarity of rarefied gas flow are formulated.

Section 2

Hypersonic Flows $M_\infty \to \infty$

Hypersonic Flow $M_\infty \to \infty$

(I) Two Dimensional Case

a) The inclined Shock

$$\tan\beta = \tan\alpha \cdot \frac{\gamma-1}{\gamma+1}$$

$$p_2 = \frac{2}{\gamma+1}\rho_1 v_1^2 \sin^2\alpha$$

$$M_2^2 = (1+\cot^2\beta)\frac{\gamma-1}{2\gamma} = \left(1+\cot^2\alpha\cdot\left(\frac{\gamma+1}{\gamma-1}\right)^2\right)\frac{\gamma-1}{2\gamma}$$

$$M_1^2 = \frac{\gamma-1}{2\gamma}\frac{1}{\sin^2\alpha} + \frac{2}{\gamma-1}\cot^2\alpha$$

$$= \frac{\gamma-1}{2\gamma}\frac{1}{\sin^2\alpha} + \frac{2}{\gamma-1}\left[\frac{1}{\sin^2\alpha} - 1\right]$$

$$M_2^2 = \frac{(\gamma+1)^2}{2\gamma(\gamma-1)}\frac{1}{\sin^2\alpha} - \frac{2}{\gamma-1}$$

$$\cot\beta = \cot\alpha\left(\frac{\gamma+1}{\gamma-1}\right)$$

b) Subsequent Expansions

We shall use the formula

[illegible]

[illegible]

$$- \left[\frac{M}{2} - \frac{1}{\sqrt{M^2-1}} + \frac{1}{3} \frac{1}{(M^2-1)^{3/2}} - \cdots \right]$$

[illegible]

$$+ \left[\frac{M_2}{2} - \frac{1}{\sqrt{M_2^2-1}} + \frac{1}{3} \frac{1}{(M_2^2-1)^{3/2}} - \cdots \right]$$

[illegible]

We have the formula

$$1 + \frac{\gamma-1}{2} M^2 = \left(\frac{p_0'}{p}\right)^{\frac{\gamma-1}{\gamma}}, \qquad 1 + \frac{\gamma-1}{2} M_2^2 = \left(\frac{p_0'}{p_2}\right)^{\frac{\gamma-1}{\gamma}}$$

One can write the ratio p/p_2 in terms of $\theta_0 - \theta$.

$$\frac{1 + \frac{\gamma-1}{2} M^2}{1 + \frac{\gamma-1}{2} M_2^2} = \left(\frac{p_2}{p}\right)^{\frac{\gamma-1}{\gamma}}$$

$$\theta_2 - \theta = \frac{2}{\gamma+1}\frac{1}{M_2}\left(1+\frac{\gamma-1}{4}M_2^2\right)\left[\left(1-\left(\frac{p_1}{p_2}\right)^{\frac{\gamma-1}{\gamma}}\right)\left(1-\frac{\gamma-1}{2}\frac{p_1}{p_2}\left(1-\left(\frac{p_1}{p_2}\right)^{\frac{\gamma-1}{\gamma}}\right)\right)^{-\frac{1}{2}}\cdots\right]$$

$$-\frac{4}{3}\frac{3\gamma}{\gamma-1}\frac{1}{M_1^2}\left(1-\left(\frac{p_1}{p_2}\right)^{\frac{3(\gamma-1)}{2\gamma}}\right)\cdots\Bigg]$$

$$-\frac{4}{3}\frac{4\gamma}{\gamma-1}\left[1-\left(\frac{p_1}{p_2}\right)^{\frac{3(\gamma-1)}{2\gamma}}\right]\Bigg)\frac{1}{M_1^2}$$

(c) Small θ_0

$$\tan(\alpha-\theta_0) = \frac{\gamma-1}{\gamma+1}\tan\alpha$$

$$\frac{1+\tan\alpha\tan\theta_0}{} = \frac{}{\gamma+1}$$

$$\tan\alpha - \tan\theta_0 = \frac{\gamma-1}{\gamma+1}\tan\alpha + \frac{\gamma-1}{\gamma+1}\tan^2\alpha\tan\theta_0$$

$$\cdots\alpha = \tan\theta_0 + \frac{\gamma-1}{\gamma+1}\tan^3\alpha\cdots$$

$$\frac{4}{(\gamma+1)^2}\frac{\sin\alpha}{1-\sin^2\alpha} = \tan^2\theta_0 + 2\frac{\gamma-1}{\gamma+1}\tan^2\theta_0\frac{\sin^2\alpha}{1-\sin^2\alpha} + \left(\frac{\gamma-1}{\gamma+1}\right)^2\tan^2\theta_0\frac{\sin^4\alpha}{(1-\sin^2\alpha)^2}$$

$$\frac{4}{(\gamma+1)^2}\left[\sin^2\alpha - \sin^4\alpha\right] = \tan^2\theta_0\left[1 - 2\sin^2\alpha + \sin^4\alpha\right] + 2\frac{\gamma-1}{\gamma+1}\tan^2\theta_0\sin^2\alpha$$

$$+ \left(\frac{\gamma-1}{\gamma+1}\right)^2\tan^2\theta_0\sin^4\alpha$$

$$\left[1 - \frac{2}{\gamma+1}\tan^2\theta_0 + \frac{4}{(\gamma+1)^2}\sin^4\alpha + \left(2\frac{\gamma-1}{\gamma+1} - 2\right)\tan^2\theta_0 - \frac{\gamma-1}{\gamma+1}\sin^2\alpha\right.$$

$$\left. + \tan^2\theta_0 = 0\right.$$

$$\left(\frac{2}{\gamma+1}\right)^2(\tan^2\theta_0+1)\sin^4\alpha - 2\frac{2}{\gamma+1}\left[\tan^2\theta_0 + \frac{1}{\gamma+1}\right]\sin^2\alpha + \tan^2\theta_0 = 0$$

$$(\tan^2\theta_0+1)\sin^4\alpha - 2\left(\frac{\gamma+1}{2}\right)\left[\tan^2\theta_0 + \frac{1}{\gamma+1}\right]\sin^2\alpha + \left(\frac{\gamma+1}{2}\right)^2\tan^2\theta_0 = 0$$

$$\sin^2\alpha = \cos^2\theta_0\left[\frac{\gamma+1}{2}\tan^2\theta_0 + 1 - \sqrt{\tan^2\theta_0 + \gamma\tan^2\theta_0 + 1 - \left(\frac{\gamma+1}{2}\right)^2\tan^2\theta_0 - \left(\frac{\gamma+1}{2}\right)^2\tan^2\theta_0}\right]$$

$$= \cos^2\theta_0\left[\frac{\gamma+1}{2}\tan^2\theta_0 + \frac{1}{2} - \sqrt{\frac{1}{4} - \frac{\gamma^2-1}{4}\tan^2\theta_0}\right]$$

$$= \frac{1}{2}\cos^2\theta_0\left[(\gamma+1)\tan^2\theta_0 + 1 - \sqrt{1-(\gamma^2-1)\tan^2\theta_0}\right]$$

$$\frac{1}{2}\cos^2\theta_0\left[\cdots\tan^2\theta_0 + 1 - 1 + \frac{\gamma^2-1}{2}\tan^2\theta_0 + \frac{1}{8}(\gamma^2-1)^2\tan^4\theta_0 - \cdots\right]$$

$$\sin^2\alpha = \left(\frac{\gamma+1}{2}\right)^2\sin^2\theta_0 + \frac{1}{16}(\gamma^2-1)^2\sin^2\theta_0\cdot\tan^2\theta_0 - \cdots$$

$$\sin\theta_0 = \theta_0\left(1 - \frac{1}{6}\theta_0^2 - \cdots\right)$$

$$\sin^2\theta_0 = \theta_0^2\left(1 - \frac{1}{3}\theta_0^2 - \cdots\right),$$

$$\sin^2\alpha = \left(\gamma\frac{M^2+1}{2}\right)^2\left[\theta_0^2\left(1-\frac{1}{3}\theta_0^2-\cdots\right)+\frac{1}{4}(\gamma-1)^2\theta_0^4-\cdots\right]$$

$$\boxed{\sin^2\alpha = \left(\gamma\frac{M^2+1}{2}\right)^2\theta_0^2\left[1-\left|\frac{1}{3}-\left(\frac{M^2-1}{2}\right)^2\right|\theta_0^2-\cdots\right]}$$

$$\frac{1}{M_2^2} = \frac{\gamma(\gamma-1)}{2}\theta_0^2\left[1-\left\{\frac{1}{3}-\left(\frac{M^2+1}{2}\right)^2\right\}\theta_0^2-\cdots\right]\left[1+\gamma\theta_0^2-\cdots\right]$$

$$\frac{1}{M_2^2} = \frac{\gamma(\gamma-1)}{2}\theta_0^2\left[1+\left|\gamma+\left(\frac{M^2-1}{2}\right)^2-\frac{1}{3}\right|\theta_0^2-\cdots\right]$$

$$\frac{1}{M_1^2} = \gamma\frac{\gamma-1}{2}\left[1+\frac{1}{3}\gamma+\gamma^2-\frac{1}{4}\theta_0^2-\cdots\right]$$

$$\theta_0 - \theta = \sqrt{\frac{2}{\gamma-1}}\,\theta_0\left[1+\frac{1}{2}\left\{\gamma+1\left(\frac{\gamma-1}{2}\right)^2-\frac{1}{3}\right\}\theta_0^2-\cdots\right]$$

$$\left[1-\left\{\frac{1}{2}\,\frac{\gamma-1}{\gamma}\left(1+\frac{\gamma}{4}\right)-\frac{\gamma+3}{3}+2\left(\frac{1}{2}\,\frac{\gamma-1}{\gamma}-\frac{3-\gamma}{3}\left(\frac{1}{2}\right)\right.\right.\right.$$

[illegible]

$$\theta - \theta_0 = \sqrt{\frac{2}{\gamma-1}}\,\theta_0\left[\left(1-\left(\frac{1}{2}\right)\right)^{\frac{\gamma-1}{2\gamma}}\right.$$

[illegible]

[illegible]

$$-\theta = \sqrt{\frac{2}{\gamma-1}}\,\theta_0\left[1+\left\{\frac{1}{2}\left[\gamma+1\left(\frac{\gamma-1}{2}\right)^2-\frac{1}{3}\right]-\frac{\gamma(\gamma+1)}{12}\right\}\theta_0^2-\cdots\right]-\theta_0$$

$$\sim\left(\sqrt{\frac{2}{\gamma-1}}-1\right)\theta_0 \qquad \text{и} \quad \gamma=1.405, \quad \sqrt{\frac{2}{\gamma-1}}-1=1632$$

Two-Dimensional Flow

The general differential equation is

$$a_0^2 = a^2 + \frac{\gamma-1}{2}\left[u^2 + 2u\frac{\partial\varphi}{\partial x} + \left(\frac{\partial\varphi}{\partial x}\right)^2 + \left(\frac{\partial\varphi}{\partial y}\right)^2\right]$$

$$a^{*2} = a_0^2 - \frac{\gamma-1}{2}u^2 \qquad a_0^2 = a^{*2} + \frac{\gamma-1}{2}u^2$$

$$a^2 = a^{*2} + \frac{\gamma-1}{2}u^2 - \frac{\gamma-1}{2}\left[u^2 + 2u\frac{\partial\varphi}{\partial x} + \left(\frac{\partial\varphi}{\partial x}\right)^2 + \left(\frac{\partial\varphi}{\partial y}\right)^2\right]$$

$$\frac{u^2}{a^2} = \frac{u^2 + 2u\frac{\partial\varphi}{\partial x} + \left(\frac{\partial\varphi}{\partial x}\right)^2}{a^{*2}\left[1 - \frac{\gamma-1}{2}\left(2M^*\frac{1}{a^*}\frac{\partial\varphi}{\partial x} + \frac{1}{a^{*2}}\left(\frac{\partial\varphi}{\partial x}\right)^2 + \frac{1}{a^{*2}}\left(\frac{\partial\varphi}{\partial y}\right)^2\right)\right]}$$

$$\frac{M^2 + 2M^*\frac{1}{a^*}\frac{\partial\varphi}{\partial x}}{1 - (\gamma-1)M^*\frac{1}{a^*}\frac{\partial\varphi}{\partial x} - \frac{\gamma-1}{2}\frac{1}{a^{*2}}\left(\frac{\partial\varphi}{\partial y}\right)}$$

Transform the differential equation becomes

$$+\left[(1-(\gamma-1)M^2)\frac{1}{a^2}\frac{\partial\phi}{\partial x}-\frac{\gamma+1}{2}\frac{1}{a^2}\left(\frac{\partial\phi}{\partial y}\right)^2-\frac{1}{a^2}\left(\frac{\partial\phi}{\partial z}\right)^2\right]\frac{\partial^2\phi}{\partial y^2}=0$$

$$+\left[1-(\gamma-1)M^2\frac{1}{a^2}\frac{\partial\phi}{\partial x}-\frac{\gamma+1}{2}\frac{1}{a^2}\left(\frac{\partial\phi}{\partial y}\right)^2\right]\frac{\partial^2\phi}{\partial y^2}=0$$

Let $y=a^2b\frac{1}{M^2}f(\xi,\eta)$

$$x=b\xi$$

$$y=b\eta\left(\frac{f}{b}\right)^n$$

Boundary conditions, at ∞, $\frac{\partial f}{\partial\xi}=\frac{\partial f}{\partial\eta}=0$

at $\eta=0$, $\left(\frac{\partial^2 f}{\partial\eta^2}\right)_{\eta=0}=a^2M$

at $\eta=0$, $a^2b\frac{1}{M^2}\left(\frac{\partial f}{\partial\eta}\right)_{\eta=0}\frac{1}{b}\frac{1}{\left(\frac{f}{b}\right)^n}=a^2\left(M^2\frac{f}{b}\right)(\xi,\eta)$

or $\left(\frac{\partial f}{\partial\eta}\right)_{\eta=0}=\left[M^2\left(\frac{f}{b}\right)\right]\left[M^2\left(\frac{f}{b}\right)^n\right](\xi,\eta)$

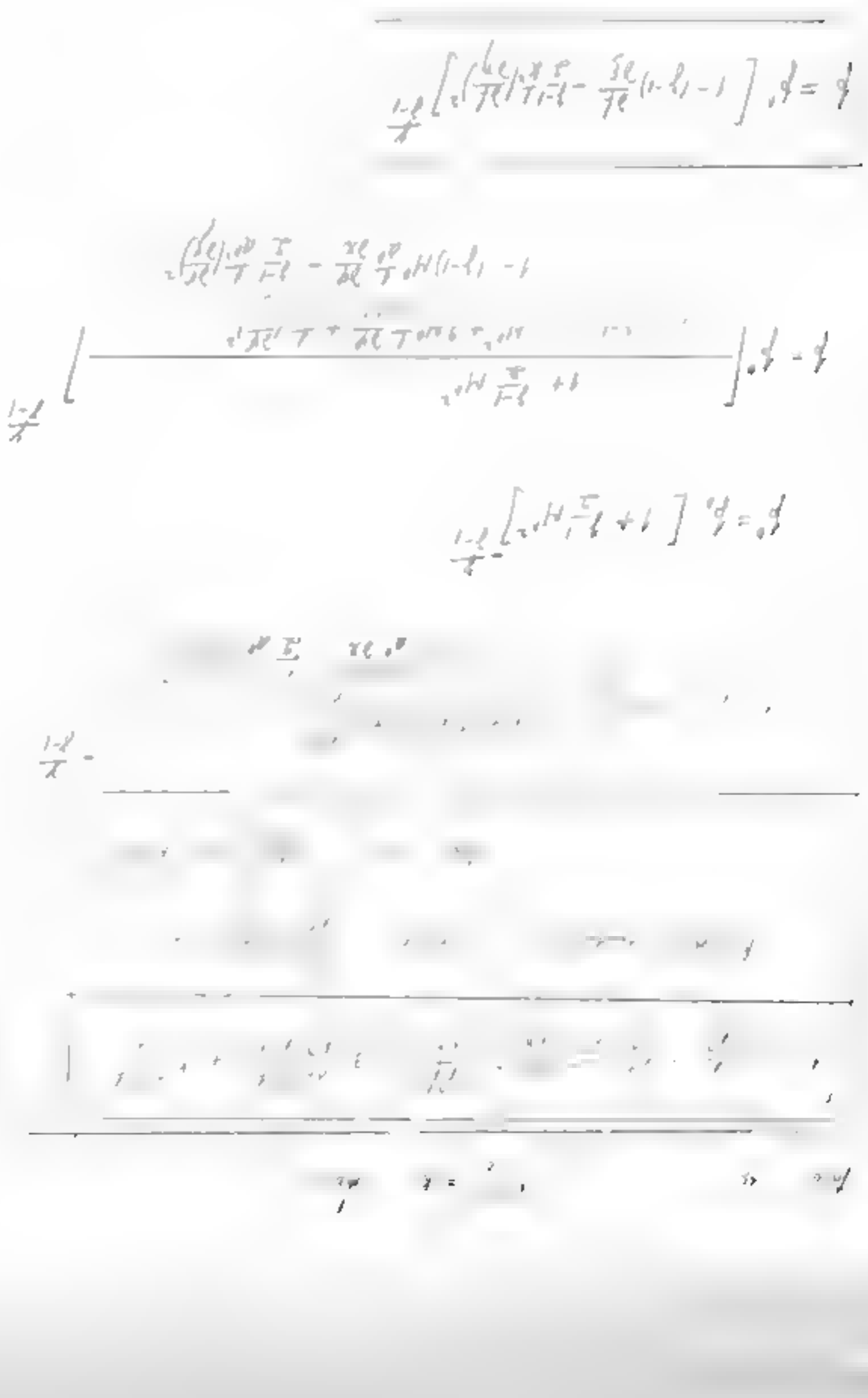

$$C_L = \frac{D}{\quad} = \frac{D}{\quad} = \frac{\quad}{\quad}$$

$$C_D = \frac{1}{M^{*3}} \mathcal{D}(M^* \tfrac{x}{b})$$

$$C_L = \frac{1}{M^{*2}} \mathcal{L}(M^* \tfrac{x}{b})$$

Clearly symmetric flows

$$+ \left[(1-\gamma) M^{*2} \frac{1}{a^*} \frac{\partial \varphi}{\partial x} - \frac{\gamma-1}{2} \frac{1}{a^{*4}} \left(\frac{\partial \varphi}{\partial y}\right)^2 \right] \frac{1}{y} \frac{\partial \varphi}{\partial y}$$

Boundary conditions, at ∞,

At $y=0$, $\left(v = \frac{\partial \varphi}{\partial y}\right)_{y=0} = a^* M^* f'(s)$

$$- 2 \frac{\partial \varphi}{\partial y} \frac{\partial^2 \varphi}{\partial x \partial y} + \left[M^* \left(\frac{1}{a^*}\right)^2 \right] \frac{\partial^2 \varphi}{\partial y^2}$$

Section 3

Application of Tschaplygin's Transformation to Two Dimensional Subsonic Flow

PART (III)

Application of Tschaplygin's Transformation to Two Dimensional Subsonic Flow

in case of ~~two~~ bodies where direction accor

process is very tedious and the method ~~is~~ not

circular function. The chief disa

or the hodographic plane

In the first section, the general theory [illegible]
[illegible] second section the theory [illegible]
[illegible] [illegible]

Section (I)

If p is the pressure and v is the density of gas, the adiabatic process is expressed as a

[illegible]

tangent at this point. The equation of the tangent at this point can be written as

$$p_1 - p = C(v_1 - v_0) = C\left(\rho_1^{-1} - \rho_0^{-1}\right) \qquad (31)$$

where ρ is the density of the gas. Now the slope

[illegible]

Therefore $C = -a_1^2 \rho_1^2$

Hence the approximate p-ρ relation near p_1, ρ_1 can be written as

$$p_1 - p = a_1^2 \rho_1^2 \left(\frac{1}{\rho} - \frac{1}{\rho_1}\right) \qquad (32)$$

integrate, the following relation is obtained

Here if $w_3 = 0$, $w_2 = w$, $\rho_3 = \rho_0$ and $\rho_2 = \rho$, then

(a)

increase

on Eq. (13.7), the ratio

ratio will increase. But

(4 1.7) and # 3.8) the upper limit is for the $\frac{E}{}$

$$\left(\frac{w'}{w}\right)_{max} = \frac{1}{\frac{w}{a}+1}\sqrt{\frac{\frac{E}{}}{\frac{E}{}+1}\left(\frac{E}{}+1\right)^2\left(\frac{}{}+1\right)}$$

In the factor $i^2 = \gamma\frac{E}{e}$ the ratio

to

$$\left(\frac{w'}{w}\right)_{max} = \frac{1}{\frac{w}{a}+1}\sqrt{\frac{}{}\left(\frac{}{}+1\right)^2\left(\frac{}{}+1\right)}$$

The values of $\left(\frac{w'}{w}\right)_{max}$ for different values of $\frac{}{}$ are shown Table 3 1

Table

	0.7	75
	24	
	12	
	9	

It is plain also that for small fractional values of the theory will approximate to the Newtonian due to large deviations from the character known at higher velocities until finally, when the ratio $\frac{E}{}$ is

or $$\left|\frac{s}{s_0}\right| = \sqrt{1 - \frac{\omega^2}{a^2}} \qquad (37)$$

Furthermore, from Eq. (36), $s_1^2 a_1^2 = s_1^2 a_0^2$, thus Eq (3.7) can also be written as

(3 8)

Now if the flow is irrotational, there exists a velocity potential Φ such that

$$\frac{\partial \Phi}{\partial x} = u, \quad \frac{\partial \Phi}{\partial y} = v \qquad (39)$$

x & y components of the velocity w

Now if the angle of inclination of the velocity w to the

$$d\phi = w \cos\beta \, dx + w \sin\beta \, dy \qquad (3\,11)$$

$$\left.\begin{aligned} dx &= \frac{\cos\beta}{w} d\phi - \frac{\sin\beta}{w} \frac{s_0}{s} d\psi \\ dy &= \frac{\sin\beta}{w} d\phi + \frac{\cos\beta}{w} \frac{s_0}{s} d\psi \end{aligned}\right\} \qquad (3\,12)$$

[illegible] (4)

[illegible]

$$d\phi = \phi'_w\, dw + \phi'_\beta\, d\beta \qquad (3\,13)$$
$$d\psi = \psi'_w\, dw + \psi'_\beta\, d\beta$$

[illegible]

[illegible]

(3.16)

Using Eq. (3.7), Eqn (3.16) becomes

[illegible]

(3.17)

[illegible]

new variable to be introduced.

[illegible]

Then Eq (3.18) becomes

[illegible]

[illegible] a new variable W is used instead [illegible]

such that

$$W = a_0 e^{-} \qquad (3.20)$$

On by integrating Eq (3.19),

$$W = \frac{2a_0 w}{\sqrt{a_0^2 + w^2} + a_0} \qquad (3.21)$$

Hence by inversion

$$w = \frac{4a_0^2 W}{4a_0^2 - W^2}$$

[illegible] into Eq. (3.8)

$$\frac{4a_0^2 + W^2}{4a_0^2 - W^2}$$

$$\cos\beta\frac{\partial\psi}{\partial u}+\sin\beta\frac{\partial\psi}{\partial v}$$

$$\phi+i\psi=F(u-iv)=F(\bar{w})$$

$$\phi-i\psi=\bar{F}(u+iv)=\bar{F}(w) \qquad (3.26)$$

[illegible]

one equation by means of Eq. (326). Thus

$$dz = dx + i dy = \frac{dF}{W} - \frac{W \cdot d\bar{F}}{4a_0^2} \qquad (327)$$

[illegible]

(II) Now let $F = W_1 G(\zeta)$, where W_1 is the [illegible]

[illegible]

(III) Using the above value of F, Eq (327) can be written as

$$dz = d\zeta - \frac{1}{4}\left(\frac{W_1}{a_0}\right)^2 \left(\frac{d\bar{E}}{d\bar{\zeta}}\right)^2 d\bar{\zeta} \qquad (328)$$

of incompressible flow. The factor before the integral depends only on the Mach number of the undisturbed flow only. By using

$$\frac{1}{4}\left(\frac{W_1}{a_0}\right)^2 = \frac{\left(\frac{aW_1}{a_1}\right)^2}{1 + \frac{\gamma-1}{2}\left(\frac{W_1}{a_1}\right)^2} \qquad (3.9,1)$$

Eq (3.98) is

By means of Eqn. (3.29)

$$\frac{W}{W_1} = \frac{\frac{|W|}{W_1}}{\frac{W_0}{W_1}\left[1 - \frac{1}{4}\left(\frac{W_1}{a_0}\right)^2\left(\frac{|W|}{W_1}\right)^2\right]}$$

Thus by putting $w = w_1$, one obtains

$$\frac{W_1}{W_1} = \frac{1}{1 - \frac{1}{4}\left(\frac{W_1}{a_0}\right)^2}$$

Thus

$$\frac{w}{w_1} = 1 + \frac{1}{4}\frac{W_1^2}{a_1^2} \cdot \frac{\frac{2W_1}{W_1}}{1 - \frac{1}{4}\left(\frac{W_1}{a_0}\right)^2\left(\frac{2W_1}{W_1}\right)^2} \qquad (3\,31)$$

Using Eqns. 3 30 and 3 29) the ratio $\frac{w}{w_1}$ can be calculated easily.

17 To determine the pressure acting on the surface of the body one has to use Eq. 3 (3) with some manipulation the following relation is obtained

$$\frac{p - p_0}{\frac{\rho}{2}a^2} = \frac{1}{\frac{w_1^2}{a^2}}\left[1 - \left(\frac{w}{w_1}\right)^2\right]$$

$$= \frac{1}{2}\left[1 - \left(\frac{w}{w_1}\right)^2\right]$$

Thus finally

$$\frac{S_0}{S} = \sqrt{1 + \left(\frac{w}{w_1}\right)^2\left(\frac{W_1}{a_0}\right)^2}$$

$$= \sqrt{1 + \frac{1}{4}\left(\frac{W_1}{a_0}\right)^2\left(\frac{2W_1}{W_1}\right)^2} \qquad (3\,31)$$

Finally

$$= \frac{1}{2}\left[1 - \sqrt{1 + \left(\frac{w}{w_1}\right)^2 \cdot \left(\frac{W_1}{a_0}\right)^2}\right] \qquad (3\,32)$$

Section II

In this section the general theory developed in Section I is applied to the simple case of flow over a symmetrical Joukowsky airfoil at zero angle of attack. The complex potential in the circle-plane (see Fig 3.2) is known to be

$$w_1 = \left\{(\mu - b) + \frac{a^2}{\mu - b}\right\} \qquad (3.33)$$

where a = radius of the circle, b = eccentricity of the circle, and the relation between the circle plane and circle plane is the well known Joukowsky transformation

$$\zeta = \mu + \frac{1}{\mu} \qquad (3.34)$$

If the radius of the transforming circle is unity, in the starting form of the calculation is the function Φ to be found $\Phi(\bar{z})$ and

$$W = \frac{d\Phi}{d\bar{z}} = \frac{d\Phi}{d\mu}\frac{d\mu}{d\bar{z}} = \frac{\frac{d\Phi}{d\mu}}{\frac{d\bar{z}}{d\mu}} \qquad (3.35)$$

Transformation $\zeta = \mu + \frac{r^2}{\mu}$ [illegible]

From the expression term in Eqn (3.28) we

$$\frac{1}{2\pi i}\oint \frac{W}{z}\,dz = \frac{1}{2\pi i}\oint \frac{W^2}{z}\,dz + I_2 + I_3 \qquad (3.35)$$

$$\dots \left(- \frac{\dots}{\dots} + \frac{a^{k}}{\mu - b^{k}} \right) d\mu$$

$$\dots \left(- \frac{\dots}{\dots} + \frac{a^{k}}{\mu - b^{k}} \right) \frac{d\mu}{\mu - 1}$$

$$\dots \left(\frac{\dots}{\dots} + \frac{a^{k}}{\mu - b^{k}} \right) \frac{d\mu}{\mu + 1}$$

These integrals can be easily computed & simplified noting that $a - \dots$, $\dots \bar{\mu} \dots$ $a e^{i\theta}$ and $\lambda = \frac{a}{b}$

$$I_1 = a \left\{ e^{i\theta} + \lambda e^{-i\theta} - \frac{1}{3} e^{-i3\theta} \right\} \qquad (36)$$

$$I_2 = \frac{1}{2} \left\{ \frac{1}{6} - e^{-i\theta} + \frac{1}{2} e^{-2i\theta} + \frac{1}{3} e^{-3i\theta} + \log(a e^{i\theta}) \right\}$$

$$= \left(\dots \right) \log a e^{i\theta} - \frac{1}{4} + \lambda^{2} \left(\frac{1}{2} - 1 \right) \log a \dots$$

$$+ \lambda^{3} (1 - \lambda^{2}) e^{-i\theta} + \frac{\lambda^{2}}{2} e^{-2i\theta} - \frac{\lambda}{3} e^{-3i\theta} \Bigg\}$$

[illegible] the real and imaginary parts and after

$$\mathrm{Re}\,(I_1 + I_2 - I_3) = a \left(3\cos\theta - \frac{1}{3}\cos 3\theta \right)$$

$$+ \frac{1}{2} \left[\dots \log \left(\dots \right) + \lambda^{3} \dots \right]$$

$$+ \frac{1}{2} (1 - \lambda^{2}) \cos 2\theta + \frac{1}{3} (1 + \lambda) \cos 3\theta \Bigg\} \qquad (37)$$

$$\mathrm{Im}\,(I_1 + I_2 - I_3) = a \left(-\sin\theta + \frac{1}{3}\sin 3\theta \right)$$

$$+ \frac{1}{2} \left[\dots \lambda^{2} \sin 2\theta - \frac{1}{3} (1 + \lambda) \sin 3\theta \right.$$

$$\left. - (1 - \lambda^{2})^{2} \tan^{-1} \frac{\sin\theta}{\cos\theta + \lambda} + (1 - \lambda^{2}) \theta \right\}$$

is neglected the second term is a second order quantity

The determination of harmonic conjugates can be carried out by using the method developed by von Seggern and Tuttle [ref] The same practical means the Seggern Tuttle method is somewhat modified.

[illegible]

[illegible]

[illegible]

[illegible]

$$\text{Since } \zeta_1 = \zeta_2 \left[1 + f(\zeta_2)\right] \qquad (39)$$

where $\zeta_1 = \zeta_2$ have their origin at the center O and the ~~or~~ absolute value $|f(\zeta_2)|$ is small compared with 1

Then it is shown ~~that~~ (Ref. 7)" that

$$g(\theta) + \mathrm{Re.}\,[f(\zeta_2)] = 0. \qquad (340)$$

To In order to calculate $f(\zeta_2)$ we develope the function $g(\theta)$ in a Fourier series.

$$g(\theta) = \sum_0^\infty a_n \cos n\theta \qquad (341)$$

There only cosine terms appear because the origin is symmetrical with the chord. On the other hand the complex function $f(\zeta_2)$ has the form for $|\zeta_2| > 1$

$$f(\zeta_2) = \sum_0^\infty \frac{c_n}{\zeta_2^n} \qquad (342)$$

In fact $\zeta_2 = \infty$ then 340 is satisfied by

$$c_n = -a_n$$

Then
$$f(\zeta_2) = -\sum_0^\infty \frac{a_n}{\zeta_2^n} \qquad (343)$$

It can be easily seen that the velocity ~~at the~~ across the trailing edge is proportional to the circulation

$$w = w_J \left|\frac{d\zeta_1}{d\zeta_2}\right| \qquad (344)$$

where w_J = velocity around the Joukowsky airfoil

Now from Eqs (3 39) and (3 43)

$$\frac{1}{\rho} = \frac{1}{r} + \sum_{0}^{\infty} \frac{n^2 a_n}{r^{n+1}} = \frac{1}{r} + \sum_{0}^{\infty} \frac{n^2 a_n}{r^{n+1}} \cos n\theta$$

$$= \frac{1}{r} + \sum_{0}^{\infty} n a_n \cos n\theta - \sum_{0}^{\infty} a_n \cos n\theta$$

$$= 1 + \sum_{0}^{\infty} n a_n \cos n\theta - \sum_{0}^{\infty} a_n \cos n\theta$$

$$= 1 + \frac{1}{2\pi} \sum_{0}^{\infty} a_n \sin n\theta - g(\theta) \qquad \text{Eq (3 45)}$$

[illegible]

(346)

Integrating by parts, the integral

$$\frac{1}{2\pi}\int_0^{2\pi} g(\theta+\xi)+g(\theta-\xi)\,\cos n\theta\,d\theta + \frac{1}{2\pi}\int_0^{2\pi}\frac{g(\theta+\xi)+g(\theta-\xi)}{\tan\frac{\xi}{2}}\sin n\theta\,d\theta$$

$$\frac{1}{\pi}\int_0^{\pi} g(\theta+\xi)+g(\theta-\xi)\,\cos n\theta\,d\theta + \frac{1}{\pi}\int_0^{\pi}\frac{g(\theta+\xi)+g(\theta-\xi)}{2(1-\cos\xi)}\sin n\theta\,d\theta$$

Hence Since Eq (345) can be written as

$$\frac{1}{\pi}\int_0^{\pi}\frac{g(\theta+\xi)+g(\theta-\xi)}{2(1-\cos\xi)}\sin n\theta\,d\theta \qquad (346)$$

The integral is evaluated by numerically integrating the function $g(\theta)$ because then the [illegible] is known [illegible]

[illegible] the results of calculations for a [illegible] with the thickness parameter b [illegible] at two speeds [illegible] are given in the author's [illegible] speaks of considerably higher wall heights and [illegible] Also the [illegible] because tanks tend to have [illegible] with increasing speed [illegible] are in agreement with the experimental results of

shown by J Stack (Ref 3) ~~the computed~~ [illegible] The values of $\frac{t-l}{\frac{1}{2}\rho u^2}$ [illegible]
which a ~~wave~~ can will attain a velocity ~~of~~ equal
to the local sound velocity. It is thus seen
that the effect of compressibility on pressure
distribution is appreciable even ~~at~~ ~~speed~~ when
no shock the local sonic velocity is reached.
One should however bear in mind that the effect
on the free settlement of the airfoil will not
be so marked as with the pressure distribution.
because, the free is the algebraic difference of pressure
free stream & the sides of the section

Appendix to PART (III)

Comparison with Other Methods

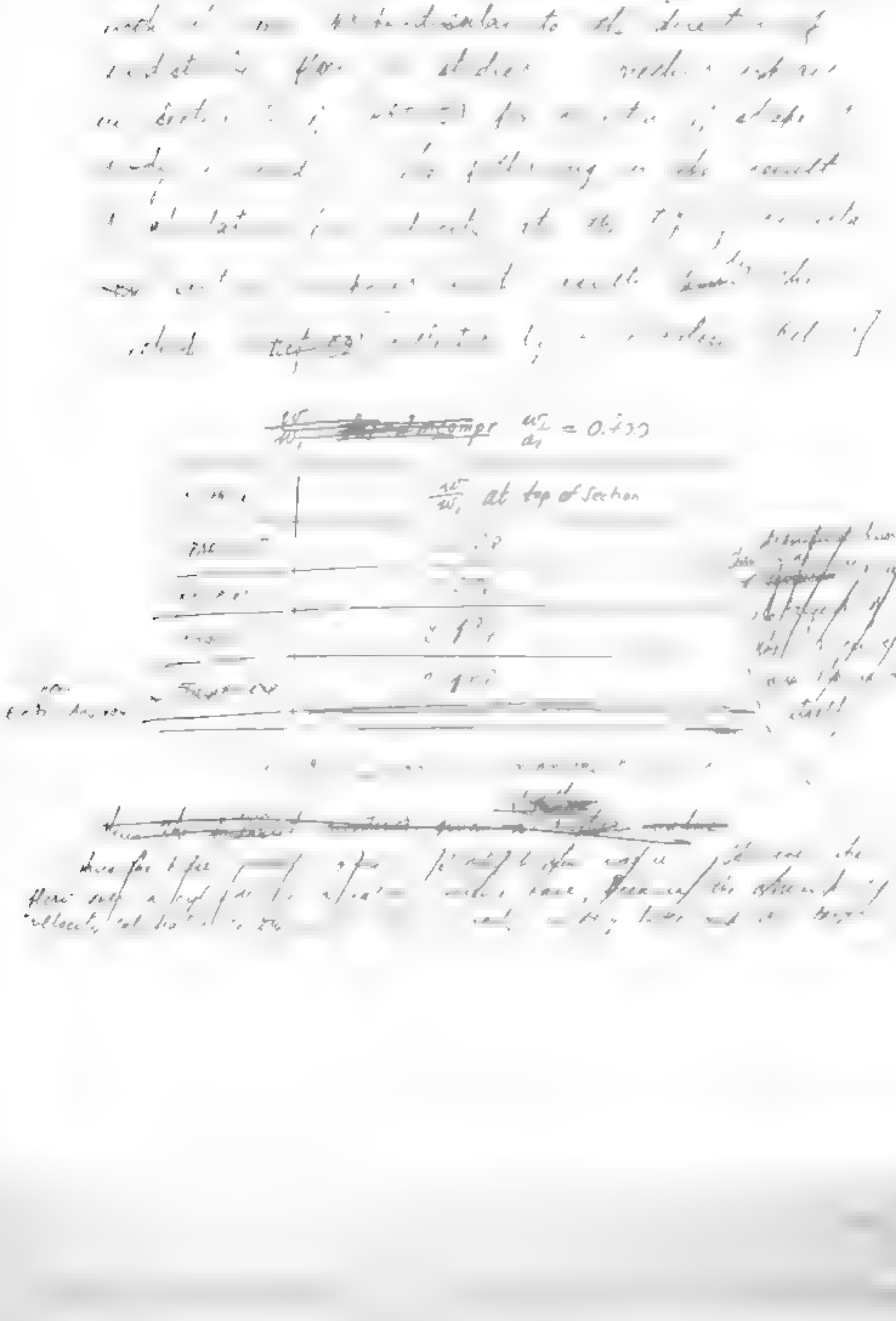

thus the present method gives a [illegible] higher value [illegible]
however the flow over a cylinder is rather an exception
this because the difference between
to be calculated and the undisturbed velocity
large and this [illegible]

References on PART (II)

Annahme eines Geschwindigkeitspotentials
Arch. d. Mathem. u. Phys, Grunert Hoppe (1890), Reihe 2,
Bd 9 S 157

Two Methods of Solving the Equations for the Flow of a Compressible

Comptes Rendus Vol 194, p. 1218 (1932)

Also Variation de la résistance aux faibles vitesses sous l'influence
de la compressibilité Comptes Rendus Vol 194, p. 1220 (1932)

(5) A Busemann Die Expansionsberichtigung der Kontraktionsziffer von
Blenden Forschung Bd 6, S 186-187 (1935)

Also Hodographenmethode der Gasdynamik ZAMM Bd 12, S 73-79 (1932)

(6) W F Durand Aerodynamic Theory Vol 2, p 21-24 1st Edition,
Julius Springer, Berlin (1935)

(7) Th. von Kármán, E Trefftz: Potentialströmung um

Proc. of London Math Soc. (2) Vol. 24, pp 241-246 (1925)

(9) J Stack. The Compressible Bubble

[See back side]

(10) E. Pistolesi: La portanza alle alte velocità (Portanza a alte velocità)

Atti del V Convegno "Volta", fasc 300, (1936)
Reale Accademia d'Italia, Rome

Section 4

Report on the Present State of Theory of Thin Plate and Cylindrical Shells in Compression

Report on the Present State of Theory of Thin Plates and Cylindrical Shells in Compression

H.S Tsien

References

(I) General Theory

(2) K Marguerre

ZAMM 14. 57-73 (1938)

(6) T E Schmidt

RM 1465 (1932)

Trans ASME 56 · 795-806 (1934)

(III) Conical shell without [illegible]
[illegible]

Ing.-Arch. 8 151-172 (1937)

(II) Uffened Cylindrical Shell

(9) [illegible]

H Wagner Einiges über schalen [illegible]

RM 1679 (1936)

TM 866

Punkten

4)
Hohlzylinder infolge axialer Belastung.
Ing-Arch 6: 334—337 (1935)

5) [illegible]
[illegible]
[illegible]
[illegible]
gerader Stäbe Der Bauingenieur 19: 499-505 (1938)

I.

fracture assumes the validity of Navier beam

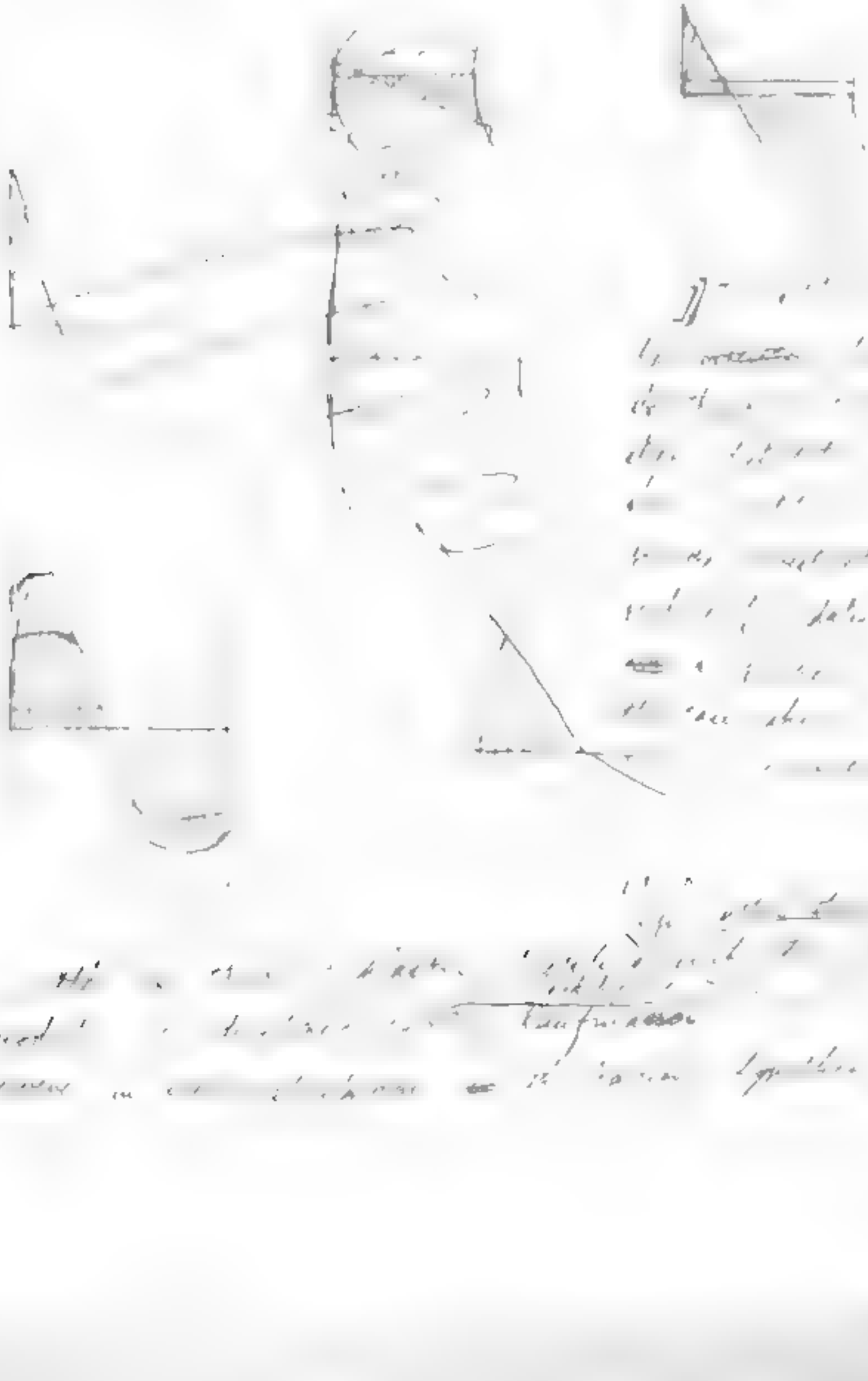

1) $\beta = \frac{2.5^\circ}{5\sqrt{3}} = 0.0436$, $\geq$ 0.0436

$\sin 4\alpha_1 \sqrt{\frac{L}{a}} = 3.46\sqrt{0.125} = 0.254$

retained. But due to the fact that only thick plate I sheets
fail in plastic buckling it seems necessary to combine them
[illegible] ground. They (1) to give a
[illegible]

[illegible]

Plate

[illegible]

= Shells of Revolution

[illegible] 1) [illegible] 2) [illegible] 3) [illegible] 4) W Flügge 5) W Flügge

[illegible] the end conditions more [illegible]

[illegible] pure no metallic [illegible] 9)
[illegible] gradually grow deeper and deeper
[illegible] welding. But if the element
[illegible] the cylinders fail to sudden
[illegible] accompanied by the emission [illegible]
[illegible] metallic [illegible]
[illegible] W. Hugo and later [illegible]
Dannel (7) also introduced the [illegible]
[illegible] of the specimen [illegible]
[illegible] "Volland" [illegible]
[illegible]
[illegible] could [illegible]
[illegible]
[illegible] for at least the [illegible]
[illegible]
[illegible]

[illegible] a natural [illegible]
[illegible] this shell, originally developed by
[illegible]
[illegible]
[illegible]

V

especially for large curvatures. However, a more

shall

For almost all cases, the second method

for large deflections

terms, the extremum condition is not linear.

each load condition. ∴ To decide which is

the true minimum, one has to use the second variation

equilibrium differential equations
used by K Magnuson (15) and L.H Donnel (17) have
to be critically examined in the case of
small deflection which is no longer true in the

Section 5

The Buckling of Thin Cylindrical Shells under Axial Compression

THE BUCKLING OF CYLINDRICAL SHELLS UNDER

Th. von Karman and Hsue-shen Tsien
Guggenheim Aeronautical Laboratory, California Institute of Technology

In two previous papers (Ref.1 and Ref.2), the authors have discussed in detail the inadequacy of the classical theory of thin shells in explaining the buckling phenomenon of ~~both~~ cylindrical ~~shells~~ and ~~the~~ spherical shells. It was shown that not only the calculated buckling load is 4 to 5 times higher than that experimentally observed, but the buckling wave pattern found is also different from that predicted. It was pointed out, furthermore, that the different explainations for this discrepancy advanced by L.H. Donnell[1] and W.Flügge[4] are untenable when certain conclusions drawn from these explainations are compared with the experimental facts. The authors are then led by ~~both~~ the theoretical investigation on spherical shells (Ref.1) and a model exreriment (Ref.2) on 'thin columns with non-linear elastic support/to the belief that the buckling phenomenon of curved shells can only be explained by means of the non-linear large deflection theory.

to keep the shell in equilibri

buckle. This characteristic of dropping load shows, first

buckling has started, and thus explains the observed rapidity

of the buckling process. Furthermore, this characteristic also brings in the possibility of a decrease in the buckling load when there are slight imperfections in the test specimen or when there are vibrations during the testing process.

In this paper, the authors will show by means of an approximate calculation the dropping load characteristic of a uniform, thin cylindrical shell under axial compression. Consequently, they hope that they have thus offered an aceptable explaination of the observed facts.

Stresses in the Median Surface and the Expression for the Total Energy of the System

If u, v, and w (fig 1) are the displacement of a point on the median surface of the shell in the axial, x-direction, the circumferential, y-direction, and the radial direction, then the unit strains in the x and y directions, ε_x, ε_y and the unit shear γ_{xy} at a point in the median surface can be expressed in the following form, including terms

$$\varepsilon_x = \frac{\partial u}{\partial x} + \frac{1}{2}\left(\frac{\partial w}{\partial x}\right)^2$$

$$\varepsilon_y = \frac{\partial v}{\partial y} + \frac{1}{2}\left(\frac{\partial w}{\partial y}\right)^2 - \frac{w}{R} \qquad (1)$$

$$\gamma_{xy} = \frac{\partial u}{\partial y} + \frac{\partial v}{\partial x} + \left(\frac{\partial w}{\partial x}\frac{\partial w}{\partial y}\right),$$

where R is the radius of the undeformed median surface of the shell. The strain energy in the median surface of the shell is, known, as the following

expressed by the following equations in case of thin shells:

$$\left.\begin{aligned}\frac{\partial \sigma_x}{\partial x} + \frac{\partial \tau_{xy}}{\partial y} &= 0 \\ \frac{\partial \tau_{xy}}{\partial x} + \frac{\partial \sigma_y}{\partial y} &= 0\end{aligned}\right\} \quad (4)$$

introducing the well-known Airy stress function, F, defined by the relations

$$\sigma_x = \frac{\partial^2 F}{\partial y^2}, \qquad \tau_{xy} = -\frac{\partial^2 F}{\partial x \partial y}, \qquad \sigma_y = \frac{\partial^2 F}{\partial x^2}$$

Eliminating the variables u and v between Eqns. (3) and (5)

This equation is very similar to the large deflection equation for flat plate derived by the senior author. (Ref 5) L.H.Donnell (Ref; 3) first obtained this equation in its present form. With a given form of the radial deflection component of the displacement, Eq.(6) gives the induced stresses in the median surface of the shell. [illegible] extensional

[illegible]

$$[illegible] \quad (7)$$

where a and b are the half wave lengths in the axial and the circumferential direction respectively

[illegible]

necessary first to find the expressions for the change of curvatures and unit twist of the median surface. In [illegible] simplified expressions will be

$$\chi_x = \frac{\partial^2 w}{\partial x^2}, \qquad \chi_y = \frac{\partial^2 w}{\partial y^2}, \qquad \chi_{xy} = \frac{\partial^2 w}{\partial x \partial y} \qquad (8)$$

In Eq. (8), certain additional terms in χ_y and χ_{xy} involving v are neglected. It was shown by L.H.Donnell (Ref.8) [illegible] differ from the terms retained in Eq.(8) by a factor $1/n^2$, where n is the number of waves in the circumferential direction. For thin cylindrical shells, the value of n is usually around 10; therefore the neglection is justified. With these expressions for the change of the curvatures and the twist of the median surface, the bending

for one complete wave panel

can be obtained as

The lowering of the potential of the applied force on the end of the cylindrical shell can be calculated as the product of the change in length of the shell and the

The equilibrium condition of the shell is obtained by equating the first variation of the sum of energies, W_1, W_2 and W_3 to zero. In the following calculation, the Rayleigh-Ritz method or the energy method will be used by assuming a plausible form for the function w.

Calculation of the Total Energy

To obtain a plausible form for w, one has to resort to

It is known that

values of the wave amplitude, the waves are so-called diamond shaped. This particular wave shape can be approximately expressed by

$$\cos^2\frac{(mx+ny)}{2R}\cos^2\frac{(m'x-ny)}{2R} \qquad (11)$$

where the squares are introduced to account for the fact that the shell has a definite preference to buckle inward. Eq. (11)

can be rewritten as

[illegible]

On the other hand, the classical theory which is correct for infinitesimal values of the wave amplitude, requires the waves to be of the form

$$\cos\frac{n\pi x}{R}\cos\frac{n\pi y}{R} \tag{13}$$

In order to satisfy this requirement, the wave form assumed in the following calculations is of the

[illegible]

$$+\frac{1}{4}f_2\left[\cos\frac{2n\pi x}{R}+\cos\frac{2n\pi y}{R}\right]$$

where f_0, f_1, and f_2 are unknowns to be determined by conditions of minimum totel energy of the system. f_0 is introduced inorder to allow the shell to expand

[illegible] .(14) into Eq.(6), the differentia

equation for the Airy stress function F is obtained:

[illegible]

$$+B\cos\frac{2n\pi x}{R}\Big)$$

[illegible]

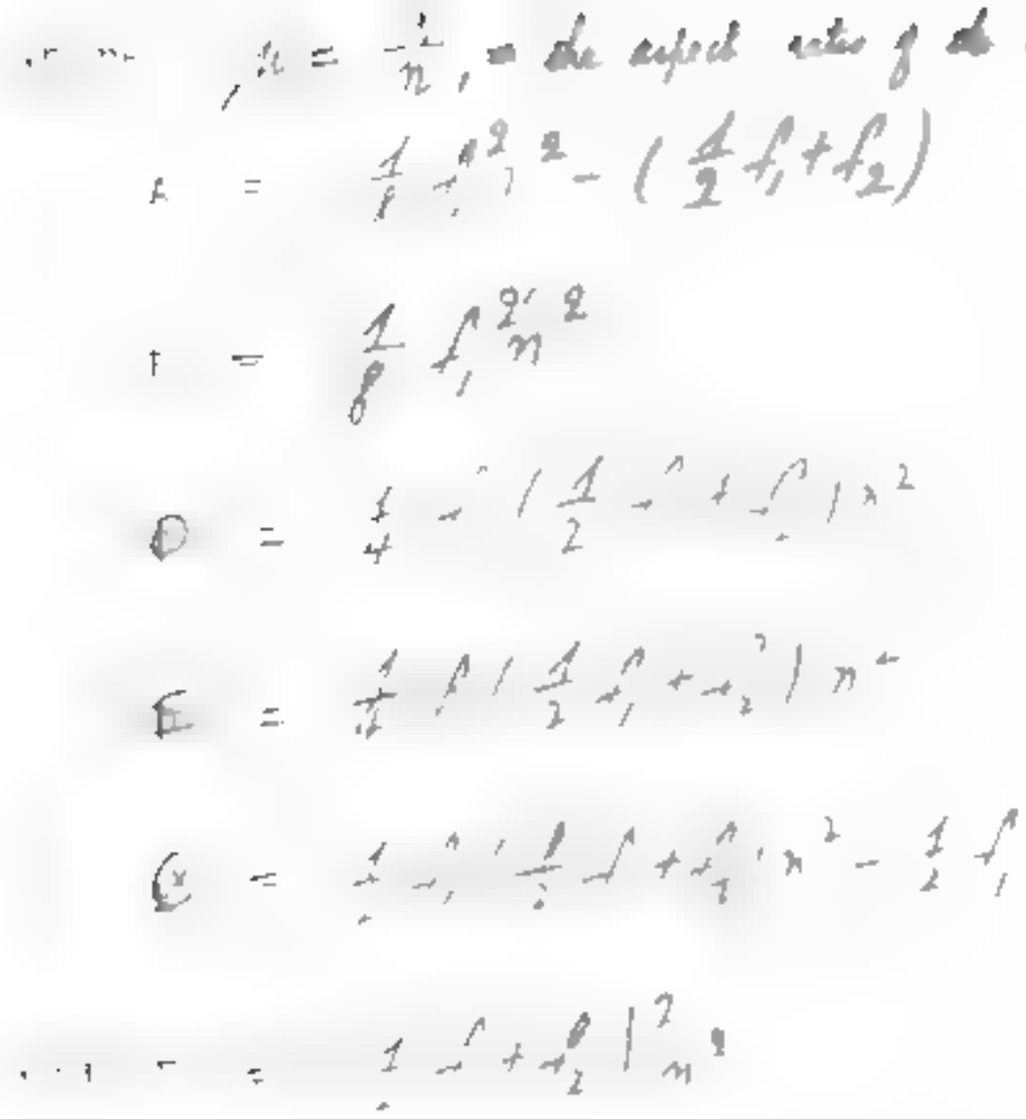

The solution of this differential equation can be easily obtained as

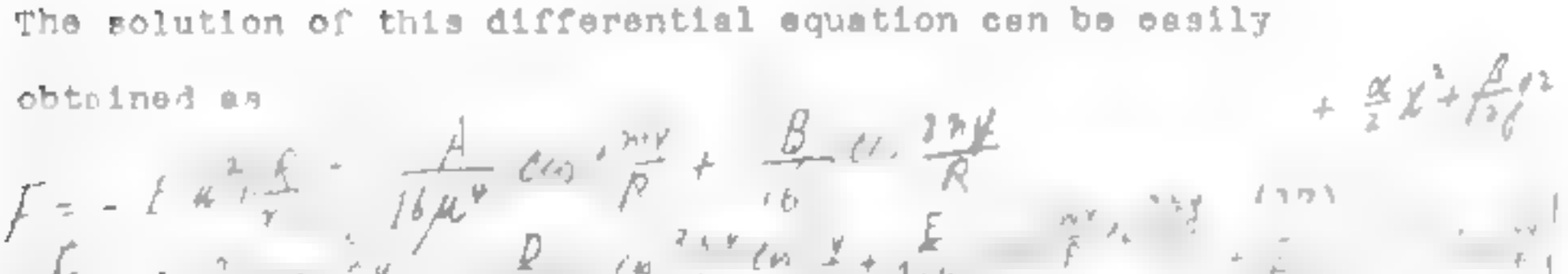

obtained as can be written as

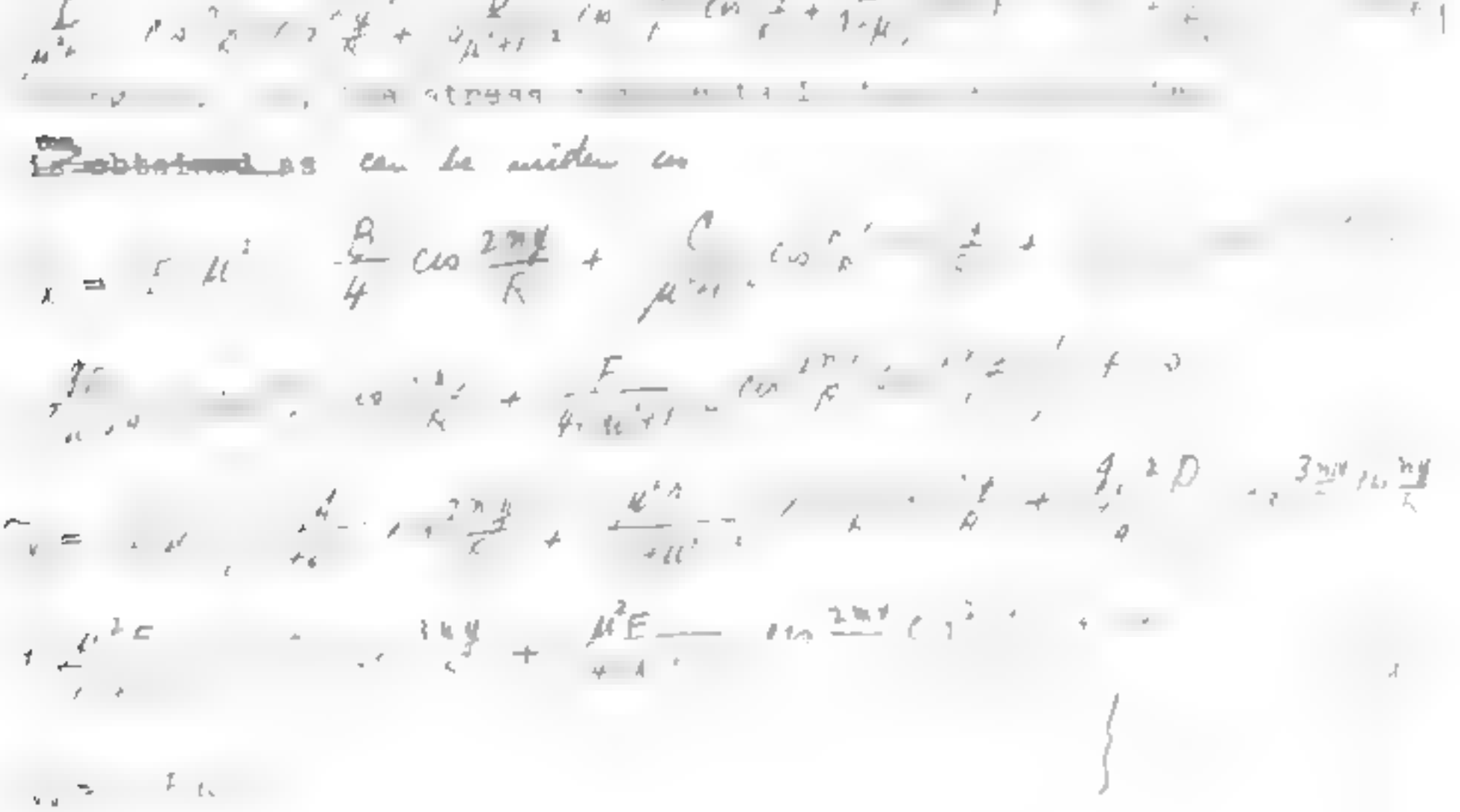

In all experimental results, the data is usually expressed in term of the average compression stress σ_A in the axial direction. It can be easily seen from Eq.(18) that

$$\beta = -\sigma \tag{19}$$

By ~~solving~~ Using Eq.(3), ~~and solving~~ for the following expressions for $\frac{\partial u}{\partial x}$ and $\frac{\partial v}{\partial y}$ can be obtained:

$$\frac{\partial u}{\partial x} = \frac{1}{E}(\sigma_x - \nu\sigma_y) - \frac{1}{2}\left(\frac{\partial w}{\partial x}\right)^2$$

$$\frac{\partial v}{\partial y} = \frac{1}{E}(\sigma_y - \nu\sigma_x) - \frac{1}{2}\left(\frac{\partial w}{\partial x}\right)^2 + \frac{w}{R}$$

By substituting Eqs.(14) and (18) into Eq.(20), it is found that

[illegible] cosine Term (21)

Since y-~~direction~~ measured is the circumferential direction, v must be a periodic function; therefore the constant term in $\frac{\partial v}{\partial y}$ must be equal to zero. ~~Thus~~ σ_x

This is the condition for the determination of α.

Using Eqs. (18) and (22), the extensional energy of the shell is obtained as

$$-\frac{W_1}{\frac{1}{2}Et\,ab} = 4\Big[(1-\nu^2)\Big(\frac{\pi}{E}\Big)^2 + n^4\Big\{\frac{3}{64}f_1^2 + \frac{1}{16}f_1f_2 + \frac{1}{16}f_2^2\Big\}^2$$

$$+ \Big(f_0 + \frac{1}{4}f_1\Big)^2 - 2n^2\Big\{\frac{3}{64}f_1^2 + \frac{1}{16}f_1f_2 + \frac{1}{16}f_2^2\Big\}\Big(f_0 + \frac{1}{2}f_1\Big)\Big]$$

$$+ \Big\{\frac{A^2}{8} + \frac{B^2\mu^4}{8} + \frac{\mu^4}{(1+\mu^2)}C^2 + \frac{\mu^4}{14\mu^2+1}D^2 + \frac{\mu^4}{\mu^2+0.1}E^2$$

$$+ \frac{\mu^4}{16(1+\mu^2)^2}F\Big\}$$

Using Eqs. (9) and (16),,the bending energy of the shell can be calculated as

$$\frac{W_2}{\frac{1}{2}Et\,ab} = \frac{1}{(1-\nu^2)}\Big(\frac{\pi}{E}\Big)^2\Big\{f_1^2\Big[\frac{1}{8}(1+\mu^2)^2 + \frac{1}{4}(1+\mu^2)$$

$$+ (1+\mu^2)f_1f_2 + (1+\mu^2)f_2^2\Big\} \qquad (24)$$

The lowering in potential of the applied force can be obtained by means of Eqs.(10), (18),(21),and (22): The result is

$$\frac{W_3}{\frac{1}{2}Et\,ab} = -2(1-\nu^2)\Big(\frac{\pi}{E}\Big)^2 + n^2\Big\{\frac{3}{32}(\mu^2+\nu)f_1^2$$

$$+ \frac{1}{8}(\mu^2+\nu)f_1f_2 + \frac{1}{8}(\mu^2+\nu)f_2^2\Big\}\frac{\pi}{E} - 2\nu\Big(f_0 + \frac{1}{4}f_1\Big)\frac{\pi}{E}\Big]$$

Relation between the Compression Stress and the Amplitude of Waves

To find the relation between the compression stress and the amplitude of the waves, the conditions which will make the sum of the energies W_1, W_2, and W_3 a minimum have to be obtained. It was found that the calculations can be simplified to a certain extend by first using the condition that

$$\frac{\partial}{\partial f_0}(W_1 + W_2 + W_3) = 0 \tag{26}$$

This condition will determine the relation between f_0 and f_1 and f_2, which can be written as

$$f_0 + \frac{1}{4}f_1^2 = \pi^2\left(\frac{3}{64}f_1^4 + \frac{1}{16}f_1^2 f_2^2 + \frac{1}{16}f_2^4\right) - \nu\frac{\sigma}{E} \tag{27}$$

Substituting Eq.(27) into the expressions for W_1, W_2 and W_3 as given by Eqs. (23), (24) and (25) and using Eq. (16), the total energy of the system is expressed finally in the following form:

$$\frac{W}{\frac{1}{2}E\lambda^2} = \pi^2 f_1^2 + \frac{1}{2}\pi^2 f_2^2 + \frac{1}{4}\left(\frac{\mu^4}{\mu^2+1} + \frac{1}{4}\frac{\mu^4}{(\mu^2+1)^2} + \frac{1}{16}\frac{\mu^4}{(\mu^2+1)^3}\right)\pi^4 f_1^4$$

$$+ \frac{1}{2}\left(\frac{\mu^4}{\mu^2+1} + \frac{\mu^4}{4(\mu^2+1)^2}\right)\pi^4 f_1^2 f_2^2 + \frac{1}{4}\left(\frac{\mu^4}{\mu^2+1} + \frac{\mu^4}{4(\mu^2+1)^2}\right)\pi^4 f_2^4 + \cdots \tag{28}$$

The equilibrium conditions are then obtained by differentiating the expression for total energy, Eq.(28), with respect to f_1 and f_2 , and then set these expressions equal to zero. The results can be written in a simpler form by introducing the following parameters

$$\rho = f_2/f_1$$
$$\gamma = n^2 \frac{t}{R} \qquad (29)$$
$$\xi = f_1 \frac{R}{t} - \frac{\rho}{t}$$

where [illegible] is the unit solution of the matrix [illegible] of the shell.

Then the equilibrium conditions are

[illegible]

Eliminating $\frac{\partial R}{\partial t}$ from the above equations, the following equation for ρ is obtained

$$A_3\rho^3 + A_2\rho^2 + A_1\rho + A_0 = 0$$

where the coefficients are

$$A_3 = (\gamma\xi)^2\left[\frac{3\mu^4}{(\mu^2+1)^2} + \frac{\mu^4}{(9\mu^2+1)^2} + \cdots\right]$$

A_2

A

A_0

(32)

Thus with a given value of μ and γ, the coefficients for various values of the wave amplitude ξ can be first calculated by using the Eq.(32). Then Eq.(31) can be solved for different values of ρ corresponding to this particular value of μ and γ at various wave amplitude ξ. When the value of ρ is known, Eq.(30) can be used to calculate the corresponding value of the compression stress $\frac{\partial \zeta}{\partial t}$. It is found, however, that the following expression for the compression stress which is obtained from Eq. (30) by

eliminating the third powers of ζ ,is more suitable for numerical computation:

These calculation was carried out for two values of ~~the ratio of the wave lengths in circumferential direction and in axial direction.~~ definitely the ratio of the wave lengths in circumferential direction and in axial direction. These values of μ are] and 0.5. The former value was chosen, because the experiments indicates that at large wave amplitudes, the diamond waves have ~~almost~~ equal sides. The latter value of μ was chosen, because the experiments made by N. Nojima and S.Kanemitsu (Ref.2) shows the occurance of this type of waves. The results of these computations are shown in Fig.2 and Fig.3 where the compression stress is plotted against the wave amplitudes.

The parameter in the figures is ~~the number of waves in the circumferential direction~~ λ. The values written in the parenthesis is the actual number of waves in circumferential direction for ~~the~~ R/t = 1000. The dropping

the actual load taken by the specimen under a testing machine can not be predicted from these figures. In a testing machine, the only factor under the control of the operator is the distance between the end plates and this is the factor ~~which determine~~ geometrical restraining the specimen must conform. Therefore, it is clear that the compression stress on the shell is not determined by the wave amplitude, but by the end shortening. The unit end shortening, i.e.,

from Eq.(21). It is found that

$$\frac{\varepsilon R}{t} = \frac{\sigma R}{Et} + \frac{\mu^2}{16}\xi(1+\xi)\left(\xi^2+\xi+\frac{3}{4}\right) \qquad (A)$$

Thus the unit end shortening can be easily calculated by

taking two pairs of values of β and $\frac{\sigma}{E}$ in Fig. 4 and [illegible] the corresponding pressure ratio is plotted against the unit end shortenings, for [illegible] $\mu = 1$ and $\mu = 0.5$ respectively

It is immediately clear from this two figures that if

the [illegible] process is [illegible] even [illegible], once the

[illegible] start [illegible] or [illegible] will have

[illegible] increase,

[illegible] which means that [illegible] the [illegible] of the [illegible] will [illegible] the [illegible] of the [illegible] ~~must first~~ jump to the point P (Fig4 or 5) which has the same end shortening as the starting point of buckling process, but has a much lower compression stress . This jump definitely involves a release of elastic energy and thus explains the rapidity of buckling process observed [illegible].

However, it is still difficult to say the shell will jump to a state with narrow waves, as shown by Fig.5, or to a state with almost square waves, as shown by Fig.4. Superficially, one might conclude that narrow waves are probable because it gives a much compression stress, as can be seen by comparing Fig.4 with Fig.5. But at a given end shortening, the true criteri[illegible] fundamental concept of mechanics for the most probable equilibrium position is that the elastic energy stored in

shell should be the lowest. An approximate calculation of the elastic energy of the shells shows that for values of $\left|\ < 0.012\right|$, the occurance of narrow waves is improbable, because the elastic energy is higher than that for square waves at same value of end shortening. However, for $\frac{\epsilon R}{t}$ near 0.6, the elastic energy stored in the shell for narrow waves is comparable to that for the square waves at same values of [illegible] This indicates the possibility of the occurance of narrow waves [illegible]. This is in agreement with the experimental findings of N.Nojima and S.Kanemitsu as reported in a previous paper by the present authors (Ref.2).

In any case it is definite that there are equilibrium positions of a buckled cylindrical shell which involve (8) the beginning of buckling. For instance, the square wave mode, the lowest compression stress is given by

$$\frac{\sigma}{E} = 0.194\left(\frac{t}{R}\right) \qquad (35)$$

This value corresponds closely to most of the experimental [illegible] (Ref.7)

In the two previous papers (Ref.1 and Ref.2) the authors have pointed out that due to imperfections present in test specimen and vibrations in the surroundings, [illegible] the test buckling load will probably nearer to

the minimum load necessary to keep the shell in buckled

classical theory.

The Effect of the Elastic Characteristic of the Testing Machine on the Buckling Behavior

In the previous paragraphs, it is stated that the compression on the specimen is determined by the distance between the end plates which is in turn determined by the loading mechanism. However, in actual cases, there is always a certain amount of elasticity in the testing machine and thus the distance between the end plates is not only determined by the loading mechanism but also by the compression force on the specimen. With the loading mechanism

will force the end plates apart and thus reduce the end shortening

a linear elastic behavior, the compression load is related to the end shortening by parallel straight lines for constant values of number of turns of the loading crank of the testing machine. If the loading crank is held at a fixed position, then the compression load of the specimen must follow the straight line corresponding to this crank position.

In Fig.6, the load-end shortening curves of different [illegible] plotted on a system of straight lines representing the characteristics of the testing machine. It is evident that after the maximum, or initial buckling load is reached, the shell will jump to an equilibrium state involving much lower compression load. The new equilibrium state is determined by the first [illegible] the slope of the load-end shortening curve. A (Fig.6) will give higher load than the curve B (Fig.6). Secondly, the elastic character of the testing machine. A more elastic machine will give a set of characteristic straight lines having smaller slopes. Therefore, in case of Curve A, a more elastic machine will result in a higher load, while in case of curve B, a more elastic machine will result in a lower load. Therefore, the buckling behavior of a cylindrical shell is only determined by the elastic characteristics of the shell itself, but also influenced by [illegible] of the testing machine.

This fact is first discussed by the senior author in connection with the elastic buckling of [illegible] in an early paper (Ref. [illegible]).

[illegible] is a slight imperfection in the testing shell [illegible] than

Concluding Remarks

In the previous paragraphs, the authors have shown that there are equilibrium positions in the buckled shape involving much lower load than the buckling load predicted by classical theory, and thus if the specimen is slightly imperfect, it is reasonable to expect much lower buckle loads

order observed in the laboratory. They have also pointed out that the elastic behavior of the testing machine has a profound influence on the buckling phenomenon and this might be another cause of the large scattering of experimental data obtained by different experimenters.

However, due to complexity of the problem, the results given in this paper can be only considered as a rough approximation and most of the discussion made are qualitative rather than quantitative. To put the new theory on a solid footing, a more accurate solution of the differential equations of equilibrium is necessary. Particular attention must be given to the calculation of the elastic energy stored

the buckled cylindrical shell, but rather the elastic energy stored.

Perhaps, a inquisitive investigator would be pleased by a rigorous proof of the validity of all the large deflection equations. All the equations used are

intuitive arguments rather by systematic

For instance, it is not certain whether the curvature of the shell has to be calculated more accurately by taking into account the second order terms, or the extensions of median surface should be more accurately determined. It is the belief of the present authors that an investigation of these problems

by starting from the general non-linear elasticity theory
of Cosserat (Ref.9) and others very desirable
The senior author has already expressed this
opinion in his 1949 Gibbs Lecture of the American Mathematical
Society

THE BUCKLING OF THIN CYLINDRICAL SHELLS UNDER AXIAL COMPRESSION

Theodore von Kármán and Hsue-shen Tsien
California Institute of Technology

In two previous papers (Ref. 1 and Ref. 2), the authors have discussed in detail the inadequacy of the classical theory of thin shells in explaining the buckling phenomenon of cylindrical and spherical shells. It was shown that not only the calculated buckling load is 3 to 5 times higher than that found by experiments, but the observed wave pattern of the buckled shell is also different from that predicted. Furthermore, it was pointed out that the different explanations for this discrepancy advanced by L. H. Donnell (Ref. 3) and W. Flügge (Ref. 4) are untenable when certain conclusions drawn from these explanations are compared with the experimental [illegible]. The authors were then led to [illegible] the buckling [illegible] this point [illegible] with non-linear [illegible]. 2 it is evident from these investigations that the load necessary to keep the shell in equilibrium drops very rapidly with increase in wave amplitude once the shell started to buckle. This characteristic shows, first of all, that there is a release of the elastic energy stored in the shell once the buckling has started, and thus explains the observed rapidity of the buckling process. Furthermore, it also brings in the possibility of a decrease in the buckling load when there are slight imperfections in the test specimen and when there are vibrations during the testing process.

In this paper, the authors will show by means of an approximate

calculation that in case of a thin uniform cylindrical shell under axial compression, the load sustained by the shell drops with increasing deflection. Consequently, they hope that they have thus offered an acceptable explanation of the observed facts.

Stresses in the Median Surface and the Expression for the Total Energy of the System

Let x and y be measured in the axial and the circumferential direction in the median surface of the undeformed cylindrical shell and u, v, and w be the components of displacement of a point on the median surface of the shell in the x-direction, the y-direction, and the radial direction. Then the unit strains in the x and y-directions, ε_x, ε_y and the unit shear γ_{xy} at a point in the median surface can be expressed in the following

where

stresses and the strains in the median surface of the shell are, however, related to each other by the following equations:

$$\sigma_x = \frac{E}{1-\nu^2}(\varepsilon_x + \nu\varepsilon_y)$$
$$\sigma_y = \frac{E}{1-\nu^2}(\varepsilon_y + \nu\varepsilon_x) \qquad (2)$$
$$\tau_{xy} = \frac{E}{2(1+\nu)}\gamma_{xy}$$

where E is Young's modulus of elasticity and ν is Poisson's ratio. Therefore by substituting Eq. (1) into Eq. (2), the following connections between the components of stress in the median surface and the components of displacement of the median surface are obtained:

$$\varepsilon_x = \frac{1}{E}\left(\sigma_x - \nu\sigma_y\right) = \frac{\partial u}{\partial x} + \frac{1}{2}\left(\frac{\partial w}{\partial x}\right)^2 + \nu\frac{w}{R}$$

$$\varepsilon_y = \frac{1}{E}\left(\sigma_y - \nu\sigma_x\right) = \frac{\partial v}{\partial y} + \frac{1}{2}\left(\frac{\partial w}{\partial y}\right)^2 - \frac{w}{R} + \nu\frac{\partial u}{\partial x}$$

$$\gamma_{xy} = \frac{E}{2(1+\nu)}\left[\frac{\partial u}{\partial y} + \frac{\partial v}{\partial x} + \frac{\partial w}{\partial x}\frac{\partial w}{\partial y}\right]$$

It is generally accepted that the equilibrium conditions of thin shells in terms of stresses in the median surface of a thin shell can be approximately expressed by the following equations:

$$\frac{\partial \sigma_x}{\partial x} + \frac{\partial \tau_{xy}}{\partial y} = 0$$
$$\frac{\partial \tau_{xy}}{\partial x} + \frac{\partial \sigma_y}{\partial y} = 0 \qquad (4)$$

These partial equations can be satisfied by introducing the well-known Airy's stress function, $F(x,y)$ defined by the relations

$$\sigma_x = \frac{\partial^2 F}{\partial y^2}, \quad \tau_{xy} = -\frac{\partial^2 F}{\partial x \partial y}, \quad \sigma_y = \frac{\partial^2 F}{\partial x^2}$$

Eliminating the variables u and v in Eqs. (3) and (5) a relation between Airy's stress function F and the deformation of the median surface, w is obtained:

$$\frac{\partial^4 F}{\partial x^4} + 2\frac{\partial^4 F}{\partial x^2 \partial y^2} + \frac{\partial^4 F}{\partial y^4} = E\left[\frac{\partial^2 w}{\partial x \partial y}\right]^2 - \frac{\partial^2 w}{\partial x^2}\frac{\partial^2 w}{\partial y^2} + \frac{1}{R}\frac{\partial^2 w}{\partial x^2}$$

This equation expresses the condition of compatibility between stress and strain. When $R \to \infty$, it reduces to the corresponding equation for a flat plate derived by the senior author (Ref. 6). L. H. Donnell (Ref. 3) first obtained this equation in its present form. With a given form of the radial component of the displacement, w, Eq. (6) gives the induced stresses in the median surface of the shell.

For the complete wave panel, the extensional elastic energy, corresponding to these stresses can be written as

$$U_1 = \frac{1}{2}\int_0^a \int_0^b \left(\sigma_x \varepsilon_x + \sigma_y \varepsilon_y + \tau_{xy}\gamma_{xy}\right) dx\, dy$$

where a and b are the half wave lengths in the axial and the circumferential directions respectively.

To calculate the bending elastic energy, it is necessary to find the expressions for the change of curvatures and the unit twist of the median surface. [illegible] are

$$\chi_x = \frac{\partial^2 w}{\partial x^2}, \quad \chi_{xy} = \frac{\partial^2 w}{\partial x \partial y}, \quad \chi_y = \frac{\partial^2 w}{\partial y^2} \tag{8}$$

[illegible] terms in χ_y and χ_{xy} are [illegible] 8) that those neglected terms differ from the terms retained in Eq. (8) by a factor $\frac{1}{n^2}$, where n is the number of waves in the circumferential direction. For thin cylindrical shells, the value of n is around 10; therefore the neglection is justified. With these expressions for the change of curvatures and the unit twist of the median surface, the bending energy W_2 for one complete wave panel can be written as

$$W_2 = \frac{t^3 E}{[illegible]} \int_0^a \int_0^b [illegible] \, dx \, dy$$

[illegible] of the cylindrical shell can be calculated as the product of the change in length of the shell and the applied force. Therefore the following expression is obtained for one complete wave panel:

$$W_3 = -t \int_0^b (\sigma_x)_{x=a} dy \int_0^a \frac{\partial u}{\partial x} dx \tag{10}$$

The equilibrium condition of the shell can be obtained either by equating to zero the variation of the energy [illegible] zero, or by actually analyzing the moments and the stresses in the median surface of the shell. Using the approximations stated previously, Donnell (Ref. 8) derived the equilibrium equation as

[illegible] $\frac{Et}{} \nabla^4 w = \frac{\partial^2}{} \frac{\partial^2 F}{} + \frac{\partial^2}{} \frac{\partial^2 F}{} - \frac{\partial^2 w}{} + \frac{\partial^2 w}{} + \sigma_y \frac{\partial^2 w}{}$

where p is the external radial pressure on the surface of the shell. In the case concerned, $p = 0$, then using Eq. (5), the second equation [illegible] Airy's stress function F [illegible] displacement, w is obtained as

[illegible]

When [illegible], Eq. (12) reduces to the corresponding [illegible] plate.

There are two different ways to solve the problem of the buckling of a thin uniform cylindrical shell under axial compression. The more exact method is to solve Eqs. (6) and (12) simultaneously, using appropriate boundary conditions. The approximate method is to first assume a plausible function for w, with undetermined parameters and then use Eq. (6) to determine the stresses in the median surface of the shell. The energies W_1, W_2 and W_3 can then be calculated by means of Eqs. (7), (9), and (10). The undetermined parameters can be ascertained by the condition that the sum of energies W_1, W_2, and W_3 must be a minimum. This approximate method will be used in the following calculations.

Calculation of the Total Energy

To obtain a plausible form for w, one has to resort to the experimental results. It is observed that, for large values of the wave amplitude, the waves show a so-called diamond shaped pattern. This particular wave shape can be approximately expressed by

$$\frac{w_1}{R} = \cos^2 \frac{(mx+ny)}{2R} \cos^2 \frac{(mx-ny)}{2R}.$$

where the squares are introduced to account for the fact that the shell has a definite preference to buckle inward. Eq. (13) can be re-written as

$$\frac{w_1}{q} = \frac{1}{4} + \frac{1}{2}\left[\cos\frac{mx}{R}\cos\frac{ny}{R} + \frac{1}{4}\cos\frac{2mx}{R} + \frac{1}{4}\cos\frac{2ny}{R}\right]$$

On the other hand, the classical theory which is correct for infinitesimal values of the wave amplitude, requires the wave to be of the form

$$\frac{w_2}{R} = \cos\frac{mx}{R}\cos\frac{ny}{R} \qquad (15)$$

In order to satisfy this requirement, the wave form assumed in the following calculation is

[illegible] (16)

where f_0 , f_1 , f_2 are unknowns to be determined by conditions of minimum total energy of the system. f_0 is introduced in order to allow the shell to expand radially. The amplitude of the wave pattern defined as the maximum difference in the radial deflection, w is evidently given by f_1 . The wave lengths in the axial and the circumferential direction are [illegible] circumference of the shell is equal to n . It is evident that no end effect can be accounted for by this form of wave pattern, and therefore the following calculation really corresponds to the case of a very long cylindrical shell. This simplification is justified by the experimental findings of N. Nojima and S. Kanemitsu as reported in a previous paper (Ref. 2). It was found that there is no appreciable length effect when the length of the cylindrical is greater than 1.5 times the radius of the shell. Furthermore, it is seen that by setting $f_0 = f_1 = 0$, Eq. (16) is reduced to Eq. (14); while by setting $\frac{f_1}{4} + \frac{f_2}{2} = 0$ and $f_0 + \frac{f_2}{4} = 0$, Eq.

(16) is reduced to Eq. (15). With other values of these parameters, wave patterns intermediate between these two limits can be obtained.

Substituting Eq. (16) into Eq. (6), the differential equation for Airy's stress function $F(x,y)$ is obtained:

$$[illegible]$$

where $\mu = \frac{m}{n}$, the aspect ratio of the waves. If $\mu > 1$ the waves are longer in the circumferential direction; if $\mu < 1$, the waves are longer in the axial direction. The coefficients in Eq. (17) are given by the following relations:

$$A = \frac{1}{8} f_1^2 n^4 - \left(\frac{1}{2} f_1 + f_2\right)$$

$$B = \frac{1}{8} f_1^2 n^4$$

$$= [illegible]$$

$$D = \frac{1}{4} f_1 n^2 \left(\frac{1}{2} f_1 + f_2\right)$$

$$C = \frac{1}{4} f_1 n^2 \left(\frac{1}{2} f_1 + f_2\right)$$

and $$H = n^2 \left(\frac{1}{2} f_1 + f_2\right)^2$$

The solution of this differential equation can be easily obtained as

$$[illegible]$$

$$+ \frac{\alpha}{2} x^2 + \frac{\beta}{2} y^2$$

Using Eq. (5), the stress components in the median surface can be written as

$$[illegible] \qquad (20)$$

the average compression stress σ in the axial direction. It can be easily seen from Eq. (20) that

$$\beta = -\sigma \tag{21}$$

Using Eq. (3), the following expressions for $\frac{\partial u}{\partial x}$ and $\frac{\partial v}{\partial y}$ can be obtained:

$$\frac{\partial u}{\partial x} = \frac{1}{E}(\sigma_x - \nu\sigma_y) - \frac{1}{2}\left(\frac{\partial w}{\partial x}\right)^2$$
$$\frac{\partial v}{\partial y} = \frac{1}{E}(\sigma_y - \nu\sigma_x) - \frac{1}{2}\left(\frac{\partial w}{\partial y}\right)^2 + \frac{w}{R} \tag{22}$$

By substituting Eqs. (16) and (20) into Eq. (22), it is found that

(23)

Since y is measured along the circumference of the shell, v must be a periodic function of y; therefore, the constant term in $\frac{\partial v}{\partial y}$ must be equal to zero. Or

This is the condition for the determination of α.

Using Eqs. (7), (20) and (24), the extensional energy W_1 of the shell is obtained as

Using Eqs. (9) and (16), the bending energy W_2 of the shell can be calculated as

The lowering of the potential of the applied force can be obtained by means of Eqs. (10), (20), (23) and (24). The result is

Relation between the Compression Stress and the Amplitude of Waves

To find the relation between the compression stress and the amplitude of the waves, the conditions which will make the sum of the energies W_1, W_2, and W_3 a minimum have to be obtained. It was found that the calculations can be simplified to a certain extent by first using the condition that the sum of energies must be minimum with respect to .

Or

$$\frac{\partial}{\partial f_0}(W_1+W_2+W_3)=0 \tag{28}$$

This condition determines a relation between f_0 and f_1 and f_2, which can be written as:

$$f_0+\frac{3}{4}f_1=\pi^2\left(\frac{3}{64}f_1^2+\frac{1}{16}f_1f_2+\frac{1}{16}f_2^2\right)-\nu\frac{\sigma}{E} \tag{29}$$

Using this relation and Eq. (24), it is easily seen that $\alpha=0$. In other words, the shell will expand radially to such an extent that the average of the circumferential stress σ_θ is equal to zero. Substituting Eq. (29) into the expressions for W_1, W_2 and W_3 as given by Eqs. (25), (26) and (27) and using Eq. (18), the total energy of the system is expressed finally in the following form:

$$+\left[\left(\frac{1}{32}+\frac{1}{4}\frac{\mu^6}{(1+\mu^4)^3}\right)f_1^2+\frac{1}{8}f_1f_2+\frac{1}{8}f_2^2\right]+ \qquad (30)$$

The equilibrium conditions are then obtained by differentiating the expression for total energy, Eq. (30), with respect to f_1 and f_2, and then set these expressions equal to zero. The results can be written in a simpler form by introducing the following parameters:

$$\zeta=\frac{f_2}{f_1} \qquad \eta=\pi^2\frac{t}{R}, \qquad \xi=f_1\frac{R}{t}=\frac{\delta}{t} \qquad (31)$$

where δ is the wave amplitude of the buckled shape of the cylindrical shell. Then the equilibrium conditions are

$$+\left[\frac{1}{4}\xi+\frac{1}{\rho}\right]+\frac{1}{3(1-\nu^2)}\eta^2\left[(1+\mu^4)\xi+\frac{1}{2}(1+\mu^4)\right]$$

is obtained

$$A_3\xi^3+A_2\xi^2+A_1\xi+A_0=0 \qquad (33)$$

where the coefficients are

$$A_3=$$

$$A_2=$$

$$A_1=$$

$$A_0=$$

$$-\frac{2}{3(1-\nu^2)}\eta^2\left\{(1+\mu^4)-\frac{1}{4}(1+\mu^2)^2\right\}$$

Therefore, when $\xi=0$, i.e., when the wave amplitude approaches zero

Eq. (32) gives $A_3=A_2=0$; and

$$A_1 = -\frac{5}{3(1-\nu^2)}\eta^2\left[2(1+\mu^2) - \frac{1}{2}(1+\mu^2)^2\right]$$

$$A_0 = -\frac{2}{3(1-\nu^2)}\eta^2\left[(1+\mu^2) - \frac{1}{4}(1+\mu^2)^2\right] = \frac{A_1}{2}$$

Substituting into Eq. (31) it is seen that $f = -\frac{1}{2}$, or $f_2 = -\frac{1}{2}f_1$. Putting this relation between f_1 and f_2 into Eq. (14), the wave pattern is reduced to that represented by Eq. (15), i.e., the classical wave pattern for infinitesimal wave amplitude.

With a given value of μ and η, the coefficients for various values of the wave amplitude ξ can be first calculated by using the Eq. (34). Then Eq. (33) can be solved for ρ corresponding to this particular set of values of μ and η at various wave amplitude ξ. When the value of ρ is known, Eq. (32) can be used to calculate the corresponding value of the compression stress $\frac{\sigma R}{E t}$. It is found, however, that the following expression for the compression stress $\frac{\sigma C}{E t}$ which is obtained from Eq. 3 by eliminating the third powers of ρ is more suitable for numerical computations:

$$\frac{\sigma R}{E t} = \left[\frac{1}{3}\frac{\mu^2}{(1+\mu^2)^2} + \frac{1}{12(1-\nu^2)}\frac{\eta(1+\mu^2)^2}{\mu^2}\right]$$

Therefore, when $\xi \to 0$, i.e., when the wave amplitude becomes very small, Eq. (35) reduces to

$$\left(\frac{\sigma R}{E t}\right)_{\xi \to 0} = \frac{1}{\eta}\frac{\mu^2}{(1+\mu^2)^2} + \frac{1}{12(1-\nu^2)}\frac{1}{\frac{1}{\eta}\frac{\mu^2}{(1+\mu^2)^2}} \qquad (36)$$

[illegible]

$$Min\left(\frac{\sigma R}{E t}\right)_{\xi \to 0} = \frac{1}{\sqrt{3(1-\nu^2)}} \qquad (37)$$

[illegible]

deflections. This minimum value is obtained when

$$\eta \frac{1+\mu^2}{\mu^2} = 2\sqrt{3(1-\nu^2)} \qquad (38)$$

It is interesting to notice that for infinitesimal wave amplitude, the minimum value of average compression stress is not determined by separate parameters η or μ, but by a combined parameter shown in Eq. (38).

These calculations were carried out for two values of the parameter μ , the ratio of the wave lengths in circumferential direction and in axial direction. These values of μ are 1 and 0.5 . The value 1 was chosen because the experiments indicate that at large values of wave amplitude, the diamond waves have almost equal sides. The value 0.5 was chosen to investigate the possibility of occurrence of narrow waves. The results of these computations are shown in Fig. 2 and Fig. 3, where the compression stress $\frac{\sigma_c}{E}\frac{R}{t}$ is plotted against the wave amplitudes ξ . The parameter in the figures is η . The values written in the parenthesis after η is the actual number of waves n in circumferential direction for $R/t = 1000$. For a given value of η and μ, i.e., a fixed size of the wave, the load sustained by the shell, $\frac{\sigma R}{E t}$ first decreases as the wave amplitude, ξ , is increased. After a minimum is reached, the load will rise with increase in wave amplitude. When the waves are larger, the initial buckling

load, i.e., the value of $\frac{\sigma R}{Et}$ at $\xi = 0$, is higher. However, the minimum load reached tends to a lower value, except for $\eta < 0.169$ and $\mu = 1.0$. For $\mu = 0.5$, the lowest value of the minimum load is not yet reached at $\eta = 0.081$.

The Relation between the Compression Stress and the Shortening in the Axial Direction

Although the load characteristic of the cylindrical shell shown in the Figs. 2 and 3 give the possible equilibrium relations between load and amplitude of the deflection wave, the actual behaviour of a specimen in a testing machine cannot be directly seen from these figures. In a testing machine, the only factor under the control of the operator is the distance between the end plates; this is the geometrical restraint the specimen must conform. Therefore, in order to determine the behaviour of the specimen the compression stress will have to be plotted as function of the end shortening. The unit end shortening, ε, i.e., the total shortening in one wave length of the shell in axial direction divided by the wave length, can be easily calculated from Eq. (23). It is found that

$$\frac{\varepsilon R}{t} = \frac{\sigma R}{Et} + \frac{\mu^2}{16}\xi(\eta\xi)\left(\xi^2+\xi+\frac{3}{4}\right) \qquad (39)$$

This equation for the unit end shortening contains only quantities already [illegible] as the ordinates of Figs. 4 and 5, the compression [illegible] plotted against the unit end shortening $\frac{\varepsilon R}{t}$ for [illegible] and $\mu = 0.5$, respectively. It is immediately clear from this two figures that if the buckling process follows the curves drawn, after the shell starts to buckle the end shortening has to decrease. In other words, the end plates of the testing machine have to move apart. Therefore, the process of buckling in this region is highly unstable, since before the operator has

times to separate the end plates, the shell will jump to the point P (Figs. 4 or 5) which has the same end shortening as the starting point of the buckling process, but has a much lower compression stress. This jump in equilibrium positions involves a release of elastic energy and thus explains the rapidity of the buckling process observed and the accompanied vibration.

However, it is still difficult to say whether the shell will jump to a state with almost square waves, as shown in Fig. 4, or to a state with narrow waves, as shown in Fig. 6. Superficially, one might conclude that the narrow waves are the more probable shape because it gives a much lower compression stress, as can be seen by comparing Figs. 4 and 5. But, according to the fundamental concept of mechanics, the true criterion for the most probable equilibrium position compatible with a given value of the end shortening is that the elastic energy stored in the shell should be the lowest. An approximate calculation of the elastic energy of the shells shows that for values of $\eta < 0.12$, the occurrence of the narrow waves is improbable, because the elastic energy stored is higher than that for the square waves at same value of the end shortening. However, for $\frac{\varepsilon R}{t}$ near 0.6, and $\eta \geq 0.12$ the elastic energy stored in the shell for the narrow waves is comparable to that for the square waves at the same value of the end shortening. This indicates the possibility of the appearance of narrow waves during the very initial stages of the buckling process.

In any case, it is certain that there are equilibrium positions of a buckled cylindrical shell which involve much lower average compression stress $\frac{\sigma R}{E t}$ than that at the beginning of buckling. For instance, in the case of square wave pattern, the lowest compression stress is given by

$$\frac{\sigma}{E} = 0.194 \frac{t}{R} \tag{40}$$

Incidentally, this value corresponds closely to most of the experimental results obtained by L. H. Donnell (Ref. 3) and E. E. Lundquist (Ref. 7).

The corresponding value of the parameter η which determines the number of waves is equal to 0.225. In case of $R/t = 1000$, the number of waves, n, will be 15 which also agrees well with the experimental evidence. For this particular value of the radius to thickness ratio, the number of waves along the circumference decreases from the $n = 26$ at the beginning of the buckling to $n = 15$ at the calculated minimum buckling stress. This gradual increase in the size of waves with the unit shortening is also observed by the experiments reported in an earlier paper (Ref. 2).

It is particularly interesting, however, to trace the gradual change in the wave pattern during the buckling process. Figs. 6 and 7 show the lines of equal deflection of the wave surfaces corresponding to different equilibrium states for two values of the aspect ratio of the wave pattern, $\mu = 1.0$ and $\mu = 0.5$. These particular equilibrium states are denoted in Figs. 2, 3, 4 and 5 by a small circle in order to indicate their relative position during the buckling process. It is seen that there is a rapid shift from the rectangular waves bounded by lines, x = const., and y = const., as predicted by the classical theory for infinitesimal wave amplitudes, to staggered rows of circular or elliptical waves. Whereas, the rectangular waves are directed alternatively inward and outward, the circular or elliptical waves are all directed inwards. The transition is practically completed for $\xi = 4$ or 6, i.e., when the wave amplitude is only 4 or 6 times the thickness of the shell. The occurrence of such inwardly directed circular and elliptical waves at this stage of the buckling process is in good agreement with the experimental observations (Ref. 2). If the experiment $(\xi \sim \xi_0)$ is continued to larger deflections, these staggered waves

obtain characteristic diamond shapes. The present approximate theory fails to give these sharp diamond shaped waves. It is obviously not sufficiently exact for such large deflections. Furthermore, when these diamond shaped waves occur, the load on the specimen actually falls to a very low value such as $\frac{\sigma}{E} \approx 0.06$, whereas the theory shows a slight increase of the stress at least for the case $\mu = 1.0$. Therefore, the present calculation can be only considered as a good approximation to the earlier stages of buckling when the wave amplitude is only a few times the thickness of the shell. Nevertheless, it reproduces the characteristic features of the buckling process observed in the laboratory.

The Effect of the Elastic Characteristic of the Testing Machine on the Buckling Phenomenon

It was stated in the previous paragraph that the state of the specimen is determined by the distance between the end plate and that this distance is the independent parameter controlled by the experimenter. This statement is correct only insofar the elasticity in the mechanism of the testing machine is neglected. Since there is always a certain amount of elastic deflection in the loading mechanism and this deflection is a function of the load. Hence, if, for example, the loading crank is held at a certain position, the compression force acting on the specimen will force the end plates apart and thus reduce the amount of end shortening of the specimen. The actual shortening is determined by the load-deflection characteristics of the specimen and the testing machine. Assuming that the testing machine has a linear elastic characteristic, the compression load is related to the end shortening by parallel straight lines, each line corresponding to, say, a constant number of turns of the loading crank. If the loading crank of

the machine is held at a fixed position, corresponding values of the compression load and end shortening of the specimen must lie on the straight line for this crank position. If the load-end shortening characteristics of the specimen itself are given, it is evident that the equilibrium positions of the entire system are determined by intersections of the curves representing the characteristics of the specimen with the straight lines representing the characteristics of the machine.

Fig. 8 shows representative curves for the characteristics of the specimen and two families of straight lines representing the characteristics of two different testing machines. It is evident that after the maximum or initial buckling load is reached, the shell will jump to a new equilibrium position involving much lower compression load. But this new equilibrium position is determined not only by the load-end shortening relationship and also by the elastic characteristic of the testing machine. A more elastic machine will give a set of characteristic straight lines with smaller slopes. Therefore, in case of curve A (Fig. 8), a more elastic machine will make the shell to jump to a higher load, while in case of curve B, a more elastic machine will make the shell to jump to a lower load. This influence of the elasticity of the testing machine has been discussed by the senior author in connection with the plastic buckling of columns (Ref. 8).

Concluding Remarks

In the previous paragraphs, the authors have shown that there are equilibrium positions in the buckled shape involving much lower load than the buckling load predicted by the classical theory, and thus if the specimen is slightly imperfect, it is reasonable to expect much lower buckling loads. They have also pointed out that the elastic characteristic

of the testing machine might have quite a large influence on the buckling process and this might be another cause of the large scattering of the data obtained by different experimenters. However, due to the complexity of the problem, the results given in this paper can be only considered as a rough approximation and most of the statements made are qualitative rather than quantitative. To put the new theory on a solid footing, a more accurate solution of the differential equations of equilibrium is necessary. Particular attention must be given to the calculation of the elastic energy stored in the shell, because it is found that the most probable equilibrium depends on the magnitude of the elastic energy stored in the various equilibrium positions compatible with the constraint exerted by the loading process.

Furthermore, an inquisitive mind will, perhaps, be pleased by a rigorous proof of the validity of all the large deflection equations. These equations are established by intuitive arguments, not by systematic reasoning. For instance, due to the appearance of sharp curvatures in the diamond shaped wave surfaces at large deflections, it is not certain whether the curvature of the shell has to be calculated more accurately by taking into account the second order terms, or the extensions of the median surface should be more accurately determined. It is the belief of the authors that an investigation of these problems by starting from the general non-linear theory of elasticity developed by G. Kirchhoff, J. Boussinesq and others is very desirable. The recent work by R. Kappus (Ref. 9) is a noteworthy contribution in this field of investigation. The senior author has already expressed this opinion in his 1939 Gibbs Lecture (Ref. 10) given before the American Mathematical Society.

Section 6

Take-off from Satellite Orbit

Rough draft

Take-Off from Satellite Orbit

W. Tsien

Summary.

The mass ratio or the characteristic velocity for a take-off from the satellite orbit is computed for two cases: the radial thrust and the circumferential thrust. The circumferential thrust is much more efficient in that the required mass ratio is much less than for the radial thrust. Both cases show, however, an increase of the required mass ratio and the characteristic velocity with a reduction in acceleration. With circumferential thrust, the characteristic velocity increases by a factor of two when the acceleration is reduced from ½ g to 1/3000 g.

For take-off of a rocket from the earth surface, it is convenient to have the initial [illegible] in the vertical direction and then the thrust should be considerably larger than the total weight of the rocket. [illegible] the sum of the aerodynamic drag and the weight, the initial ratio of the thrust and the weight should be between 2 and 3 for minimum expenditure of the propellant. The situation is quite different for a space ship taking off from the satellite orbit. In a satellite orbit the gravitational attraction is completely balanced by the centrifugal force, and the [illegible] a weightless state. [illegible] dreamers of interplanetary travel to conclude that take off from satellite orbit [illegible] [illegible] at only at [illegible] [illegible] interplanetary [illegible] [illegible] [illegible] larger acceleration [illegible] [illegible] for take off from the satellite orbit [illegible] acceleration [illegible] to be used. The ion-beam rocket is only possible for very small accelerations; [illegible] moderate accelerations [illegible] rocket is required. Therefore the question of the magnitude of acceleration is an important one for interplanetary flight. [illegible] this note is to demonstrate clearly the relation between [illegible] [illegible] [illegible] engineers a more rational basis for designing space ships.

Basic Equations

The problem considered is the motion of a space ship under the [illegible] magnitude of gravitational attraction at the orbiting satellite orbit $r = r_0$ (fig 1), then the equations of motion of the space ship are

$$\frac{d^2r}{dt^2} = R + r\left(\frac{d\theta}{dt}\right)^2 - g\left(\frac{r_0}{r}\right)^2$$

and

$$\frac{d}{dt}\left(r^2\frac{d\theta}{dt}\right) = r\Theta$$

given by

$$r_0\left(\frac{d\theta}{dt}\right)_0^2 = g \qquad (3)$$

Initially, the radial velocity is zero, i.e.,

$$\left(\frac{dr}{dt}\right)_0 = 0 \qquad (4)$$

These are the initial conditions for the space ship to have sufficient forward flight, the sum of the kinetic energy and the potential [illegible] be denoted by the subscript 1. Thus at $t = t_1$

$$\frac{1}{2}\left[\left(\frac{dr}{dt}\right)_1^2+\left(r\frac{d\theta}{dt}\right)_1^2\right]-g\frac{r_1^2}{r_1}=0 \qquad (5)$$

With any specified variation of the thrust force R and Θ as functions of time, the above system of equations determine completely the take-off trajectory of the space ship. In the following sections, two special cases of practical significance will be discussed in detail: the case of constant, $\hat{T}$ = 1, finite radial thrust, and the case of constant, finite circumferential thrust.

Radial Thrust

If the thrust is always radial and is proportional to the instantaneous mass of the vehicle, a non-dimensional thrust factor μ can be introduced as

$$R=\mu g \qquad (9)$$

Furthermore, let

$$\rho=r/r_0, \qquad \tau=\sqrt{\frac{g}{r_0}}\,t \qquad (11)$$

Then Eqs (1) and (2) can be written in the non-dimensional form as

$$\frac{d^2\rho}{d\tau^2}=\mu+\rho\left(\frac{d\theta}{d\tau}\right)^2-\frac{1}{\rho^2} \qquad (17)$$

and

$$\frac{d}{d\tau}\left(\rho^2\frac{d\theta}{d\tau}\right)=0 \qquad (18)$$

Eq (18) can be immediately integrated and by using the initial condition of the trajectory, we obtain

$$\frac{d\theta}{d\tau}=\frac{1}{\rho^2} \qquad (19)$$

By substituting the equation into Eq (17), the final equation for ρ is

$$\frac{d^2\rho}{d\tau^2}=\mu+\frac{1}{\rho^3}-\frac{1}{\rho^2} \qquad (10)$$

The non-dimensional radial velocity is $d\xi/d\tau$. This is related to the physical radial velocity dr/dt as follows

$$\frac{dr}{dt} = \sqrt{\frac{3}{2}r_0}\,\frac{d\xi}{d\tau} \tag{11}$$

Eq (10) can be rewritten as

$$\frac{d}{d\xi}\left[\frac{d\xi}{d\tau}\right]^2 = u + \frac{1}{\xi} - \frac{1}{\xi^2}$$

Since $d\xi/d\tau = 0$ when $\tau = 0$ and $\xi = 1$ according to Eq. (6), the result of integrating the above equation is

$$\left(\frac{d\xi}{d\tau}\right)^2 = 2u(\xi - 1) + \left(1 - \frac{1}{\xi^2}\right) - 2\left(1 - \frac{1}{\xi}\right) \tag{12}$$

Therefore the non-dimensional time τ can be calculated as a function of the radius ξ as follows

$$\tau = \int \frac{\xi\, d\xi}{\sqrt{(\xi-1)(2u\xi^2 - \xi + 1)}} \tag{13}$$

With Eqs. (9) and (12), the end condition of Eq. (5) can be written as

$$\frac{1}{2}\left[\left[2u(\xi_1 - 1) + \left(1 - \frac{1}{\xi_1^2}\right) - 2\left(1 - \frac{1}{\xi_1}\right)\right] + \frac{1}{\xi_1^2}\right] - \frac{1}{\xi_1} = 0$$

Or simply

$$\xi_1 = 1 + \frac{1}{2u} \tag{14}$$

Then the velocities at the end of acceleration period are

$$\left(\frac{dr}{dt}\right)_1 = \sqrt{\frac{3}{2}r_0}\,\sqrt{\frac{1}{2u}}$$

and

$$\left(\frac{dr}{dt}\right)_1 = \sqrt{\frac{3}{2}r_0}\,\frac{1}{\sqrt{2u}}$$

In the τ_1 given in Eq. (12), μ at t_1 can be obtained from Eq. (13), by setting the upper limit of integration to ξ_1. Thus

$$\tau_1 = \frac{2}{\mu}\sqrt{\frac{\mu^2+\mu}{2\mu+1}} + F\left(\frac{1}{\sqrt{2\mu^2}}, \cos^{-1}\frac{\mu^2-1}{2\mu+1}\right) + E\left(\frac{1}{\sqrt{2\mu^2}}, \cos^{-1}\frac{2\mu+1}{2\mu+1}\right) \quad (14)$$

where F and E are the elliptical integrals of first kind and second kind respectively.*

If $M(t)$ is the instantaneous mass of the space ship, and c the effective exhaust velocity of the rocket, then

$$RM = \mu g M = -c\frac{dM}{dt} = -c\sqrt{\frac{g}{r_0}}\frac{dM}{d\tau}$$

Therefore the mass ratio M_0/M_1 can be calculated as follows:

$$\log(M_0/M_1) = \frac{\sqrt{2gr_0}}{c}\mu\tau_1$$

By using the result of Eq. (16),

$$\log(M_0/M_1) = 2\mu\sqrt{\frac{\mu+1}{2\mu+1}} + \sqrt{2\mu}\,F\left(\frac{1}{\sqrt{2\mu}}, \cos^{-1}\frac{2\mu}{2\mu+1}\right) \cdot E\left(\frac{1}{\sqrt{2\mu}}, \cos^{-1}\frac{2\mu}{2\mu+1}\right) \quad (17)$$

When the acceleration is very large, $\mu \gg 1$, the integrand in Eq. (13) can be expanded in terms of the fraction $\frac{1}{2\mu}$ and integrated term by term, to obtain

$$\frac{c}{\sqrt{gr_0}}\log(M_0/M_1) = 1 + \frac{1}{2\cdot 3\cdot 2\mu} - \frac{1}{4\cdot 5\cdot 2\mu^2} + \cdots \quad (18)$$

The relation of Eqs. (17) and (18) is plotted in Fig. 2. For $\mu = \frac{1}{2}$, the mass ratio becomes infinite. The reason is that at this value

The author is indebted to Dr. Y. T. Wu who kindly supplied the solution of Eq. (11)

...acceleration, there is a radial position where the thrust force is equal to the gravitational attraction and no further increase in the energy of the vehicle can occur. Therefore the radial thrust per unit mass, of maintained constant throughout the powered flight, should be larger than 1/8 g. With increasing thrust, the optimal mass ratio for

...

...in going to higher thrust than 1g. The strong dependence of mass ratio upon the acceleration factor is contrary to opinion that for take-off from satellite orbit only very small thrust is required.

Circumferential Thrust

If the thrust is always circumferential and horizontal to the plane of the ecliptic, then

$$\Theta = \nu \rho \tag{19}$$

By using the same non-dimensional variables as defined in Eq (6), the equations of motion are

$$\frac{d^2\rho}{d\tau^2} = \rho\left(\frac{d\theta}{d\tau}\right)^2 - \frac{1}{\rho^2} \tag{20}$$

$$\frac{d}{d\tau}\left(\rho^2 \frac{d\theta}{d\tau}\right) = \nu\rho \tag{21}$$

The initial conditions of Eqs (3) and (4) are

$$\left(\frac{d\theta}{d\tau}\right)_0 = 1\,, \quad \left(\frac{d\rho}{d\tau}\right)_0 = 0\,, \quad \text{at } \rho = 1,\ \tau = 0 \tag{22}$$

Therefore Eq (20) gives another initial condition that

$$\left(\frac{d^2\rho}{d\tau^2}\right)_0 = 0 \tag{23}$$

By elimination of ν from Eqs. (20) and (21)

[illegible]

This is a third order differential equation with three initial conditions [illegible] the single initial condition [illegible] determined in terms centered around approximations that are [illegible] of ν

For very large values of ν, the acceleration [illegible] is expected to [illegible] The value of ρ must be very close to the initial value of unity. By taking ρ to be unity, Eq. (24) becomes

$$\frac{d}{d\tau}\left(\frac{d^2\rho}{d\tau^2}+1\right)^{\frac{1}{2}} = \nu$$

Then

$$\frac{d^2\rho}{d\tau^2}+1 = C^2 + 2C\nu\tau + \nu^2\tau^2$$

where C is the integration constant. C, however, must be 1 because of the initial condition of Eq. (23). The appropriate approximate solution for ρ for very large ν is thus

$$\rho \cong 1 + \frac{1}{3}\nu\tau^3 + \frac{1}{12}\nu^2\tau^4 \qquad (25)$$

To obtain higher terms in this power series, the second order [illegible] method may be used. The calculation is somewhat lengthy and therefore will not be reproduced here. The result is

$$\rho = 1 + \frac{1}{3}\nu\tau^3 + \frac{1}{12}\nu^2\tau^4 - \frac{\pi}{10}\tau^5 - \frac{23\pi^2}{360}\tau^6 + \cdots \qquad (26)$$

By using the result of Eq (26), the radial velocity is obtained by [illegible]tion. Then Eq (10) gives the circumferential velocity. The end condition of Eq. (5) can be modified into the following more convenient form by multiplying it by r^2.

$$0 = \left[(\rho \frac{\partial \varepsilon}{\partial \tau})^2 + (\rho^2 \frac{\partial \theta}{\partial \tau})^2 - 2\rho \right]_{\tau_1}$$

obtaining τ_1 is obtained:

$$0 = -1 + 2V\tau_1 + V^2\tau_1^2 - \frac{2}{3}V\tau_1^3 + V^2\tau_1^4 + \frac{V}{30}(1+2kV^2)\tau_1^5 - \frac{V^2}{90}(4-13V^2)\tau_1^6 + \dots \quad (27)$$

$$\frac{c}{\sqrt{g r_0}} \ln(M_0/M_1) = V\tau_1 = x \quad (28)$$

$$x' = \frac{1}{2(1+x^{(1)})}\left[\frac{2}{3}x^{(0)3} - x^{(1)4} - \right.$$

(30)

$$x^{(0)2} + 2x^{(1)} - 1 = 0$$

(The acceleration will be very small and)

$$x^{(0)} = \sqrt{2} - 1 = 0.4142$$
$$x^{(1)} = 0.002349$$
$$x^{(2)} = -0.0000479$$

(41)

We complete the calculation of mass ratio for large values of the acceleration factor V.

For the other extreme case of very small values of V, it is to be expected that in Eq. (30) the term $\rho^3 \frac{d^2\rho}{d\tau^2}$ will be very much smaller than ρ. Therefore a good approximation of Eq. (30) at small V is

$$\frac{d}{d\tau}\left(\frac{d\rho}{d\tau}\right)^2 = V\rho \quad \text{or} \quad \frac{1}{2}\frac{d\rho}{\rho^{3/2}} = V\,d\tau$$

The solution of this equation with the initial condition of $\rho = 1$ at $\tau = 0$ is

$$\rho = \frac{1}{(1 - V\tau)^2} \tag{35}$$

$$\frac{d\rho}{d\tau} = \frac{2V}{(1-V\tau)^3}, \quad \frac{d^2\rho}{d\tau^2} = \frac{6V^2}{(1-V\tau)^4} \tag{36}$$

At $\tau = 0$, the radial velocity and the radial acceleration are thus not zero as required by the initial conditions of Eqs. (22) and (23). They are however very small, because V is very small. Therefore the solution of Eq. (35) is a good approximation to the exact solution.

To the same approximation, Eq. (16) becomes

$$\rho\frac{d^2\rho}{d\tau^2} = \frac{1}{\rho^2} = (1 - V\tau) \tag{37}$$

force per unit mass $r\left(\frac{d\theta}{dt}\right)^2$ practically balances the gravitational attraction at every instant. The end condition of Eq. 15) can then

be written as

$$\frac{6x^2}{(1-x)^6} - (1-x)^2 = 0 \qquad (9)$$

where x is $V\tau_j$. The appropriate solution for x is then

$$x = 1 - (2V)^{1/4} \qquad (10)$$

Since the mass ratio M_0/M_1 is related to x by Eq. (28), Eq (39) actually gives the mass ratio for exposing the gravitational field with very small acceleration.

The parameter x is plotted against V in Fig. 3, using both Eq (10) and Eq (39) (then V also $\ll 1$). x is always less than 1. When V is very large, x approaches $\sqrt{2}-1$. As V increases, x and hence the mass ratio M_0/M_1 decrease monotonically. Therefore, same as the result for purely radial thrust, there is a strong influence of the magnitude of acceleration on the required mass ratio. However so far as decreasing the mass ratio is concerned, there is no appreciable advantage in using V greater than $\frac{1}{2}$.

Discussion

By [illegible] thrust [illegible] thrust [illegible] large [illegible] the radial thrust is more than twice that for circumferential thrust. Furthermore, in case of radial thrust, the ratio of thrust to the acceleration must, of maintained constant, never be larger than $1/e$. In case of circumferential thrust, no such limit exist. Therefore circumferential thrust is definitely preferred

The quantity $c \log(M_0/M_1)$ is a measure of the performance of the

capability of the vehicle. It has the dimension of a velocity and is actually the increase of velocity which the vehicle is capable of in absence of [illegible] gravitation. The quantity [illegible] would be the velocity of the vehicle [illegible] would be denoted by V_0. Then for the case of circumferential thrust, Eq 12c) gives

$$V = c \log(M_0/M_1) = \sqrt{g r_0}\, x = \frac{S}{\sqrt{2\lambda}}\, x \qquad (40)$$

[illegible] λ is the ratio of the radii of the satellite orbit and the earth. S is equal to 11.2 km/sec. Fig. 3 then shows that by increasing the [illegible] x [illegible] velocity V, will increase by a factor of two. This is a very important point for the designers of space ships.

References

1. "Interplanetary Travel between Satellite Orbits" by [illegible] Journal of the American Rocket Society, Vol 22, pp 92-96 (1952)

2. "Interplanetary Transport Trajectories" by [illegible] Journal of the British Interplanetary Society, Vol. 11, pp. 173-193 (1952)

3. "Man on the Moon, The Journey" by W. von Braun Collier's. Oct. 18, 1952 p. 52

Take-Off From Satellite Orbit

H. S. Tsien*

Summary

The mass ratio or the characteristic velocity for the take-off of a space ship from the satellite orbit is computed for two cases: the radial thrust and the circumferential thrust. The circumferential thrust is much more efficient in that the required mass ratio is much less than for the radial thrust. Both cases show, however, an increase of the required mass ratio and the characteristic velocity with a reduction in acceleration. With circumferential thrust, the characteristic velocity increases by a factor of two when the acceleration is reduced from 1/2 g to 1/3000 g.

* Robert H. Goddard Professor of Jet Propulsion

For take-off of a rocket from the earth surface, it is convenient to have the initial trajectory in the vertical direction and then the thrust should be considerably larger than the initial weight of the rocket. Because of the relative magnitudes of the aerodynamic drag and the weight, the initial ratio of the thrust and the weight should be between 2 and 3 for minimum expenditure of the propellant. The situation is quite different for a space ship taking off from the satellite orbit: In a satellite orbit, the gravitational attraction is completely balanced by the centrifugal force, and the vehicle is effectively in a weightless state. This fact has led many fanciers of interplanetary travel to conclude that take-off from satellite orbit requires only a very minute thrust. For instance, L. Spitzer (Ref. 1) proposed a nuclear power plant for a space ship to be accelerated at only 1/3000 g. Another example is the extensive discussion of interorbital transport techniques by H. Preston-Thomas (Ref. 2) based upon the assumption of equally small acceleration. On the other hand, W. von Braun (Ref. 3) seems to prefer a very much larger acceleration of approximately 1/2 g for take-off from the satellite orbit.

The magnitude of the acceleration has a strong bearing on the optimum type of power plant to be used: The ion-beam rocket is only possible for very small acceleration, while for moderate acceleration, chemical rocket is required. Therefore the question of the magnitude of acceleration is an important one for interplanetary flight. The purpose of this note is to demonstrate clearly the relation between the acceleration and the velocity required for escape from the earth's gravitational field, starting from the satellite orbit. It is hoped that the present investigation will give the future generation of astronautical engineers a more rational basis for designing space ships.

Basic Equations

The problem considered is the motion of a space ship under the influence of the rocket thrust and the gravitational attraction of a single massive body, say the earth. Then if the rocket thrust is in the plane of trajectory, the trajectory of the space ship will remain in a plane. Let the position of the ship at any time instant t be given by the polar coordinates r and θ : r the distance from the center of attraction, and θ the angular position. If the components of the rocket thrust per unit mass of the vehicle are R in the radial direction and Θ in the circumferential direction, and if g is the magnitude of gravitational attraction at the starting satellite orbit $r = r_0$ (Fig. 1), then the equations of motion of the space ship are

$$\frac{d^2r}{dt^2} = R + r\left(\frac{d\theta}{dt}\right)^2 - g\left(\frac{r_0}{r}\right)^2 \qquad (1)$$

and

$$\frac{d}{dt}\left(r^2\frac{d\theta}{dt}\right) = r\Theta \qquad (2)$$

By using the subscript 0 to indicate quantities at the starting instant $t = 0$, the equilibrium condition of the satellite orbit is given by

$$r_0\left(\frac{d\theta}{dt}\right)_0^2 = g \qquad (3)$$

Initially, the radial velocity is zero, i.e.,

$$\left(\frac{dr}{dt}\right)_0 = 0 \qquad (4)$$

These are the initial conditions. For the space ship to have sufficient energy to escape the earth gravitational field at the end of the powered flight, the sum of the kinetic energy and potential energy must vanish at the end of the

end of the accelerating period. Let that instant be denoted by the subscript 1. Thus at $t = t_1$

$$\frac{1}{2}\left[\left(\frac{dr}{dt}\right)_1^2 + \left(r\frac{d\theta}{dt}\right)_1^2\right] - g\frac{r_e^2}{r_1} = 0 \qquad (5)$$

With any specified variation of the thrust forces R and Θ as functions of time, the above system of equations determine completely the take-off trajectory of the space ship. In the following sections, two special cases of practical significance will be discussed in detail: the case R = constant, $\Theta \neq 0$, purely radial thrust; and the case R = 0, Θ = constant, purely circumferential thrust.

Radial Thrust

If the thrust is always radial and is proportional to the instantaneous mass of the vehicle, a non-dimensional thrust factor μ can be introduced as

$$T = \mu M_1 \qquad (7)$$

Furthermore, let

$$\rho = \frac{r}{r_e} \qquad \tau = \frac{t}{\sqrt{r_e/g}} \qquad (6)$$

where ρ and τ are respectively the non-dimensional radial distance and time. Then Eqs. (1) and (2) can be written in the nondimensional form as

$$\frac{d^2\rho}{d\tau^2} = \mu + \rho\left(\frac{d\theta}{d\tau}\right)^2 - \frac{1}{\rho^2} \qquad (7)$$

and

$$\frac{d}{d\tau}\left(\rho^2\frac{d\theta}{d\tau}\right) = 0 \qquad (8)$$

Eq. (8) can be immediately integrated and by using the initial condition of Eq. (3), the result of integration is

$$\frac{d\theta}{d\tau} = \frac{1}{\rho^2} \qquad (9)$$

By substituting this equation into Eq. (7), the final equation for ζ is

$$\frac{d^2\zeta}{d\tau^2} = \mu + \frac{1}{\zeta^3} - \frac{1}{\zeta^2} \tag{10}$$

The nondimensional radial velocity is $d\zeta/dt$. This is related to the physical radial velocity dr/dt as follows

$$\frac{dr}{dt} = \sqrt{gr_0}\,\frac{d\zeta}{d\tau} \tag{11}$$

Eq. (10) can be rewritten as

$$\frac{1}{2}\frac{d}{d\zeta}\left(\frac{d\zeta}{d\tau}\right)^2 = \mu + \frac{1}{\zeta^3} - \frac{1}{\zeta^2}$$

Since $d\zeta/dt = 0$ when $t = 0$ and $\zeta = 1$ according to Eq. (4), the result of integrating the above equation is

$$\left(\frac{d\zeta}{d\tau}\right)^2 = 2\mu(\zeta - 1) + \left(1 - \frac{1}{\zeta^2}\right) - 2\left(1 - \frac{1}{\zeta}\right) \tag{12}$$

Therefore the non-dimensional time τ can be calculated as a function of the radius ζ as follows

$$\tau = \int \frac{\zeta\, d\zeta}{\sqrt{(\zeta - 1)[2\mu\zeta^2 - \zeta + 1]}} \tag{13}$$

With Eqs. (9) and (12), the end condition of Eq. (5) can be written as

Or simply

$$\eta_1 = 1 + \frac{1}{2\mu} \tag{14}$$

Then the velocities at the end of acceleration period are

and

The time τ_1 for the powered flight can be obtained from E_1 (15) by setting the upper limit of integration to ξ_1. Thus the result of this integration is*

$$\tau_1 = \frac{1}{\mu} \left[\frac{2}{2n+1} + F\left(\frac{\pi}{4}, \sin\frac{\xi_1}{2}\right) + E\left(\frac{\pi}{4}, \sin\frac{\xi_1}{2}\right) \right] \qquad (16)$$

where F and E are the elliptical integrals of first kind and second kind respectively.

If $M(t)$ is the instantaneous mass of the space ship, and c the effective exhaust velocity of the rocket, then

$$RM = \mu g M = -c \frac{dM}{dt} = -c\sqrt{\frac{g}{r_0}} \frac{dM}{d\tau}$$

Therefore the mass ratio M_0/M_1 can be calculated as follows:

$$\log(M_0/M_1) = \sqrt{\frac{g r_0}{c}}\, \mu \tau_1$$

By using the result of Eq. (16),

$$\frac{c}{\sqrt{g r_0}} \log(M_0/M_1) = \frac{2}{2n+1} + F\left(\frac{\pi}{4}, \sin\frac{\xi_1}{2}\right) + E\left(\frac{\pi}{4}, \sin\frac{\xi_1}{2}\right) \qquad (17)$$

When the acceleration is very large, $\mu >> 1$, the integrand in Eq. (15) can be expanded in terms of this parameter. Then the mass ratio

$$\frac{c}{\sqrt{g r_0}} \log(M_0/M_1) = 1 + \frac{1}{24\mu^2} - \frac{1}{40\mu^4} + \cdots \qquad (18)$$

The relation of Eqs. (17) and (18) is plotted in Fig. 2. For $\mu = \frac{1}{\xi}$, the mass ratio becomes infinite. The reason is that at this value of

---

* The author is indebted to Dr. Y. T. Wu who kindly supplied the relation of Eq. (16).

Insert for p. 6

97'

Eq (15) shows that at very large values of the acceleration factor p, the acceleration is accomplished in so short an interval that the circumferential velocity at the end of the acceleration remains at the initial value of $\sqrt{gr_0}$. The radial velocity increases from nothing at the initial instant to the final value of $\sqrt{gr_0}$. The total kinetic energy is thus gr_0 at the end of acceleration and this is equal to the negative of potential energy at that instant, since the radial position r must be [illegible] r_0 [illegible]
work of the rocket is to produce the radial velocity $\sqrt{gr_0}$. Thus it is evident that the value of $c' \log (M_0/M_1)$ must be $\sqrt{gr_0}$, as the calculation shows.

acceleration, there is a radial position where the thrust force is equal to the gravitational attraction and one further increase in the energy of the vehicle can occur. Therefore the radial thrust per unit mass, if maintained constant throughout the powered flight, should be larger than 1/8 g. With increasing thrust, the required mass ratio for escape from the earth's gravitational field decreases. The asymptotic value of [illegible] However there is no appreciable improvement in energy for a thrust greater than 1 g. This strong dependence of the mass ratio upon the acceleration factor is contrary to our notion that for take-off from earth the most economical thrust is required.

>

Circumferential Thrust

If the thrust is always circumferential and proportional to the mass of the vehicle, then a new thrust factor Θ can be introduced such that

$$\Theta = \nu g \tag{19}$$

By using the same non-dimensional variables as defined in Eq. (6), the equations of motion are

[illegible] (21)

[illegible] (21')

The initial conditions of Eqs. (3) and (4) are

$$\left(\frac{dL}{dT}\right)_0 = 1, \quad \left(\frac{d\ell}{dT}\right)_0 = 0, \quad \text{at} \quad \zeta = 1, \quad \tau = 0 \tag{22}$$

Therefore Eq. (20) gives another initial condition that

$$\left(\frac{d^2\ell}{dT^2}\right)_0 = 0 \tag{23}$$

By eliminating β from Eqs. (20) and (21),

$$\frac{d}{dt}\left(\zeta^3\frac{d^2\rho}{dt^2}+\rho\right)^{\frac{1}{2}}=\nu\rho \tag{24}$$

This is a third order differential equation with three initial conditions specified by Eqs. (18) and (23). No simple general solution can, however, be obtained. The following discussion is thus centered around approximations that are valid for large values of ν or small values of ν.

For very large values of ν, the acceleration period is expected to be short and the change of the radial position to be small. Then the value of ρ must be very close to the initial value of unity. By taking ζ to be unity, Eq. (24) becomes

$$\frac{d}{dt}\left(\frac{d^2\rho}{dt^2}+1\right)^{\frac{1}{2}}=\nu$$

Then

$$\frac{d^2\rho}{dt^2}+1=C^2+2C\nu t+\nu^2t^2$$

where C is the integration constant. C, however, must be 1 because of the initial condition of Eq. (23). The appropriate approximate solution for ζ for very large ν is thus

$$\zeta\cong 1+\frac{1}{3}\nu t^3+\frac{1}{12}\nu^2t^6 \tag{25}$$

To obtain higher terms in this power series, the usual series substitution method may be used. The calculation is somewhat lengthy and therefore will not be reproduced here. The result is

$$\zeta=1+\frac{1}{3}\nu t^3+\frac{1}{12}\nu^2t^6-\frac{\nu}{60}t^5-\frac{23\nu^2}{360}t^6+\cdots \tag{26}$$

By using the result of Eq. (26), the radial velocity is obtained by differentiation. Then Eq. (28) gives the circumferential velocity. The end condition of Eq. (5) can be modified into the following more convenient form by multiplying it by $\frac{1}{2}r^2$:

$$0 = \left[\left(\rho \frac{df}{dz}\right)^2 + \left(\rho^2 \frac{dh}{dz}\right)^2 - 2\rho\right]_1$$

By substituting the solution of Eq. (26) into this condition, an equation for determining T_1 is obtained.

$$[\text{illegible}] \qquad (27)$$

The mass ratio M_0/M_1 can be calculated in the same way as in the previous section and can be determined through the new parameter x defined as follows:

$$\frac{c}{\sqrt{g r_0}} \log (M_0/M_1) = V T_1 = X \qquad (28)$$

Eq. (28) then can be written as

$$[\text{illegible}] \qquad (29)$$

Since the calculation is designed for large values of V, the appropriate expansion of x should be a series in inverse powers of V. Eq. (29) suggests specifically

$$X(V) = X^{(0)} + \frac{X^{(1)}}{V^2} + \frac{X^{(2)}}{V^4} + \cdots \qquad (30)$$

where $x^{(0)}$, $x^{(1)}$ and $x^{(2)}$ are constants independent of V. By substituting Eq. (30) into Eq. (29) and equating equal powers of V, the following set of equations results:

$$x^{(0)2} + 2x^{(0)} - 1 = 0 \tag{31}$$

$$x^{(1)} = \frac{1}{2(1+x^{(0)})}\left[\frac{2}{3}x^{(0)3} - x^{(0)4} - \frac{13}{15}x^{(0)5} - \frac{13}{90}x^{(0)6}\right] \tag{32}$$

$$x^{(2)} = \frac{1}{2(1+x^{(0)})}\left[\frac{1}{3}x^{(0)4} + \frac{2}{3}x^{(0)5} + \frac{1}{6}x^{(0)6} - \frac{13}{3}x^{(0)}x^{(1)2} - \frac{26}{3}x^{(0)2}x^{(1)2} - \frac{13}{3}x^{(0)3}x^{(1)2} - 13x^{(0)}x^{(1)}x^{(2)} - 13x^{(0)2}x^{(1)}x^{(2)} - 13x^{(1)2}x^{(2)} - 13x^{(0)}x^{(2)2} - 13x^{(1)}x^{(2)2}\right] \tag{33}$$

The explicit numerical solutions are then

$$x^{(0)} = \sqrt{2} - 1 = 0.41421 \tag{34}$$

$$x^{(1)} = 0.002349$$

$$x^{(2)} = -0.0000479$$

This completes the calculation of mass ratio for large values of the acceleration factor V.

For the other extreme case of very small values of V, it is to be expected that in Eq. (28), the acceleration will be very small and the term $\rho^{1/2}\frac{d\rho}{d\tau}$ will be very much smaller than ρ. Therefore a good approximation of Eq. (28) at small V is

$$\frac{d\rho}{d\tau} = 0 \quad \text{or} \quad \frac{1}{2}\frac{d\rho}{\rho^{1/2}} = V\,d\tau$$

The solution of this equation with the initial condition of $\rho = 1$ at $\tau = 0$ is

$$\rho = \frac{1}{(1 - V\tau)^2} \tag{35}$$

Then

$$\frac{dL}{dT} = \frac{2V}{(1-VT)^3} \quad , \quad \frac{d^2L}{dT^2} = \frac{6V^2}{(1-VT)^4} \tag{37}$$

At $T=0$, the radial velocity and the radial acceleration are thus not zero as required by the boundary conditions of Eqs. (22) and (24). They are however very small, because V is very small. Therefore the solution of Eq. (36) is a good approximation to the exact solution.

To the same approximation, Eq. (20) becomes

$$\frac{dH}{dL} = \frac{1}{g^{1/2}} = (1-VT) \tag{38}$$

This means that because of the extremely small acceleration the centrifugal force per unit mass $r\left(\frac{dL}{dT}\right)^2$ practically balances the gravitational attraction at every instant. The end condition of Eq. (5) can then be written as

$$\frac{4V^2}{(1-X)^6} - (1-X)^2 = 0 \tag{39}$$

where X is $\hat{VT_1}$. The appropriate solution for X is then

$$X = 1 - (2V)^{1/4} \tag{40}$$

Since the mass ratio M_0/M_1 , is related to X by Eq. (28), Eq. (39) actually gives the mass ratio for escaping the gravitational field with very small acceleration.

The parameter X is plotted against V in Fig. 3, using both Eq. (30) with Eq. (34) and Eq. (39). When V approaches zero, X approaches 1.

with positively no change in
Invert for ϕ 11__ the radial position.

Q4

The ii. acceleration factor V is very large the [illegible] note like an impulse since the thrust is in [illegible] transversal direction, the rocket action only [illegible] the [illegible] transversal velocity V the radial transversal velocity $= V\sqrt{2gr_0}$ the required circumferential velocity for circ. $= \sqrt{2gr_0}$. Thus the increase of velocity produced by the rocket act. is $(NE-1)\sqrt{gr_0}$. This explains the asymptotic value of x for very large V.

hence the mass ratio M_0/M_1, decrease monotonically. Therefore, same as the result for purely radial thrust, there is a strong influence of the magnitude of acceleration on the required mass ratio. However as far as decreasing the mass ratio is concerned, there is no appreciable advantage in using γ greater than 1/2.

Discussion

By comparing Fig. 2 with Fig. 3, it is apparent that the radial thrust is much less efficient than the circumferential thrust for take-off from the satellite orbit. For large thrusts, the value of $\log(M_0/M_1)$ for radial thrust is more than twice that for circumferential thrust. Furthermore, in case of radial thrust, the ratio of thrust to the instantaneous mass, if maintained

such limit exist. Therefore circumferential thrust is definitely preferred.

The quantity $c \log(M_0/M_1)$ is a measure of the performance or the capability of the vehicle. It has the dimension of a velocity and is actually the increase of velocity which the vehicle is capable of in space without gravitation. This quantity is conveniently called the characteristic velocity of the vehicle. Let this be denoted by V. Then for the case of circumferential thrust, Eq. (28) gives

$$V = c \log(M_0/M_1) = \sqrt{g r_0}\, x = \frac{\hat{v}}{\sqrt{2\lambda}}\, x \tag{40}$$

where $\hat{v}$ is the "escape velocity" from the surface of the earth and λ is the ratio of the radii of the satellite orbit and the earth. $\hat{v}$ is equal to 11.2 km/sec. Fig. 3 then shows that by decreasing the acceleration $\ldots$

1/2 to 1/3000 g. ℓ . Hence the required characteristic velocity V , will increase by a factor of two. This is a very important point for the designers of space ships.

REFERENCES

1. "Interplanetary Travel between Satellite Orbits" by L. Spitzer, Jr. Journal of the American Rocket Society, Vol. 22 pp 92-96 (1952)

2. "Interorbital Transport Techniques" by H. Preston-Thomas. Journal of the British Interplanetary Society, Vol. 11 pp 173-183 (1952).

3. "Man on the Moon, the Journey" by W. von Braun. Collier's, Oct. 18, 1952, p. 52.

Satellite Orbit

Satellite Orbit

Fig 2 Mass Ratio factor $\frac{c}{\sqrt{2}T_0}\log(M_0/M_1)$ against Acceleration factor [illegible] at the Satellite Orbit of Radius T_0; M_0, Initial Mass; M_1, Final Mass; p, the Ratio of Instantaneous Thrust per unit Mass and g.

Mass Ratio factor $\sqrt{\frac{1}{T_0}}\log(M_0/M_1)$ against Acceleration factor V for Circumferential Thrust. c, Effective Exhaust Velocity; g, [illegible] at the Orbit of Radius r_0 [illegible] M_0, Initial Mass, M_1, Final Mass, V, the Ratio of Instantaneous Thrust per unit Mass and g.

AMERICAN ROCKET SOCIETY, INC.
20 WEST 39TH STREET
NEW YORK 18, N. Y.

Department Aeronautical Engineering
Princeton University
Princeton New Jersey

December 4, 195[illegible]

Prof. H. S. Tsien
[illegible] Institute of Technology
[illegible] Pasadena California Street
Pasadena [illegible]

[illegible]

I have read your paper on [illegible] for the Journal. I [illegible] no reason to [illegible] publication. I have, however, sent it to seek additional reviews, as I have requested the New York Office for publication. It will appear in the March April issue of the J[illegible] forthcoming contribution.

Thank you for your evaluation of the Feldman paper. We are going ahead to publish it.

With best regards

Sincerely yours,

Martin Summerfield

Martin Summerfield
[illegible]

Section 7

Circumferential Acceleration

Incremental Acceleration

$$\frac{d}{dt}\left(r^2\frac{d\theta}{dt}\right) = 0r$$

$$\frac{d^2r}{dt^2} = r\left(\frac{d\theta}{dt}\right)^2 - g\frac{r_0^2}{r^2}$$

$$\left(r^3\frac{d^2r}{dt^2} + gr_0^2r\right)^{\frac{1}{2}} = r^2\frac{d\theta}{dt}$$

$$\frac{d}{dt}\left(\frac{dr}{dt}\right)^2 + gr_0^2r^{-1} = \left(r^2\frac{d\theta}{dt}\right)^2$$

$$r = r_0\left[1 + a_3\left(\frac{t}{r_0}\right)^{\frac{2}{3}}t^3 + a_4\left(\frac{t}{r_0}\right)^3t^4 + a_5\left(\frac{t}{r_0}\right)^{\frac{5}{3}}t^5 + a_6\left(\frac{t}{r_0}\right)^4t^6 + \cdots\right]$$

$$\frac{dr}{dt} = g\left[6a_3\left(\frac{t}{r_0}\right)^{\frac{1}{3}}t + 12a_4\left(\frac{t}{r_0}\right)t^2 + 20a_5\left(\frac{t}{r_0}\right)^{\frac{4}{3}}t^3 + \cdots\right]$$

$$r^3 = r_0^3\left[1 + 3a_3\left(\frac{t}{r_0}\right)^{\frac{2}{3}}t^3 + \cdots\right]$$

$$\frac{d^2r}{dt^2} = gr_0\left[6a_3\left(\frac{t}{r_0}\right)^{\frac{1}{3}}t + 20a_5\left(\frac{t}{r_0}\right)^{\frac{2}{3}}t^2 + \cdots\right]$$

$$gr_0^2r = gr_0^3\left[1 + a_3\left(\frac{t}{r_0}\right)^{\frac{2}{3}}t^3 + a_4\left(\frac{t}{r_0}\right)^3t^4 + \cdots\right]$$

$$r\frac{d^2r}{dt^2} + gr_0r = gr_0^3\left[1 + 10a_3\left(\frac{t}{r_0}\right)^{\frac{2}{3}}t^3 + 15a_4\left(\frac{t}{r_0}\right)^3t^4 + (30a_5 + a_3^2)\left(\frac{t}{r_0}\right)^{\frac{5}{3}}t^5 + \cdots\right]$$

$$r^2\left(\frac{d\theta}{dt}\right)^2 = gr_0^3\left[1 + 4a_3\left(\frac{t}{r_0}\right)^{\frac{2}{3}}t^3 + 6a_4\left(\frac{t}{r_0}\right)^3t^4 + \left(15a_5 + \frac{9}{2}a_3^2\right)\left(\frac{t}{r_0}\right)^{\frac{5}{3}}t^5 + \cdots\right]$$

$$-\frac{1}{9}a_3^2\left(\frac{t}{r_0}\right)^2t^4 - \frac{1}{9}(4a_4 + 3a_3a_5)\left(\frac{t}{r_0}\right)^{\frac{7}{3}}t^7 + \cdots$$

$$-\frac{5}{18}a_3^3\left(\frac{t}{r_0}\right)^{\frac{4}{3}}t^6 + \frac{5}{11}(3a_3^2a_4 + 2a_5)\left(\frac{t}{r_0}\right)^{\frac{8}{3}}t^8 + \cdots$$

$$-\frac{55}{432}a_3^4\left(\frac{t}{r_0}\right)^2t^8 + \cdots\Big]$$

$$\text{Lit} \qquad \Theta = n\eta$$

$$n\left[1 + \cdots + a_3\left(\frac{r}{r_0}\right)^{3k} t^3 + \cdots\right]$$

$$= a_3 + 2\left[10a_4 - \frac{9}{2}a^2\right]\left(\frac{\rho}{r_0}\right)^{1/2} t + 3\left[10a_5 + \frac{a_3}{2} - 18\,a_3 a_4 + \frac{21}{2}a_3^3\right]\frac{\rho}{r_0} t^2$$

$$+ \cdots \frac{a_3}{2} + \cdots a_2 + a_3 a_2^2 - 18 a_4^2 - \frac{3}{2}a_3(20a_2 + a_3) + 81\,a_3^2 a_4 - \frac{5\times 21}{8}a_3^4\left(\frac{\rho}{r_0}\right)^{3/2} t^3 + \cdots$$

Then $n = 3a_3$,

$$a_3 = \frac{n}{3}$$

$$10a_4 = \frac{9}{2}a_3^2 \qquad a_4 = \frac{n^2}{12}$$

$$a_5 \cdots - \frac{a_3}{20} + \frac{9}{10}a_3 a_4 - \frac{3}{20}a_3^3 = -\frac{n}{60} + n^3\,\frac{14}{10}\,\frac{1}{3}\,\frac{1}{12} - n^3\,\frac{27}{20}\,\frac{1}{27}$$

$$a_5 = -\frac{n}{60}$$

$$\cdots^2 = \frac{a_3^2}{4} + \cdots a_4 + \cdots^2 - 18\,\frac{n^2}{144} - \frac{n}{2}\left(-\frac{1}{3} + \frac{2}{3}\right) + 9n^2\,\frac{n^2}{12} \qquad \frac{\cdots n^4}{8}$$

$$15\,a_6 = -\frac{23}{24}n^2 \qquad a_6 = -\frac{23n^2}{15\times 24}$$

$$\eta - r_0\left[1 + \frac{n}{3}t^3 + \frac{n^2}{12}t^4 - \frac{n}{60}t^5 - \frac{23n^2}{15\times 24}t^6 + \cdots\right] \qquad t = \sqrt{\frac{g}{r_0}}\,t$$

$$\frac{dr}{dt} = \sqrt{\frac{g}{r_0}}\,\frac{dr}{dt}$$

$$u - \frac{dr}{dt} = \sqrt{\frac{g}{r_0}}\left[\cdots t^2 + \frac{n^2}{3}t^3 - \frac{n}{12}t^4 - \frac{23}{60}n^2 t^5 + \cdots\right]$$

$$u^2 = gr_0\left[n^2 t^4 + \frac{2}{3}n^3 t^5 + \left(\frac{n^4}{9} - \frac{n^2}{6}\right)t^6 + \cdots\right]$$

$$r^2\left(\frac{d\theta}{dt}\right)^2 = r_0^3 g\left[1 + 2n\tau + \left(n^2 + \frac{n}{10}\right)\tau^2 + \left(\frac{n^2}{5} + \frac{n}{70}\right)\tau^3 - \left(\frac{n^2}{70} - \frac{n}{350}\right)\tau^4 + \cdots\right]$$

$$r^2\left(\frac{d\theta}{dt}\right)^2 = r_0^3 g\left[1 + 2n\tau + \left(n^2 + \frac{n}{10}\right)\tau^2 + \left(\frac{n^2}{5} + \frac{n}{70}\right)\tau^3 - \left(\frac{n^2}{70} - \frac{n}{350}\right)\tau^4 + \cdots\right]$$

$$\left(r^2\frac{d\theta}{dt}\right)^2 = r_0^3 g\left[1 + 2n\tau + \left(n^2 + \frac{n}{10}\right)\tau^2 + \left(\frac{n^2}{5} + \frac{n}{70}\right)\tau^3 - \left(\frac{n^2}{70} - \frac{n}{350}\right)\tau^4 + \cdots\right]$$

$$= r_0^3 g\left[1 + 2n\tau + \left(n^2 + \frac{n}{10}\right)\tau^2 + \left(\frac{n^2}{5} + \frac{n}{70}\right)\tau^3 - \left(\frac{n^2}{70} - \frac{n}{350}\right)\tau^4 + \cdots\right]$$

$$r^2\left(n^2 + \frac{1}{r^3}\right) = r_0^3 g\left[1 + 2n\tau + n^2\tau^2 + \frac{1}{6}\tau^3 + \frac{1}{12}\tau^4 + \cdots\right]$$

$$= r_0^3 g\left[1 + 2n\tau + n^2\tau^2 + \frac{1}{6}\tau^3 - \frac{n^2}{6}\tau^4 + \cdots\right]$$

$$= r_0^3 g\left[n^2\tau^4 + \frac{2}{3}n^3\tau^5 - \frac{n^2}{6}\left(1 - \frac{2}{3}n^2\right)\tau^6 + \cdots\right]$$

$$r^2\left(n^2 + \frac{1}{r^3}\right) = r_0^3 g\left[1 + 2n\tau + n^2\tau^2 + \frac{1}{6}\tau^3 + \frac{1}{12}\tau^4 + \cdots\right]$$

$$= r_0^3 g\left[1 + 2n\tau + n^2\tau^2 + \frac{1}{6}\tau^3 - \frac{n^2}{6}\tau^4 + \cdots\right]$$

$$= r_0^3 g\left[n^2\tau^4 + \frac{2}{3}n^3\tau^5 - \frac{n^2}{6}\left(1 - \frac{2}{3}n^2\right)\tau^6 + \cdots\right]$$

r_1 is then given by

$$0 = -1 + 2n\tau_1 + n^2\tau_1^2 - \frac{2}{3}n\tau_1^3 + n^2\tau_1^4 + \frac{n}{30}\left(1 + 26n^2\right)\tau_1^5 + \left(-\frac{2}{180}n^2 + \frac{13}{90}n^4\right)\tau_1^6 + \cdots$$

$$\eta\tau_y = x$$

$$\cdot = 2x + x^2 - \frac{2}{3}\frac{x^3}{\eta^2} + \frac{x^4}{\eta^2} + \frac{x^5}{\eta^4} + \frac{13}{15}\frac{x^5}{\eta^2} - \frac{4}{14}\frac{x^6}{\eta^6} + \frac{13}{90}\frac{x^6}{\eta^2} \cdots$$

$$x = x^{(0)} + \frac{2}{\eta^2}x^{(0)} + \frac{4}{\eta^4}x^{(2)} + \cdots$$

$$x^2 = x^{(0)^2} + \frac{2}{\eta^2}x^{(0)}x^{(1)} + \frac{4}{\eta^4}\left(x^{(1)^2} + 2x^{(0)}x^{(2)}\right) + \cdots$$

$$x^3 = x^{(0)^3} + \frac{3}{\eta^2}x^{(0)^2}x^{(1)} + \cdots$$

$$x^4 = x^{(0)^4} + \frac{4}{\eta^2}x^{(0)^3}x^{(1)} + \cdots$$

$$x^5 = x^{(0)^5} + \frac{5}{\eta^2}x^{(0)^4}x^{(1)} + \cdots$$

$$x^6 = x^{(0)^6} + \frac{6}{\eta^2}x^{(0)^5}x^{(1)} + \cdots$$

$$= x^6 + x^{(1)^2} + \frac{1}{\eta^2}\left(2x^{(1)}x^{(2)} + x^{(1)^3} + 3x^{(0)^2}x^{(2)} + 3x^{(0)}x^{(1)^2} + x^{(1)^3} + 6x^{(0)^2}x^{(2)}\right)$$

$$+ \frac{1}{\eta^4}\Big(2x^{(2)} + x^{(1)^2} + 2x^{(0)}x^{(2)} - \frac{2}{3}3x^{(0)^2}x^{(2)} + 4x^{(0)^2}x^{(2)}$$

$$+ \frac{1}{30}x^{(2)^2} + \frac{13}{15}5x^{(0)^4}x^{(2)} - \frac{4}{140}x^{(2)^6} + \frac{13}{90}6x^{(0)^5}x^{(2)}\Big)$$

$$x^7 = x^{(0)^7}$$

$$\cdot\ \eta = \frac{\pi M}{R^2}$$

$$\cdot\ \cdot\ \frac{\Delta}{\rho_1} - \frac{1}{2}\pi g t = \frac{4\beta\sigma}{c}\pi\tau_y$$

$$\text{[illegible]}\quad M_c - \text{[illegible]}\quad x$$
$$M_1$$

[illegible] $\ll 1$, then

$$r^3 \frac{d^2r}{dt^2} \ll g r_0^2 r$$

So as a first approximation,

$$r_0 n \sqrt{g}\, \frac{dr}{dt} = n g r$$

$$\frac{1}{2} r_0 n \sqrt{g}\, \frac{dr}{r^{3/2}} = n g\, dt$$

$$r_0 n \sqrt{g} \left\{ \frac{1}{r_0^{1/2}} - \frac{1}{r^{1/2}} \right\} = n g t$$

whence

$$\frac{1}{r_0^{1/2}} - \frac{1}{r^{1/2}} = n \frac{1}{r_0^{1/2}} \sqrt{\frac{g}{r_0}}\, t$$

$$\frac{1}{r_0^{1/2}} \left(1 - n \sqrt{\frac{g}{r_0}}\, t \right) = \frac{1}{r^{1/2}}$$

$$r = r_0 \frac{}{(1 - n \sqrt{\frac{g}{r_0}}\, t)^2}$$

$$\frac{dr}{dt} = r_0 \frac{-2r}{1 - n \sqrt{\frac{g}{r_0}}\, t}$$

$$r \frac{dr}{dt} = r_0^2 n \sqrt{\frac{g}{r_0}} + n g \int_0^t r_0 \frac{dt}{(1 - n \sqrt{\frac{g}{r_0}}\, t)^2}$$

$$= r_0 n \sqrt{g r_0} \left\{ 1 + \int_0^{n \sqrt{\frac{g}{r_0}}\, t} \frac{d\xi}{(1-\xi)^2} \right\}$$

$$= r_0 n \sqrt{g r_0} \left\{ 1 + \frac{n \sqrt{\frac{g}{r_0}}\, t}{1 - n \sqrt{\frac{g}{r_0}}\, t} \right\}$$

$$r \frac{dr}{dt} = n \sqrt{g r_0}\, (1 - n \sqrt{\frac{g}{r_0}}\, t)$$

At $t=t_1$ $\quad x\sqrt{\frac{2}{r_0}}\,t_1 = x\tau_1 = x$

$$0 = \left[\frac{dx}{dt}\right]^2 + \left[\frac{dy}{dt}\right]^2 - 2\frac{2r_0^2}{\tau}$$

$$0 = \frac{4n^2}{(1-x)^6} + (1-x)^2 - 2(1-x)^2$$

$$4n^2 = (1-x)^8$$

$$1-x = 2^{1/4} n^{1/4}$$

$$\tau^2 \left[\frac{dx}{dt}\right]^2 = r_0^4 \left(\frac{1}{\tau^6}\right) \frac{n^2 \frac{g}{r_0}}{\left(1-x\right)^6}$$

$$g r_0^2 = g r_1^2 \left(1-\tau_1^2\right)$$

$$\tau \left[\frac{dx}{dt}\right] g r_0^2 = \frac{n^2}{\left(1-\tau_1^2\right)^3}$$

Circumferential Acceleration

$$\frac{1}{dt}\left(r^2\frac{d\theta}{dt}\right) = \Theta r$$

$$\frac{d^2r}{dt^2} = r\left(\frac{d\theta}{dt}\right)^2 - g\frac{r_0^2}{r}$$

$$\left(r^3\frac{d^2r}{dt^2} + gr_0^2 r\right)^{\frac{1}{2}} = r^2\frac{d\theta}{dt}$$

$$\frac{d\theta}{dt}\left(r^3\frac{d^2r}{dt^2} + gr_0^2 r\right)^{\frac{1}{2}} = \Theta r$$

$$r = r_0\left[1 + a_2\left(\frac{g}{r_0}\right)^{\frac{1}{2}}t^3 + a_4\left(\frac{g}{r_0}\right)^2 t^4 + a_5\left(\frac{g}{r_0}\right)^{\frac{5}{2}}t^5 + \cdots\right]$$

$$\frac{d^2r}{dt^2} = \cdots + 10a_3\left(\frac{g}{r_0}\right)^{\frac{3}{2}}t + 12a_4\left(\frac{g}{r_0}\right)t^2 + 20a_5\left(\frac{g}{r_0}\right)^{\frac{5}{2}}t^3 + \cdots$$

$$r^3 = r_0^3\left[1 + \cdots\right]$$

$$r^3\frac{d^2r}{dt^2} = r_0^3 g\left[10a_3\left(\frac{g}{r_0}\right)^{\frac{1}{2}}t + 12a_4\left(\frac{g}{r_0}\right)t^2 + 20a_5\left(\frac{g}{r_0}\right)^{\frac{3}{2}}t^3 + \cdots\right]$$

$$gr_0^2 r = r_0^3 g\left[1 + a_3\left(\frac{g}{r_0}\right)^{\frac{1}{2}}t^3 + \cdots\right]$$

$$r^3\frac{d^2r}{dt^2} + gr_0^2 r = r_0^3 g\left[1 + 10a_3\left(\frac{g}{r_0}\right)^{\frac{1}{2}}t + 12a_4\left(\frac{g}{r_0}\right)t^2 + 15a_5\left(\frac{g}{r_0}\right)^{\frac{3}{2}}t^3 + \cdots\right]$$

$$\left(r^3\frac{d^2r}{dt^2} + gr_0^2 r\right)^{\frac{1}{2}} = r_0^{\frac{3}{2}}g^{\frac{1}{2}}\left[1 + 5a_3\left(\frac{g}{r_0}\right)^{\frac{1}{2}}t + 6a_4\left(\frac{g}{r_0}\right)t^2 + 7a_5\left(\frac{g}{r_0}\right)^{\frac{3}{2}}t^3 + \cdots\right]$$

$$-\frac{1}{8}36a_3^2\left(\frac{g}{r_0}\right)t^2 - \frac{1}{8}144a_3a_4\left(\frac{g}{r_0}\right)^{\frac{3}{2}}t^3 + \cdots$$

$$-\frac{1}{6}r^3a_3^3\left(\frac{g}{r_0}\right)^{\frac{3}{2}}t^3 + \cdots\Big]$$

$$\Theta = n\varphi$$

$$n\left[1 + \cdots\right] = 3a_3 + 2\left(4a_4 - \frac{9}{2}a_3^2\right)\left(\frac{\varepsilon}{r_0}\right)^{1/2} t$$

$$+ 3\left[10a_5 + \frac{a_1}{2} - 18a_3a_4 + \frac{27}{2}a_3^3\right]\left(\frac{\varepsilon}{r_0}\right) t^2 +$$

$$3a_3 = n, \qquad a_3 = n/3$$

$$a_4 = \frac{9}{12}a_3^2 = \frac{n^2}{12}$$

$$a_5 = -\frac{a_1}{20} + \frac{9}{5}a_3a_4 - \frac{27}{20}a_3^3$$

$$= -\frac{n}{20} + \frac{9}{5}\cdot\frac{n^3}{8} - \frac{27}{20}\cdot\frac{n^3}{81} = -\frac{n}{40}$$

$$\frac{I}{I_0} - 1 = \frac{2}{3}\left(\frac{\varepsilon}{r_0}\right)^{3/2} t^3 + \frac{n^2}{12}\left(\frac{\varepsilon}{r_0}\right)^2 t^4 - \frac{n}{40}\left(\frac{\varepsilon}{r_0}\right)^{5/2} t^5 +$$

$$u = \frac{dr}{dt} = \sqrt{\frac{\varepsilon}{r_0}}\left[n\left(\frac{\varepsilon}{r_0}\right)^{1/2} t^2 + \frac{1}{2}\left(\frac{\varepsilon}{r_0}\right)^{3/2} t^3 - \frac{n}{12}\left(\frac{\varepsilon}{r_0}\right)^2 t^4\right.$$

$$\left. + \frac{1}{8}n\left(\frac{\varepsilon}{r_0}\right)^{5/2} t^5 + \cdots\right]$$

$$\frac{r^2}{r_0^2}\frac{d\theta}{dt} = n\sqrt{\frac{\varepsilon}{r_0}}\left[1 + \frac{1}{2}n\left(\frac{\varepsilon}{r_0}\right)^{1/2} t + \frac{1}{4}n^2\left(\frac{\varepsilon}{r_0}\right) t^2 + \frac{1}{8}n^3\left(\frac{\varepsilon}{r_0}\right)^{3/2} t^3\right.$$

$$\left. + \frac{1}{16}n^4\left(\frac{\varepsilon}{r_0}\right)^2 t^4 + \cdots\right]$$

$$\frac{r^2}{r_0^2} = 1 + n\left(\frac{\varepsilon}{r_0}\right)^{1/2} t + \frac{n^2}{2}\left(\frac{\varepsilon}{r_0}\right) t^2 + \frac{n^3}{8}\left(\frac{\varepsilon}{r_0}\right)^{3/2} t^3$$

$$+ \frac{n^4}{48}\left(\frac{\varepsilon}{r_0}\right)^2 t^4 + \cdots$$

2) Case $R = 0$

$$\frac{d}{dt}\left(r^2 \frac{d\theta}{dt}\right) = \Theta r$$

$$r^2 \frac{d\theta}{dt} = r_0^2 \left(\frac{d\theta}{dt}\right)_0 + \int_0^t \Theta r \, dt$$

$$\frac{d^2r}{dt^2} = \frac{1}{r^3}\left[r_0^2 \left(\frac{d\theta}{dt}\right)_0 + \int_0^t \Theta r \, dt \right]^2 - g\frac{r_0^2}{r^2}$$

But $$r_0 \left(\frac{d\theta}{dt}\right)_0^2 = g,$$

$$\frac{d^2r}{dt^2} = g\frac{r_0^2}{r^2}\left[\frac{r}{r_0} + \frac{1}{r_0}\int_0^t \Theta r \, dt - 1\right]$$

So $$\frac{d^2r}{dt^2} = 0 \quad \text{at} \quad t = 0, \quad r = r_0$$

Thus $$(r - r_0) \sim t^3$$

$$\frac{dr}{dt} \sim t^2 \sim (r - r_0)^{2/3}$$

But $$\int_0^t \Theta r \, dt = n\eta \frac{1}{\sqrt{g r_0}} \int_{r_0}^{r} \frac{r \, dr}{\left(\frac{r}{r_0} - 1\right)^{2/3}}$$

$$= n\sqrt{\frac{8}{r_0}}\, r_0^2 \int_1^{r/r_0} \frac{\eta \, d\eta}{(\eta - 1)^{2/3}}$$

$$= n\sqrt{\frac{8}{r_0}}\, r_0^2 \left[\frac{3}{4}(\eta - 1)^{4/3} + 3(\eta - 1)^{1/3}\right]_1^{r/r_0}$$

$$= n\sqrt{\frac{8}{r_0}}\, r_0^2 \left[\frac{3}{4}\left(\frac{r}{r_0} - 1\right)^{4/3} + 3\left(\frac{r}{r_0} - 1\right)^{1/3}\right]$$

$$\rightarrow \pi^2 g\left(\frac{r_0}{r}\right)^3\left[\frac{3}{4}\left(\frac{r_0}{r}-1\right)^{4/3}+3\left(\frac{r_0}{r}-1\right)^{1/3}\right]^2$$

$$=\frac{1}{2}\left[\frac{r_0^3}{r^3}-\frac{r_0^6}{r^6}+\frac{3\pi}{2}\left(\frac{r_0}{r}\right)^3\left(\frac{r}{r_0}-1\right)^{4/3}+6\pi\left(\frac{r_0}{r}\right)^3\left(\frac{r}{r_0}-1\right)^{1/3}\right.$$

$$-\frac{1}{\eta^2}d\eta=dt$$

$$=\int_0^1 \zeta^{2/3-1}(1-\zeta)^{4/3-1}d\zeta-\int_0^{r_0/r}\zeta^{2/3}(1-\zeta)^{4/3}d\zeta$$

$$=\frac{\Gamma\left(\frac{2}{3}\right)\Gamma\left(\frac{4}{3}\right)}{2}-\int_0^{r_0/r}\zeta^{2/3}(1-\zeta)^{1/3}d\zeta$$

$$=\frac{1}{3}\frac{1}{3}\frac{1}{2}\Gamma\left(1-\frac{1}{3}\right)\Gamma\left(\frac{1}{3}\right)-\int_0^{r_0/r}\zeta^{2/3}(1-\zeta)^{1/3}d\zeta$$

$$\int_1^{r/r_0} \frac{d\eta}{\eta^3}(\eta-1)^{1/6} = \frac{\pi}{9\sin\frac{\pi}{3}} - \int_0^{r_0/r} \xi^{1/6}(1-\xi)^{1/2}\,d\xi$$

$$\int_1^{r/r_0} \frac{d\eta}{\eta^3}(\eta-1)^{1/3} = \int_{r_0/r}^{1} \xi^{-1/6}(1-\xi)^{1/3}\,d\xi$$

$$= \int_0^1 \xi^{1/3-1}(1-\xi)^{1/2-1}\,d\xi - \int_0^{r_0/r} \xi^{-1/6}(1-\xi)^{1/3}\,d\xi$$

$$\int_1^{r/r_0} \frac{d\eta}{\eta^3}(\eta-1)^{1/3} = \frac{2}{9}\frac{\pi}{\sin\frac{\pi}{3}} - \int_0^{r_0/r} \xi^{-1/6}(1-\xi)^{1/3}\,d\xi + \int_0^{r_0/r} \xi^{1/3}(1-\xi)^{1/3}\,d\xi$$

$$\int_1^{r/r_0} \frac{d\eta}{\eta^3}(\eta-1)^{2/3} = \int_{r_0/r}^{1} \xi^{1/3}(1-\xi)^{1/3}\,d\xi$$

$$\int_1^{r/r_0} \frac{d\eta}{\eta^3}(\eta-1)^{2/3} = \frac{\pi}{9\sin\frac{\pi}{3}} - \int_0^{r_0/r} \xi^{1/3}(1-\xi)^{1/3}\,d\xi$$

$$\int_1^{r/r_0} \frac{d\eta}{\eta^3}(\eta-1)^{5/3} = \int_{r_0/r}^{1} \xi^{-1/3}(1-\xi)^{5/3}\,d\xi$$

$$\int_1^{r/r_0} \frac{d\eta}{\eta^3}(\eta-1)^{5/3} = \frac{5}{9}\frac{\pi}{\sin\frac{\pi}{3}} - \int_0^{r_0/r} \xi^{-1/3}(1-\xi)^{2/3}\,d\xi + \int_0^{r_0/r} \xi^{1/3}(1-\xi)^{1/3}\,d\xi$$

$$\int_1^{r/r_0} \frac{d\eta}{\eta^3}(\eta-1)^{4/3} = \int_1^{r/r_0} \eta^{-\frac{1}{3}} d\eta \left(1-\frac{1}{\eta}\right)^{4/3}$$

$$= \left[\frac{3}{2}\eta^{2/3}\left(1-\frac{1}{\eta}\right)^{4/3}\right]_1^{r/r_0} - \frac{3}{2}\frac{4}{3}\int_1^{r/r_0} \eta^{2/3}\left(1-\frac{1}{\eta}\right)^{1/3} d\left(-\frac{1}{\eta}\right)$$

$$= \frac{3}{2}\left(\frac{r}{r_0}\right)^{2/3}\left(1-\frac{r_0}{r}\right)^{4/3} - 4\int_{r_0/r}^{1} \zeta^{-2/3}(1-\zeta)^{1/3} d\zeta$$

$$\boxed{\int_1^{r/r_0} \frac{d\eta}{\eta^3}(\eta-1)^{4/3} = \frac{3}{2}\left(\frac{r}{r_0}\right)^{2/3}\left(1-\frac{r_0}{r}\right)^{4/3} - \frac{20}{9}\frac{\pi}{\sin\frac{\pi}{3}} + 4\int_0^{r_0/r} \zeta^{-2/3}(1-\zeta)^{1/3} d\zeta}$$

$$\frac{\pi}{\sin\frac{\pi}{3}} = \frac{2\pi}{\sqrt{3}}$$

$$\frac{1}{2}u^2\frac{1}{gr_0} = \frac{1}{2}\left(1-\frac{r_0^2}{r^2}\right) - \left(1-\frac{r_0}{r}\right) + \frac{3n}{2}\left[\frac{4\pi}{9\sqrt{3}} - f_1\left(\frac{r_0}{r}\right)\right]$$

$$+ 6n\left[\frac{2\pi}{9\sqrt{3}} - f_2\left(\frac{r_0}{r}\right)\right]$$

$$+ \frac{9}{16}n^2\left[\frac{3}{2}\left(\frac{r}{r_0}\right)^{2/3}\left(1-\frac{r_0}{r}\right)^{4/3} - \frac{40\pi}{9\sqrt{3}} + 4f_3\left(\frac{r_0}{r}\right)\right]$$

$$+ \frac{9}{2}n^3\left[\frac{10\pi}{9\sqrt{3}} - f_3\left(\frac{r_0}{r}\right)\right] + 9n^2\left[\frac{2\pi}{9\sqrt{3}} - f_4\left(\frac{r_0}{r}\right)\right]$$

$$\boxed{\begin{aligned} f_1\left(\frac{r_0}{r}\right) &= \int_0^{r_0/r} \zeta^{-1/3}(1-\zeta)^{2/3} d\zeta \\ f_2\left(\frac{r_0}{r}\right) &= \int_0^{r_0/r} \zeta^{1/3}(1-\zeta)^{1/3} d\zeta \\ f_3\left(\frac{r_0}{r}\right) &= \int_0^{r_0/r} \zeta^{-1/3}(1-\zeta)^{1/3} d\zeta \\ f_4\left(\frac{r_0}{r}\right) &= \int_0^{r_0/r} \zeta^{1/3}(1-\zeta)^{2/3} d\zeta \end{aligned}}$$

$$\frac{u^2}{2gr_0} = -\frac{1}{2}\left(1-\frac{r_0}{r}\right)^2 + n\left[\frac{2\pi}{\sqrt{3}} - \frac{3}{2}f_1\left(\frac{r_0}{r}\right) - 6f_2\left(\frac{r_0}{r}\right)\right]$$
$$+ n^2\left[\frac{27}{32}\left(\frac{r}{r_0}\right)^{3/5}\left(1-\frac{r_0}{r}\right)^{6/5} + \frac{9\pi}{2\sqrt{3}} - \frac{9}{4}f_3\left(\frac{r_0}{r}\right) - 9f_4\left(\frac{r_0}{r}\right)\right]$$

$$\frac{u}{\sqrt{2gr_0}} = \left\{ n^2\left[\frac{27}{32}\left(\frac{r}{r_0}\right)^{3/5} \quad\quad\right] + n\left[- \quad - \right] - \frac{1}{2}\left(1-\frac{r_0}{r}\right)^2 \right\}$$

$$\frac{\Theta r}{u} = \frac{n\gamma}{N\gamma r_0}\,\frac{r}{\left(\frac{r}{r_0}-1\right)^{3/5}}$$

$$\Theta = n\gamma\left(\frac{r}{r_0}-1\right)^{-3/5}\left\{ n^2\left[\frac{27}{16}\left(\frac{r}{r_0}\right)^{3/5}\left(1-\frac{r_0}{r}\right)^{8/5} + \frac{9\pi}{\sqrt{3}} - \frac{1}{2}f_3\left(\frac{r_0}{r}\right) - 18f_4\left(\frac{r_0}{r}\right)\right]\right.$$
$$\left. + n\left[\frac{4\pi}{\sqrt{3}} - 3f_1\left(\frac{r_0}{r}\right) - 12f_2\left(\frac{r_0}{r}\right)\right] - \quad \left(1-\frac{r_0}{r}\right)^2 \right\}^{1/2}$$

$$\left[u^2 + r^2\left(\frac{d\theta}{dt}\right)^2\right] - 2g\frac{r_0^2}{r} = 0 \qquad \text{ab} \quad r = r_1$$

$$r\left[r\left(\frac{d\theta}{dt}\right)^2 - g\frac{r_0^2}{r^2}\right] - g\frac{r_0}{r}$$

$$= r\gamma\left[\frac{r_0^2}{r^2} - 2\frac{r_0^2}{r^2} + \frac{3n}{2}\left(\frac{r_0}{r}\right)^3\left(\frac{r}{r_0}-1\right)^{4/5} + 6n\left(\frac{r_0}{r}\right)^3\left(\frac{r}{r_0}-1\right)^{1/5}\right.$$
$$\left. + n^2\frac{9}{16}\left(\frac{r_0}{r}\right)^3\left(\frac{r}{r_0}-1\right)^{6/5} + n^2\frac{9}{2}\left(\frac{r_0}{r}\right)^3\left(\frac{r}{r_0}-1\right)^{7/5} + n^2\,9\left(\frac{r_0}{r}\right)^3\left(\frac{r}{r_0}-1\right)^{2/5}\right]$$

$$0 = -\left(1-\frac{r_0}{r}\right)^2 + n\left[\frac{4\pi}{\sqrt{3}} - 3f_1\left(\frac{r_0}{r}\right) - 12 f_2\left(\frac{r_0}{r}\right)\right] + n^2\left[\frac{27}{16}\left(\frac{r}{r_0}\right)^{2/3}\left(1-\frac{r_0}{r}\right)^{2/3} + \frac{9\pi}{\sqrt{3}}\right.$$

$$\left. - \frac{9}{2} f_3\left(\frac{r_0}{r}\right) - 18 f_4\left(\frac{r_0}{r}\right)\right]$$

$$+ \left(\frac{r_0}{r}\right)^2 - 2\left(\frac{r_0}{r}\right) + n\left[\frac{3}{2}\left(\frac{r_0}{r}\right)^2\left(\frac{r}{r_0}-1\right)^{2/3} + 6\left(\frac{r_0}{r}\right)^2\left(\frac{r}{r_0}-1\right)^{1/3}\right] + n^2\left[\frac{9}{16}\left(\frac{r_0}{r}\right)^2\left(\frac{r}{r_0}-1\right)^{2/3}\right.$$

$$\left. + \frac{9}{2}\left(\frac{r_0}{r}\right)^2\left(\frac{r}{r_0}-1\right)^{2/3} + 9\left(\frac{r_0}{r}\right)^2\left(\frac{r}{r_0}-1\right)^{2/3}\right]$$

$$1 = n\left[\frac{4\pi}{\sqrt{3}} - 3f_1\left(\frac{r_0}{r}\right) - 12 f_2\left(\frac{r_0}{r}\right) + \frac{3}{2}\left(\frac{r_0}{r}\right)^{2/3}\left(1-\frac{r_0}{r}\right)^{1/3} + 6\left(\frac{r_0}{r}\right)^{2/3}\left(1-\frac{r_0}{r}\right)^{2/3}\right]$$

$$+ n^2\left[\frac{27}{16}\left(\frac{r}{r_0}\right)^{2/3}\left(1-\frac{r_0}{r}\right)^{2/3} + \frac{9\pi}{\sqrt{3}} - \frac{9}{2} f_3\left(\frac{r_0}{r}\right) - 18 f_4\left(\frac{r_0}{r}\right)\right.$$

$$\left. + \frac{9}{16}\left(\frac{r}{r_0}\right)^{2/3}\left(1-\frac{r_0}{r}\right)^{1/3} + \frac{9}{2}\left(\frac{r_0}{r}\right)^{2/3}\left(1-\frac{r_0}{r}\right)^{2/3} + 9\left(\frac{r_0}{r}\right)^{2/3}\left(1-\frac{r_0}{r}\right)^{2/3}\right]$$

$$M\Theta = -c\frac{dM}{dt}$$

$$-\frac{dM}{M} = \frac{1}{c}\Theta\, dt$$

$$\log\frac{M_0}{M_1} = \frac{1}{c}\int_{r_0}^{r_1}\frac{\Theta\, dr}{\left(\frac{dr}{dt}\right)}$$

$$= \frac{n\sqrt{g}}{c\sqrt{r_0}}\int_{r_0}^{r_1}\frac{dr}{\left(\frac{r}{r_0}-1\right)^{1/3}}$$

$$= \frac{n}{c}\sqrt{g r_0}\int_{1}^{r_1/r_0}\frac{dy}{(y-1)^{1/3}} = \boxed{\frac{3n}{c}\sqrt{g r_0}\left(\frac{r_1}{r_0}-1\right)^{1/3} = \log\frac{M_0}{M_1}}$$